

**Author's response to reviewer's comments**

**Interactive comment on “Mineralization of organic matter in boreal lake sediments: Rates, pathways and nature of the fermenting substrates” by François Clayer et al.**

***Bold and Italic line numbers*** refer to lines in the annotated MS (attached below) while normal line numbers refer to lines in the original MS.

**Reviewer 1:**

**Anonymous Referee #1 Received and published: 23 March 2020**

The manuscript is a modification of previous work published by Clayer et al 2018 in *Geochimica et Cosmochimica Acta*. It builds on the hypothesis that the degradation of organic material under anaerobic conditions has two ultimate sinks – CO<sub>2</sub> or CH<sub>4</sub>, the most reduced and oxidized states of carbon. The relative abundance of these two should therefore provide information on the average oxidation state of the degraded organic material accounting for transport and other sources of CO<sub>2</sub>. This principal approach has been presented in Clayer et al (2018) *GCA*. The current paper is very similar to this published work and contains many data that are shared. It was not obvious to me where this work is a significant novel contribution beyond what has also ready been published. The authors use a simple steady state reaction transport model for diffusive and advective transport to determine microbial process rates based on sediment porewater concentration gradients. Furthermore, the isotope composition of DIC is used to improve the mass balance calculations.

**Below I question the validity of this approach to obtain a meaningful mass balance using the Berg et al model at steady state.**

Thank you for your rigorous and comprehensive comments, they have been very useful to improve the quality of the manuscript. We appreciate the time invested by the reviewer.

**#1 - This manuscript is difficult to understand manuscript and very technical in its description. What makes this manuscript so hard to read and understand is the multitude of R subscripts that are used in the text and the extensive treatment of the methodology in the appendix. The fractional equations are nowhere introduced. Deserves an explanation. In practice, one has to have a table on the side to look up what reaction a particular R subscript refers to and, in addition, know all the notations from Clayer et al (2018) to follow this work.**

We agree that the manuscript is very technical, which makes it harder to follow. In order to rigorously distinguish between net reaction rates, provided by PROFILE, and effective (or gross) reaction rates, we need these numerous R notations. We have now better introduced the effective reaction rates  $R_i$ . They were only introduced in Table 1 captions, in the original manuscript. We also better describe the term  $R_{net}^{Ox}$ . Note also that we have clarified the description of reaction r1 (see response to comment #9)

Note that all notations are described in the manuscript, there is no need to have notations from Clayer et al., 2018.

L. 228(138) now reads

“The main reactions retained in this study to describe carbon cycling in the sediments of the two lake basins are shown in Table 1.  $R_i$  and  $\alpha_i$  denote, respectively, the effective (or gross) reaction rate and the carbon isotopic fractionation factor associated with each reaction  $r_i$  (Table 1).”

Response to reviewers

Note also that each net reaction rates are explicitly defined.

L. **208**(121) " $R_{\text{net}}^{\text{solute}}$  (in  $\text{mol cm}^{-3}$  of wet sediment  $\text{s}^{-1}$ ) is the solute net production rate (or consumption rate if  $R_{\text{net}}^{\text{solute}}$  is negative)"

L. **248**(148) "the net rate of  $\text{CH}_4$  production,  $R_{\text{net}}^{\text{CH}_4}$ "

L. **250**(150) "The net rate of DIC production,  $R_{\text{net}}^{\text{DIC}}$ ,"

L. **279**(153) " $R_{\text{net}}^{\text{Ox}}$  is the net reaction rate of all relevant oxidants consumption, i.e.,  $\text{O}_2$ , Fe(III) and  $\text{SO}_4^{2-}$  only because  $\text{NO}_3^-$  and Mn(IV) are negligible (see above)." And there after (see also response to comment #15 below).

**#2 - Still, to follow the conclusions becomes increasingly confusing as one reads along, until one is either lost or exhausted. In the current form, the manuscript cannot be digested. I recommend that the authors outline the hypothesis, mathematically, in the materials and methods section, of how their methodology allows them to get at the oxidation state of oxidized organic matter. In the current form, the reader has to wade through too much text to get to this most interesting point of the manuscript. This paper requires a much better didactic approach to get methods and goals across and the authors get sidetracked in many details that make it hard to follow their ultimate goal. It is, in its current form, not streamlined enough and requires very significant rewriting and restructuring to make the approach more understandable and possible to evaluate critically. At present, I cannot evaluate the quality of the manuscript, but am left in doubt about its novelty given the similarity to the 2018 GCA paper. While the fundamental goal, to arrive at the oxidation state of metabolizable organic material, is of some significance, the presentation of the approach is not well developed and can be improved considerably. Data and basic approach (although I did get lost in the complicated  $\text{d}^{13}\text{C}$  treatment) are, in principle feasible, but overall I am concerned that the instrumental and modelling analytical uncertainty is too great to pin down the COS sufficiently (although an error is given).**

We have reorganized the method and discussion sections to better describe the approach and outline the hypothesis mathematically (see our response to comment #3). We have also modified the abstract, introduction and conclusions for consistency and to highlight to novelty compared to the 2018 GCA paper.

L. **14-28**(13-24) now read:

"To test the validity of this assumption, we modeled using reaction-transport equations vertical profiles of the concentration and isotopic composition ( $\delta^{13}\text{C}$ ) of  $\text{CH}_4$  and DIC in the top 25 cm of the sediment column from two lake basins, one whose hypolimnion is perennially oxygenated and one with seasonal anoxia. Furthermore, we modeled solute porewater profiles reported in the literature for four other seasonally anoxic lake basins. A total of seventeen independent porewater datasets are analysed.  $\text{CH}_4$  and DIC production rates associated with methanogenesis at the five seasonally anoxic sites collectively show that the fermenting OM has a mean ( $\pm\text{SD}$ ) carbon oxidation state (COS) value of  $-1.4 \pm 0.3$ . This value is much lower than the value of zero expected from carbohydrates fermentation. We conclude that carbohydrates do not adequately represent the fermenting OM in hypolimnetic sediments and propose to include the COS in the formulation of OM fermentation in models applied to lake sediments to better quantify sediment  $\text{CH}_4$  outflux. This study highlights the potential of mass balancing the products of OM mineralization to characterize labile substrates undergoing fermentation in sediments."

And L. **139-151**(68-74):

“In this study, the approach described in Clayer et al. (2018), combining concentration and  $\delta^{13}\text{C}$  inverse modeling, is applied to the two newly acquired datasets. These datasets include centimeter-scale vertical porewater profiles of the concentrations and of the stable carbon isotope ratios ( $\delta^{13}\text{C}$ ) of  $\text{CH}_4$  and dissolved inorganic carbon (DIC), as well as those of the concentrations of EAs from hypolimnetic sediments of two boreal lake basins showing contrasted  $\text{O}_2$  dynamics: one whose hypolimnion remains perennially oxygenated and the other whose hypolimnion becomes anoxic for several months annually. This procedure enables us to constrain the effective rates of OM mineralization reactions and calculate, using a mass balance equation, the COS of the substrates fermenting in the sediments in these two lake basins. In addition, we modelled solute porewater profiles gathered from the scientific literature or from our data repository for four other seasonally anoxic lake basins to estimate, using the mass balance equation, the COS of the substrates fermenting in these sediments. A total of seventeen independent datasets are analysed to provide additional insight into the COS of the fermenting OM in boreal lakes and the associated mineralization pathways.”

L. **781-790**(448–453) now read:

“Reactive-transport modelling of twelve datasets of porewater profiles from three boreal lakes, i.e., Bédard, Tantaré (Basin B) and Jacks, as well as of the sub-alpine Lake Lugano (Melide and Figino sites) consistently showed that the main substrates for sediment methanogenesis at deep seasonally anoxic hypolimnetic sites have a mean COS value of  $-1.4 \pm 0.3$ . The OM in the sediment of the three boreal lakes, as well as their  $\text{O}_2$  seasonal dynamics, is typical of boreal forest lakes. While Lake Bédard experiences prolonged episodes of extended hypolimnetic anoxia, Lake Tantaré Basin B and Jacks Lake show more moderate seasonal anoxia, where some years the hypolimnion of Lake Tantaré Basin B is only hypoxic (Clayer et al., 2016; Carignan et al., 1991). Hence, the selective mineralization of OM described by Clayer et al. (2018), involving that the most labile compounds are mineralized during OM downward migration in the water column and at the sediment surface leaving mainly reduced organic compounds to fuel methanogenesis in the sediments, likely applies to a large portion of boreal lakes.”

L. **801-807**(460-461) now read:

“Introducing the average COS values reported in this study ( $-1.4 \pm 0.3$ ) into Eq. 14, the coefficients  $a$  and  $b$  would take values of  $2.7 \pm 0.15$  and  $0.65 \pm 0.125$ , respectively, and the  $\text{CH}_4$  and  $\text{CO}_2$  stoichiometric coefficients would be  $0.68 \pm 0.04$  and  $0.32 \pm 0.04$ , respectively. Note that the same stoichiometric formulation would be obtained with any possible combination of acetoclasty and hydrogenotrophy. Under these conditions, fermentation (r1) coupled to methanogenesis (r4) yields  $2.2 \pm 0.4$  times more  $\text{CH}_4$  than DIC for the studied lake sediments. Ignoring the implications of the present study regarding the COS of the fermenting OM could lead to the underestimation of  $\text{CH}_4$  sediment outflux or of the rate of oxidant consumption required to mitigate this efflux by a factor of up to 2.6.”

**#3 -The authors provide statistical data to support their assertion, but it was not possible for me, based on the complicated description, to relate the outcome of these tests to the goal of the manuscript, i.e., the original oxidation of the degrading organic material. The authors must make sure, in a succinct and understandable and not too wordy fashion, how their methodology allows them to pin this value down sufficiently. Remove as much as possible reiterations of what has already been said and discussed in detail in Clayer et al 2018 GCA and restrict this paper to the novel information.**

Thank you for a constructive comment. In consequence, we have (i) clarified the novel aspects (see response to comment above), and (ii) better described the modelling and COS estimation approaches, (iii) edited the conclusions (see also our response to comment #4) and (iv) simplified the discussion (See also our response to comment #4 and #5).

As a consequence of including the new Eq. 9 below, Eq. 11 and 12 were removed which simplified section 4.2. COS values displayed in Table 4 are directly calculated with Eq. 9.

The description of the approach now reads:

“L. **245-247**(148)

Considering the net reaction rates obtained by inverse modelling, a realistic range of values can be given for each of the effective reaction rates  $R_i$  in each depth interval using the general equations described below (Eqs. 3, 4 and 5). The detailed calculations for each  $R_i$  at both study sites are described in section S2.

(...)

L. **291-296**(160)

Once the range of values have been determined for each of the effective rates  $R_i$  (see Table S2), they can be used in another reaction-transport equation to model the  $\delta^{13}\text{C}$  profiles of  $\text{CH}_4$  and DIC. Only sets of  $R_i$  values that yield acceptable modeled  $\delta^{13}\text{C}$  profiles, i.e., which fall within one standard deviation of the measured  $\delta^{13}\text{C}$  profiles (grey area fills in Fig. 4), were kept for COS calculation below (section 2.8). The  $\delta^{13}\text{C}$  modeling procedure is summarized below and described in detail in Section S.2. This procedure takes into account the effect of diffusion, bioirrigation (in Lake Tantaré Basin A) and the isotopic fractionation effect of each reaction  $r_i$ .

(...)

L. **334-342**(176)

## 2.8 COS calculation

Considering the complete fermentation of metabolizable OM of general formula  $\text{C}_x\text{H}_y\text{O}_z$ , and making two assumptions, described below for clarity, the COS of the fermenting molecule is given by (combining Eq. S8 and S15; see Section S2 for details):

$$\text{COS} = -4 \left( \frac{R_{\text{net}}^{\text{CH}_4} - R_{\text{net}}^{\text{DIC}} - R_{\text{net}}^{\text{Ox}} + R_2}{R_{\text{net}}^{\text{CH}_4} + R_{\text{net}}^{\text{DIC}} + (1 - \chi_M)R_{\text{net}}^{\text{Ox}} - R_2} \right) \quad (9)$$

where  $\chi_M$  is the fraction of oxidants consumed by methanotrophy. Equation (9) is only valid if i)  $r_1$  is the only source of substrates for hydrogenotrophy and acetoclasty (this assumption is discussed in Section 4.2 below); and that ii) siderite precipitation ( $r_7$ ) is negligible (Saturation Index for siderite are negative except below 10 cm depth in the sediment of Lake Bédard, this case is considered in Section S2.1.2.2). With values of  $R_{\text{net}}^{\text{CH}_4}$  and  $R_{\text{net}}^{\text{Ox}}$  obtained from PROFILE (section 2.4), values of  $R_2$ ,  $\chi_H$  and  $\chi_M$  constrained by  $\delta^{13}\text{C}$  modeling (section 2.7), Eq. (9) can be used to calculate the COS of the fermenting molecule.”

L. **665-670**(384-391) now read:

“The COS values displayed in Table 4 for all lake basins and dates were calculated by substituting the appropriate  $R_{\text{net}}^{\text{CH}_4}$ ,  $R_{\text{net}}^{\text{DIC}}$ ,  $R_{\text{net}}^{\text{Ox}}$  and  $R_2$  values in Eq. 9 and varying  $\chi_M$  between 0 and 1, except for Lake Tantaré Basin A for which  $\chi_M = 0.75$  (Table 3). When the value for  $R_2$  was not available, we assumed that  $R_2 = 0$ . Equation 9 indicates that  $R_2 > 0$ , would yield lower COS values than those reported in Table 4.”

L. **688-740** (406-442) now read:

“The COS values determined for the perennially oxygenated Basin A of Lake Tantaré (mean of  $-0.6 \pm 1.1$ ; range of  $-3.2$  to  $2.1$ ; Table 4) are much more variable than for the five other seasonally anoxic lake basins including unrealistic values for October 2015 in the  $Z_1$  ( $-3.2$ ), September 2016 ( $0.4-0.6$ ) and October 2005 ( $1.8-2.1$ ). Indeed, the very negative value of  $-3.2$  does not correspond to any degradable compound under anoxic

conditions, whereas the positive values of 0.4–0.6 and 1.8–2.1 would involve either amino acids and nucleotides which are very labile (Larowe and Van Cappellen 2011) and tend to be degraded in the water column (Burdige 2007), or oxidized compounds, such as ketones, aldehydes and esters, known to be quickly reduced to alcohols. Possible sources of uncertainty in the COS estimation include mis-quantification of bioirrigation and DIC production through HMW OM fermentation (reaction r2; Corbett et al. 2013). Clayer et al. (2016) provided evidences that sediment irrigation by benthic animals is effective in Lake Tantaré Basin A and that reaction rates are sensitive to the bioirrigation coefficient. Nevertheless, additional simulations show that changing the bioirrigation coefficient by a factor of 2 (increased and decreased) did not result in significant changes in COS values ( $<0.2$ ). Bioirrigation might also be mis-represented. Indeed, the term used in Eq. 2 to calculate this contribution, i.e.,  $\varphi\alpha_{\text{irrigation}}([\text{solute}]_{\text{tube}} - [\text{solute}])$ , is indeed an approximation of intricate 3-D processes variable in space and time (Meile et al., 2005; Boudreau and Marinelli, 1994; Forster and Graf, 1995; Gallon et al., 2008; Riisgård and Larsen, 2005). On the other hand, DIC production through HMW OM fermentation (reaction r2; Corbett et al. 2013) was constrained by default in Lake Tantaré Basin A (Table 4). Indeed, fitting with Eq. 7 the experimental  $\delta^{13}\text{C}$  data does not allow partitioning the production of DIC between r1 and r2 given that both processes share the same fractionation factor ( $\alpha_1 = \alpha_2 = 1.000$ ). Equation 9 indicates that to obtain negative COS values for Lake Tantaré Basin A in September 2006 and October 2005,  $R_2$  should be  $>11 \text{ fmol cm}^{-2} \text{ s}^{-1}$  and  $>110 \text{ fmol cm}^{-2} \text{ s}^{-1}$ , respectively. These  $R_2$  values correspond to transferring  $>9\%$  and  $>44\%$  of the rate of DIC production from  $R_1$  to  $R_2$  for September 2006 and October 2005, respectively. Hence, owing to the imperfection in the COS estimations for Lake Tantaré Basin A, COS values estimated for this site should be treated with caution. Note that the sediment surface was also oxic at the sites Melide and Figino of Lake Lugano in March 1989 (Table 4) as revealed by detectable bottom water  $[\text{O}_2]$  (Table 4), and by low  $[\text{Fe}]$ , undetectable  $\Sigma\text{S}(-\text{II})$  and  $[\text{CH}_4]$  and relatively high  $[\text{SO}_4^{2-}]$  in overlying water (Lazzaretti et al., 1992; Lazzaretti-Ulmer and Hanselmann, 1999). Despite this, the COS values determined for the two sites of Lake Lugano appear realistic and consistent with those calculated for Lakes Tantaré Basin B, Bédard and Jacks. This disparity between Lake Tantaré Basin A and Lake Lugano could be explained by the presence of benthic organisms in the former (Hare et al., 1994) but their absence in the latter, as shown by the presence of varves (Lazzaretti et al., 1992) and the absence of benthos remains in the recent sediments of Lake Lugano (Niessen et al., 1992)."

**#4 - A lot of the discussion about the CH<sub>4</sub> isotopes are not really part of the goal of this paper. This should be separated.**

Agreed, we simplified and moved the text L. 305-317 to section 3.4 to streamline the discussion. Note however that the discussion related to the importance of hydrogenotrophy in section 4.1 is kept and its implication is now emphasized in the Conclusions (see below).

L. **473-483** (305-317) now, in section 3.4, read:

"The sharp upward depletion in  $^{13}\text{C}\text{-CH}_4$  leading to a minimum  $\delta^{13}\text{C}\text{-CH}_4$  value at 2.5 cm depth in Lake Tantaré Basin A sediments (Fig. 3a) was unanticipated since it occurs in the methanotrophic zone, i.e., where the remaining  $\text{CH}_4$  is expected to be  $^{13}\text{C}$ -enriched as a result of  $\text{CH}_4$  oxidation. Marked  $^{13}\text{C}\text{-CH}_4$  depletions at the base of the sulfate-methane transition zone, where  $\text{CH}_4$  is consumed via  $\text{SO}_4^{2-}$  reduction, have often been observed in marine sediments (Burdige et al., 2017 and references therein). Such features are generally attributed to the production of  $\text{CH}_4$  by hydrogenotrophy from the  $^{13}\text{C}$ -depleted DIC resulting from the anaerobic  $\text{CH}_4$  oxidation, a process referred to as intertwined methanotrophy and hydrogenotrophy (e.g., Borowski et al., 1997; Burdige et al., 2017; Pohlman et al., 2008). Here the modelled  $\delta^{13}\text{C}\text{-CH}_4$  profile captured the minimum in  $\delta^{13}\text{C}\text{-CH}_4$  in the  $Z_1$  by simply assuming concomitant hydrogenotrophy and methanotrophy in this zone and an upward-increasing  $\alpha_4$  value from 1.085 in the  $Z_3$  to 1.094 in the  $Z_1$  (section S2.2.1 of the SI). A small variation with sediment depth in the fractionation factor  $\alpha_4$  is arguably possible since its value depends on the types of microorganisms producing  $\text{CH}_4$  (Conrad, 2005)."

L. **773-780** (444–447) now read:

“Our results show that fermentation and methanogenesis represent about 50% and 100% of OM mineralization in the top 25 cm of the sediments at the hypolimnetic sites in Lake Tantaré Basin A and Bédard, respectively, that methane is produced only by hydrogenotrophy and fermentation substrates have a negative COS at these two sites. The association of hydrogenotrophy with the fermentation of reduced OM ( $\text{COS} < -0.9$ ; implying that labile compounds are depleted) in the studied lake sediments is consistent with the fact that hydrogenotrophy becomes increasingly important when labile OM is depleted (Chasar et al., 2000; Hornibrook et al., 2000; Whitticar et al., 1986).”

**#5 - There are a few assumptions whose impact I don't understand or that are difficult to assess, e.g., that there are no anaerobic reoxidation reactions for sulfide; elemental sulfur with FeOOH. The paper does not lost O<sub>2</sub> uptake rates for the oxic part of the year, which is an important constraint on the 'background CO<sub>2</sub> levels in the buried porewaters. The paper does not constrain oxygen penetration depths or the importance of bioturbation processes for DIC levels, and does not show O<sub>2</sub> microelectrode profiles, which would be necessary to constrain the inorganic oxidative processes. Therefore the constraints for the diagenetic system, e.g., by having total O<sub>2</sub> uptake rates are far and few. In principle, non-steady state reaction transport modelling with a much more advanced model are necessary to tackle this question, if it is possible at all.**

O<sub>2</sub> microprofiles were not measured for this study, but Couture et al. (2016) reported O<sub>2</sub> micro-profile measured previously in the sediment of Lake Tantaré Basin A. These microprofiles were the basis of our estimation of  $R_{\text{net}}^{\text{O}_2}$ , see L. 129-132. For the majority of the other study sites, the bottom waters were anoxic (O<sub>2</sub> < 0.1 mg L<sup>-1</sup>), thus O<sub>2</sub> uptake was negligible. Furthermore, we acknowledge in section 4.3 (L. 406-442), the fact that bioirrigation, O<sub>2</sub> uptake and misattribution of DIC production can involve uncertainty in the COS estimation for Lake Tantaré Basin A. However, these factors are much less prominent, if not absent, for the other seasonally anoxic lake basins. We believe that the strength of our demonstration resides is the consistency among the COS estimations reported for the seasonally anoxic basins.

We also agree that the concentration profiles presented here were collected in October and are thus the result of “**background CO<sub>2</sub> levels in the buried porewaters**”, and of changing conditions at the SWI. Although our approach does not enable to resolve all aspect of the complex OM degradation cycling, e.g., explaining the magnitude of all the fluxes involved at a given depth, it allows us to estimate process rates in a given sediment zone, independently of the background concentrations.

Note that the term  $R_{\text{net}}^{\text{Ox}}$  takes into account anaerobic reoxidation reactions for sulfide; elemental sulfur with FeOOH. Admittedly, this point was not stated clearly enough. See our response to comment #6 below.

We also clarify the importance of bioturbation. L. **203-205** (122-123) now reads:

“considering steady state and negligible solute transport by bioturbation and advection. The validity of these assumptions has been previously demonstrated for the study sites (Couture et al., 2008; Couture et al., 2010; Clayer et al., 2016).”

Regarding non-steady state reaction transport modelling, see also our response to comment #17.

**#6 - Another curious observation is the omission of NO<sub>3</sub> dynamics as part of O<sub>2</sub> consumption by nitrification; also here there are no constraints on the system concerning NH<sub>4</sub><sup>+</sup> to accompany C mineralization dynamics.**

**The model also ignores O<sub>2</sub> consumption due to Fe oxidation, but curiously the authors choose to include instead sulfide oxidation with O<sub>2</sub> and FeOOH.**

Our approach, admittedly not stated clearly enough in the original manuscript, has considered all oxidants. Some of them (NO<sub>3</sub> and Mn(IV)) have been shown previously to be negligible because of their low content in the sediment and porewaters (Clayer et al., 2016). Secondary redox reaction as O<sub>2</sub> consumption due to Fe(II) oxidation are also taken into account.

To better appreciate these points, we modified section 2.3 (L. **279-299** / 153 and thereafter) as follows:

“ $R_{\text{net}}^{\text{Ox}}$  is the net reaction rate of all relevant oxidants consumption, i.e., O<sub>2</sub>, Fe(III) and SO<sub>4</sub><sup>2-</sup> only because NO<sub>3</sub><sup>-</sup> and Mn(IV) are negligible (see above). For simplicity,  $R_{\text{net}}^{\text{Ox}}$  is expressed in equivalent moles of O<sub>2</sub> consumption rate, taking into account that SO<sub>4</sub><sup>2-</sup> and Fe(III) have twice and one quarter the oxidizing capacity of O<sub>2</sub>, respectively. In practice, the value of  $R_{\text{net}}^{\text{Ox}}$  was calculated by adding those of  $R_{\text{net}}^{\text{O}_2}$ ,  $\frac{1}{4}R_{\text{net}}^{\text{Fe(III)}}$  and  $2R_{\text{net}}^{\text{SO}_4^{2-}}$  where  $R_{\text{net}}^{\text{O}_2}$ ,  $R_{\text{net}}^{\text{Fe(III)}}$  and  $R_{\text{net}}^{\text{SO}_4^{2-}}$  were estimated with PROFILE. In this calculation, we assumed that all dissolved Fe is in the form of Fe(II), and that the rate of Fe(II) consumption through reactions r7 is negligible compared to those associated with reactions r5 and r6. Under these conditions,  $R_{\text{net}}^{\text{Fe(III)}} = -R_{\text{net}}^{\text{Fe}}$ . It should be noted that using  $R_{\text{net}}^{\text{O}_2}$ ,  $-R_{\text{net}}^{\text{Fe}}$  and  $R_{\text{net}}^{\text{SO}_4^{2-}}$  to calculate  $R_{\text{net}}^{\text{Ox}}$ , we indirectly take into account the re-oxidation of reduced S and Fe(II), respectively, to SO<sub>4</sub><sup>2-</sup> and Fe(III) by O<sub>2</sub>. Indeed, with this procedure, we underestimate the terms  $\frac{1}{4}R_{\text{net}}^{\text{Fe(III)}}$  and  $2R_{\text{net}}^{\text{SO}_4^{2-}}$  because re-oxidation reactions are ignored, but we overestimate by the same amount the term  $R_{\text{net}}^{\text{O}_2}$ . In other words, omission of these re-oxidation reactions affects only the relative consumption rates of individual oxidants and not the value of  $R_{\text{net}}^{\text{Ox}}$ , which is of interest here.”

**#7 - It seems very hard to see how the boundary conditions can be reasonably constrained to continue with the approach used by the authors.**

As boundary conditions, we use for each solute their measured concentrations at top and bottom of the concentration profiles (as stated L. **217-218** / 128-129). The model assumes steady-state, and we now mention that this assumption is valid (see below). Under steady-state conditions, the concentrations of solutes at top and bottom of their profiles should not vary with time.

L. **203-205** (122-123) “considering steady state and negligible solute transport by bioturbation and advection. The validity of these assumptions has been previously demonstrated for the study sites (Couture et al., 2008; Couture et al., 2010; Clayer et al., 2016).”

**#8 - Line comments: Line 139: There are more products than acetate CO<sub>2</sub> and CH<sub>4</sub> and H<sub>2</sub>: Formate, propionate, isopropionate, lactate, butyrate, isobutyrate, pyruvate, succinate, etc.; The sum of the latter can be as high as 30% of the total VFA. Ok, acetate is low, but why should it not, if it is consumed by terminal oxidizers? Line 191: No good explanation for the low acetate concentrations?**

We agree, OM degradation occurs and produces other VFA. But eventually, to produce CH<sub>4</sub>, it will be degraded to acetate and/or CO<sub>2</sub> and/or H<sub>2</sub> (see Conrad 1999). Reaction r1 is a representation of the fermentation reaction, considering all VFA is out of the scope of this study.

Note that when measuring ions with ion chromatography (L. **195-196** / 109-111), we also looked for VFA, but those were under detection limit (not mentioned in the manuscript).

Besides, we provide evidence that acetoclasty is negligible. Acetate is just not an important degradation product in these sediments. As stated L. **496-499** (284-287):

“hydrogenotrophy becomes an increasingly important CH<sub>4</sub> production pathway: i) when labile OM is depleted (Chasar et al., 2000; Hornibrook et al., 2000; Whiticar et al., 1986), ii) with increasing sediment/soil depth (Conrad et al., 2009; Hornibrook et al., 1997), or iii) with decreasing rates of primary production in aquatic environments (Galand et al., 2010; Wand et al., 2006)”

We also replaced L. **467-471** (269-279):

“Modeled  $\delta^{13}\text{C}$  profiles were considered acceptable only when they fell within one standard deviation of the measured  $\delta^{13}\text{C}$  profiles (grey area fills in Fig. 4). Acceptable modeled  $\delta^{13}\text{C}$  profiles were obtained only when methanogenesis was 100% hydrogenotrophic, i.e., when  $R_3=0$  (see section S2.2.2.1).”

**L.155 Profile underestimates the oxidation rate because it is a fit of a net rate, not a gross rate, e.g., cryptic cycling leads to CO<sub>2</sub> production by sulfate reduction in the absence of a curvature in the gradient.**

Agreed, PROFILE provides net reaction rates. This is now clarified as:

L. **279-299** / 153 and thereafter

“ $R_{\text{net}}^{\text{Ox}}$  is the net reaction rate of all relevant oxidants consumption, i.e., O<sub>2</sub>, Fe(III) and SO<sub>4</sub><sup>2-</sup> only because NO<sub>3</sub><sup>-</sup> and Mn(IV) are negligible (see above). For simplicity,  $R_{\text{net}}^{\text{Ox}}$  is expressed in equivalent moles of O<sub>2</sub> consumption rate, taking into account that SO<sub>4</sub><sup>2-</sup> and Fe(III) have twice and one quarter the oxidizing capacity of O<sub>2</sub>, respectively. In practice, the value of  $R_{\text{net}}^{\text{Ox}}$  was calculated by adding those of  $R_{\text{net}}^{\text{O}_2}$ ,  $\frac{1}{4}R_{\text{net}}^{\text{Fe(III)}}$  and  $2R_{\text{net}}^{\text{SO}_4^{2-}}$  where  $R_{\text{net}}^{\text{O}_2}$ ,  $R_{\text{net}}^{\text{Fe(III)}}$  and  $R_{\text{net}}^{\text{SO}_4^{2-}}$  were estimated with PROFILE. In this calculation, we assumed that all dissolved Fe is in the form of Fe(II), and that the rate of Fe(II) consumption through reactions r7 is negligible compared to those associated with reactions r5 and r6. Under these conditions,  $R_{\text{net}}^{\text{Fe(III)}} = -R_{\text{net}}^{\text{Fe}}$ . It should be noted that using  $R_{\text{net}}^{\text{O}_2}$ ,  $-R_{\text{net}}^{\text{Fe}}$  and  $R_{\text{net}}^{\text{SO}_4^{2-}}$  to calculate  $R_{\text{net}}^{\text{Ox}}$ , we indirectly take into account the re-oxidation of reduced S and Fe(II), respectively, to SO<sub>4</sub><sup>2-</sup> and Fe(III) by O<sub>2</sub>. Indeed, with this procedure, we underestimate the terms  $\frac{1}{4}R_{\text{net}}^{\text{Fe(III)}}$  and  $2R_{\text{net}}^{\text{SO}_4^{2-}}$  because re-oxidation reactions are ignored, but we overestimate by the same amount the term  $R_{\text{net}}^{\text{O}_2}$ . In other words, omission of these re-oxidation reactions affects only the relative consumption rates of individual oxidants and not the value of  $R_{\text{net}}^{\text{Ox}}$ , which is of interest here.”

**#9 - Line 281 Equation 9 has not been introduced previously. I don't get those fractions.**



As stated in the text, Equation 9 is a simplification of Reaction r1, where  $x = \nu_1$ . Reaction r1 is displayed in Table 1 and explained in section 2.3. For further clarification, the description of r1 now reads (L. **230** / 138):

“Once oxidants are depleted, fermentation of metabolizable OM of general formula  $C_xH_yO_z$  can yield acetate,  $CO_2$  and  $H_2$  (r1). The coefficient  $\nu_1$  in r1 constrains the relative contribution of acetoclasty and hydrogenotrophy.”

**#10 - Line 322: This sentence is confusing, why should hydrogenotrophy produce DIC coupled to fermentation? Only fermentation r1 may produce  $CO_2$ .**

Agreed, DIC can only be produced by fermentation and not by hydrogenotrophy. We now clarify as follows:

L. **533-536**

“This high ratio indicates that DIC was not produced by fermentation (r1) alone in the  $Z_2$  of this lake. Indeed, methanogenesis through the coupling of r1 and r4 yields a  $R_1/R_4$  ratio of 2 if the fermenting substrate is carbohydrates (COS of 0) and lower than 2 if the fermenting substrate has a negative COS value.”

**#11 - L.330: To avoid confusion, a carbon mineralization process leads to the formation of a mineral acid, e.g., carbonic acid. Neither fermentation nor methanogenesis can therefore be called mineralization processes. They are carbon degradation/decomposition processes.**

We were not aware of this definition for the term “mineralization” since this term is widely used to refer to organic matter degradation/decomposition processes (i.e., transformation of organic matter to mineral molecules as DIC, Phosphate, Ammonium and  $CH_4$ ) including oxidation and fermentation reactions, e.g., Burdige 1991; Larowe and Van Cappellen 2011; Arndt et al., 2013.

To avoid any confusion with other uses of the term “mineralization”, we precise in the introduction as follows (L. **90-91** / 50):

“Nonetheless, the performance of these models depends on the correct formulation of the complete OM mineralization reactions, e.g., OM decomposition to DIC, phosphate, ammonium and  $CH_4$  through oxidation and fermentation reactions (Burdige 1991), particularly in terms of the metabolizable organic compounds involved.”

**#12 - Line 332: Please change your terminology Methanogenesis by hydrogenotrophy cannot lead to  $CO_2$  formation**

Agreed, we clarify as follows:

L. **543-544**

“Indeed, the sum of the rates of  $CH_4$  production ( $\Sigma R_4$ ), DIC production due to fermentation associated with  $CH_4$  formation ( $\Sigma R_1 - \Sigma R_4$ ) and HMW OM partial fermentation ( $\Sigma R_2$ )”

**#13 - Line 337-340 This conclusion cannot truly be validated with the approach used here.**

We agree that the text was lacking some clarity related to this conclusion. We now believe that our conclusion here is robust given our clarifications related to comment #XX regarding the use of the  $\delta^{13}\text{C}$  data to constrain reaction rates. We also precise our point as follows:

**I. 557-559**

“The inclusion of  $\delta^{13}\text{C}$  data in the present modeling study thus allowed to better constrain the effective rates of  $\text{CH}_4$  production ( $R_4$ ). Indeed, a value of  $R_4 = 119 \text{ fmol cm}^{-3}\text{s}^{-1}$  was required in Eq. (7) to produce an acceptable  $\delta^{13}\text{C}$ - $\text{CH}_4$  profile (Table 3 and Fig. S3).”

**#14 - Line 353-355 Again, the authors make the mistake of modelling net concentration profiles to extract information on gross rates. The  $\text{H}_2$  production and  $\text{CO}_2$  production rates by cryptic cycling are not reflected in curvatures of concentration gradients, these only represented the net effect.**

We now clarify the text as follows:

**L. 602-610**

“The progressive downward increases in dissolved Fe and  $\text{SO}_4^{2-}$  (Fig. 2e, f, m and n) below  $\sim 5 \text{ cm}$  depth and decrease in  $\Sigma\text{S}(-\text{II})$  (Fig. 2n) observed in the porewaters suggest a net production of  $\text{H}_2$  from r8 in both lakes. However, in the  $Z_1$  and  $Z_2$  of Lake Tantaré Basin A, the rate of solid Fe(III) reduction ( $< 3 \text{ fmol cm}^{-3} \text{ s}^{-1}$ ; calculated from Liu et al. 2015) is much lower than that required from r8 (i.e., 1 to 2 times the additional  $\text{H}_2$  production of  $4R_4 - 2R_1$ ;  $70\text{--}424 \text{ fmol cm}^{-3} \text{ s}^{-1}$ ) to produce sufficient amounts of  $\text{H}_2$  to sustain the additional hydrogenotrophy. The net production rates of dissolved Fe ( $< 10 \text{ fmol cm}^{-3} \text{ s}^{-1}$ ) and  $\text{SO}_4^{2-}$  ( $< 1 \text{ fmol cm}^{-3} \text{ s}^{-1}$ ) and the net consumption rate of  $\Sigma\text{S}(-\text{II})$  ( $< 1 \text{ fmol cm}^{-3} \text{ s}^{-1}$ ) are also consistent with this assertion (Fig. S3).”

**#15 - A cryptic sulfur cycle is only used to argue for  $\text{H}_2$  production. Why not  $\text{CO}_2$  production by sulfate reduction?**

DIC production by sulfate reduction is considered where the value of  $R_{\text{ox\_net}}$  is positive. Admittedly our phrasing was confused. We now clarify as follows:

**L. 279-299 / 153 and thereafter**

“ $R_{\text{net}}^{\text{Ox}}$  is the net reaction rate of all relevant oxidants consumption, i.e.,  $\text{O}_2$ , Fe(III) and  $\text{SO}_4^{2-}$  only because  $\text{NO}_3^-$  and Mn(IV) are negligible (see above). For simplicity,  $R_{\text{net}}^{\text{Ox}}$  is expressed in equivalent moles of  $\text{O}_2$  consumption rate, taking into account that  $\text{SO}_4^{2-}$  and Fe(III) have twice and one quarter the oxidizing capacity of  $\text{O}_2$ , respectively. In practice, the value of  $R_{\text{net}}^{\text{Ox}}$  was calculated by adding those of  $R_{\text{net}}^{\text{O}_2}$ ,  $\frac{1}{4}R_{\text{net}}^{\text{Fe(III)}}$  and  $2R_{\text{net}}^{\text{SO}_4^{2-}}$  where  $R_{\text{net}}^{\text{O}_2}$ ,  $R_{\text{net}}^{\text{Fe(III)}}$  and  $R_{\text{net}}^{\text{SO}_4^{2-}}$  were estimated with PROFILE. In this calculation, we assumed that all dissolved Fe is in the form of Fe(II), and that the rate of Fe(II) consumption through reactions r7 is negligible compared to those associated with reactions r5 and r6. Under these conditions,  $R_{\text{net}}^{\text{Fe(III)}} = -R_{\text{net}}^{\text{Fe}}$ . It should be noted that using  $R_{\text{net}}^{\text{O}_2}$ ,  $-R_{\text{net}}^{\text{Fe}}$  and  $R_{\text{net}}^{\text{SO}_4^{2-}}$  to calculate  $R_{\text{net}}^{\text{Ox}}$ , we indirectly take into account the re-oxidation of reduced S and Fe(II), respectively, to  $\text{SO}_4^{2-}$  and Fe(III) by  $\text{O}_2$ . Indeed, with this procedure, we underestimate the terms  $\frac{1}{4}R_{\text{net}}^{\text{Fe(III)}}$  and  $2R_{\text{net}}^{\text{SO}_4^{2-}}$  because re-oxidation reactions are ignored, but we overestimate by the same amount the term

$R_{\text{net}}^{\text{O}_2}$ . In other words, omission of these re-oxidation reactions affects only the relative consumption rates of individual oxidants and not the value of  $R_{\text{net}}^{\text{Ox}}$ , which is of interest here.”

**#16 - The overall problem with the approach is that a balance based on CO<sub>2</sub> and CH<sub>4</sub> and the OM oxidation state is too poorly constrained. In reality, in addition to a mass balance an independent charge balance should be achieved to constrain the original oxidation state of the OM. The current approach balances the electrons between the mass of methane and total CO<sub>2</sub> accounting for diffusive transport. This could likewise be achieved by adjusting the alkalinity.**

Agreed, an independent charge balance would have been very useful, but our current dataset does not enable to perform it. Note, however, that our mass balance is corroborated with the isotopic mass balance which add some robustness to our approach. In addition, the number of sites where our approach yields consistent results (i.e., a COS value < -1.0), especially for the seasonally anoxic sites where oxidation reactions, DIC production through partial fermentation (r<sub>2</sub>) and bioirrigation do not prevent the accurate estimation of fermentation reaction rates (see also I. **674-718** / 423 – 442), provide a strong support for the robustness of our approach.

**#17 - I think that the authors use the model the wrong way. It is perfectly fine for comparing rates in the different zones, but it is not possible to balance the inventories in the respective zones with this model. A more sophisticated reaction transport model that accounts for the cumulative amount of DIC formed during burial needs to be used to explain the amount and isotope composition of DIC. The model Profile only captures a snapshot of a concentration distribution, i.e., the steady state, and it does not allow for calculating cumulative effects during burial, which is important for a diagenetic model and for this case to account for the buried amount of DIC from oxic respiration. In addition, the steady state assumption is invalid for most natural cases except for very small distance, e.g., at the micrometer scale where diffusion is extremely fast. A time-dependent model that includes mass accumulation rates must be used here.**

We agree that our dataset only provide a snapshot of the complex OM degradation cycling. The concentration profiles presented here are the result of “**the cumulative amount of DIC formed during burial**”, and of changing conditions at the SWI. However, the inverse modelling tools used here with the assumption of steady state, whose validity has been discussed previously several times for the study sites (e.g., Clayer et al., 2016; Couture et al., 2008; Feyte et al., 2012), enables us to obtain the net reaction rates for this snapshot for CH<sub>4</sub>, DIC and Oxidants (relevant here are O<sub>2</sub>, Fe(III), and SO<sub>4</sub>) independently of the background concentrations.

We are confident that the depth distributions of the net reaction rates that we present in Fig. 3g, h, o and p for [CH<sub>4</sub>] and DIC are robust. Indeed, the statistical F-testing implemented in PROFILE allows to objectively select, among all the possible solutions, the one that gives the simplest rate profile while providing a satisfying explanation of the measured solute concentration profile. Also, as can be seen in Fig. S1, using another inverse modeling code, i.e., Rate Estimation from Concentrations (REC, Lettmann et al., 2012), produces consistent results with those obtained with the code PROFILE.

After having seriously considered the suggestion of the reviewer to use a non-steady state model, we decided to keep our inverse modeling approach since we believe it is reliable as described above. To our knowledge, a non-steady state model is not necessarily better suited to interpret the concentration profiles because it requires a high number of adjustable parameters (e.g., the flux of

labile organic carbon, of dissolved oxygen and other oxidants, the rate constants for each reaction of OM degradation) which is not the case for the inverse model.

We do not have the pretention to resolve all aspects of the complex OM degradation cycling, e.g., explaining the magnitude of all the fluxes involved at a given depth. We use the net reaction rates obtained by PROFILE in our isotopic model to constrain the gross rates and estimate process rates in a given sediment zone.

**Reviewer 2:**

**Anonymous Referee #2 Received and published: 15 April 2020**

**The paper addresses an interesting and fundamentally important question: which fraction of sedimentary organic matter is mineralized through methanogenesis. Based on modeling and analyses of data from two lakes, it argues that organic carbon in negative oxidation states is used preferentially and the hydrogenotrophic pathway of methanogenesis dominates. If true, this may have profound implications for modeling the carbon cycle and interpretations of sedimentary signatures of carbon isotopes. Both the dataset and the model go well beyond the level of detail of typical diagenetic studies, which is indeed a requirement for figuring out the important fine details of organic matter mineralization.**

**This important work, however, could be improved in several key areas.**

We are thankful to the reviewer for constructive and rigorous comments. We believe that it helped improve the manuscript.

***Style and clarity:* The clarity of the narrative deteriorates towards the end of the manuscript. In particular, stating clearly and emphasizing throughout the text the main finding of the work would greatly improve readability. Inferences from modeling of the isotopic profiles could also benefit from a clearer presentation. Key statement such as (Line 265) “practically all CH<sub>4</sub> is produced through hydrogenotrophy” are inferred from modeling  $\delta^{13}\text{C}$  profiles, but I admit I was rather lost following the description, particularly trying to separate the relative contributions of hydrogenotrophic vs acetoclastic methanogenesis.**

Thank you for a constructive comment. In consequence, we have (i) clarified the novel aspects (see response to next comment), (ii) better described the modelling and COS estimation approaches, (iii) moved and focused L. 305-317 to section 3.4, (iv) streamlined section 4.3 (L. 406-442) and (v) edited the conclusions (see comments below).

The description of the approach now reads:

“L. **245-247**(148)

Considering the net reaction rates obtained by inverse modelling, a realistic range of values can be given for each of the effective reaction rates  $R_i$  in each depth interval using the general equations described below (Eqs. 3, 4 and 5). The detailed calculations for each  $R_i$  at both study sites are described in section S2.

(...)

L. **291-296**(160)

Once the range of values have been determined for each of the effective rates  $R_i$  (see Table S2), they can be used in another reaction-transport equation to model the  $\delta^{13}\text{C}$  profiles of  $\text{CH}_4$  and DIC. Only sets of  $R_i$  values that yield acceptable modeled  $\delta^{13}\text{C}$  profiles, i.e., which fall within one standard deviation of the measured  $\delta^{13}\text{C}$  profiles (grey area fills in Fig. 4), were kept for COS calculation below (section 2.8). The  $\delta^{13}\text{C}$  modeling procedure is summarized below and described in detail in Section S.2. This procedure takes into account the effect of diffusion, bioirrigation (in Lake Tantaré Basin A) and the isotopic fractionation effect of each reaction  $r_i$ .

(...)

L. **334-342**(176)

## 2.8 COS calculation

Considering the complete fermentation of metabolizable OM of general formula  $\text{C}_x\text{H}_y\text{O}_z$ , and making two assumptions, described below for clarity, the COS of the fermenting molecule is given by (combining Eq. S8 and S15; see Section S2 for details):

$$\text{COS} = -4 \left( \frac{R_{\text{net}}^{\text{CH}_4} - R_{\text{net}}^{\text{DIC}} - R_{\text{net}}^{\text{Ox}} + R_2}{R_{\text{net}}^{\text{CH}_4} + R_{\text{net}}^{\text{DIC}} + (1 - \chi_M)R_{\text{net}}^{\text{Ox}} - R_2} \right) \quad (9)$$

where  $\chi_M$  is the fraction of oxidants consumed by methanotrophy. Equation (9) is only valid if i)  $r_1$  is the only source of substrates for hydrogenotrophy and acetoclasty (this assumption is discussed in Section 4.2 below); and that ii) siderite precipitation ( $r_7$ ) is negligible (Saturation Index for siderite are negative except below 10 cm depth in the sediment of Lake Bédard, this case is considered in Section S2.1.2.2). With values of  $R_{\text{net}}^{\text{CH}_4}$  and  $R_{\text{net}}^{\text{Ox}}$  obtained from PROFILE (section 2.4), values of  $R_2$ ,  $\chi_H$  and  $\chi_M$  constrained by  $\delta^{13}\text{C}$  modeling (section 2.7), Eq. (9) can be used to calculate the COS of the fermenting molecule."

Statement at L. **468-471** (265) has been clarified:

"Modeled  $\delta^{13}\text{C}$  profiles were considered acceptable only when they fell within one standard deviation of the measured  $\delta^{13}\text{C}$  profiles (grey area fills in Fig. 4). Acceptable modeled  $\delta^{13}\text{C}$  profiles were obtained only when methanogenesis was 100% hydrogenotrophic, i.e., when  $R_3 = 0$  (see section S2.2.2.1)."

L. **473-483** (305-317) now in section 3.4 read:

"The sharp upward depletion in  $^{13}\text{C}\text{-CH}_4$  leading to a minimum  $\delta^{13}\text{C}\text{-CH}_4$  value at 2.5 cm depth in Lake Tantaré Basin A sediments (Fig. 3a) was unanticipated since it occurs in the methanotrophic zone, i.e., where the remaining  $\text{CH}_4$  is expected to be  $^{13}\text{C}$ -enriched as a result of  $\text{CH}_4$  oxidation. Marked  $^{13}\text{C}\text{-CH}_4$  depletions at the base of the sulfate-methane transition zone, where  $\text{CH}_4$  is consumed via  $\text{SO}_4^{2-}$  reduction, have often been observed in marine sediments (Burdige et al., 2017 and references therein). Such features are generally attributed to the production of  $\text{CH}_4$  by hydrogenotrophy from the  $^{13}\text{C}$ -depleted DIC resulting from the anaerobic  $\text{CH}_4$  oxidation, a process referred to as intertwined methanotrophy and hydrogenotrophy (e.g., Borowski et al., 1997; Burdige et al., 2017; Pohlman et al., 2008). Here the modelled  $\delta^{13}\text{C}\text{-CH}_4$  profile captured the minimum in  $\delta^{13}\text{C}\text{-CH}_4$  in the  $Z_1$  by simply assuming concomitant hydrogenotrophy and methanotrophy in this zone and an upward-increasing  $\alpha_4$  value from 1.085 in the  $Z_3$  to 1.094 in the  $Z_1$  (section S2.2.1 of the SI). A small variation with sediment depth in the fractionation factor  $\alpha_4$  is arguably possible since its value depends on the types of microorganisms producing  $\text{CH}_4$  (Conrad, 2005)."

L. **674-718** (406-442) now read:

“The COS values determined for the perennially oxygenated Basin A of Lake Tantaré (mean of  $-0.6 \pm 1.1$ ; range of  $-3.2$  to  $2.1$ ; Table 4) are much more variable than for the five other seasonally anoxic lake basins including unrealistic values for October 2015 in the  $Z_1$  ( $-3.2$ ), September 2016 ( $0.4$ – $0.6$ ) and October 2005 ( $1.8$ – $2.1$ ). Indeed, the very negative value of  $-3.2$  does not correspond to any degradable compound under anoxic conditions, whereas the positive values of  $0.4$ – $0.6$  and  $1.8$ – $2.1$  would involve either amino acids and nucleotides which are very labile (Larowe and Van Cappellen 2011) and tend to be degraded in the water column (Burdige 2007), or oxidized compounds, such as ketones, aldehydes and esters, known to be quickly reduced to alcohols. Possible sources of uncertainty in the COS estimation include mis-quantification of bioirrigation and DIC production through HMW OM fermentation (reaction r2; Corbett et al. 2013). Clayer et al. (2016) provided evidences that sediment irrigation by benthic animals is effective in Lake Tantaré Basin A and that reaction rates are sensitive to the bioirrigation coefficient. Nevertheless, additional simulations show that changing the bioirrigation coefficient by a factor of 2 (increased and decreased) did not result in significant changes in COS values ( $<0.2$ ). Bioirrigation might also be mis-represented. Indeed, the term used in Eq. 2 to calculate this contribution, i.e.,  $\phi\alpha_{\text{irrigation}}([\text{solute}]_{\text{tube}} - [\text{solute}])$ , is indeed an approximation of intricate 3-D processes variable in space and time (Meile et al., 2005; Boudreau and Marinelli, 1994; Forster and Graf, 1995; Gallon et al., 2008; Riisgård and Larsen, 2005). On the other hand, DIC production through HMW OM fermentation (reaction r2; Corbett et al. 2013) was constrained by default in Lake Tantaré Basin A (Table 4). Indeed, fitting with Eq. 7 the experimental  $\delta^{13}\text{C}$  data does not allow partitioning the production of DIC between r1 and r2 given that both processes share the same fractionation factor ( $\alpha_1 = \alpha_2 = 1.000$ ). Equation 9 indicates that to obtain negative COS values for Lake Tantaré Basin A in September 2006 and October 2005,  $R_2$  should be  $>11 \text{ fmol cm}^{-2} \text{ s}^{-1}$  and  $>110 \text{ fmol cm}^{-2} \text{ s}^{-1}$ , respectively. These  $R_2$  values correspond to transferring  $>9\%$  and  $>44\%$  of the rate of DIC production from  $R_1$  to  $R_2$  for September 2006 and October 2005, respectively. Hence, owing to the imperfection in the COS estimations for Lake Tantaré Basin A, COS values estimated for this site should be treated with caution. Note that the sediment surface was also oxic at the sites Melide and Figino of Lake Lugano in March 1989 (Table 4) as revealed by detectable bottom water  $[\text{O}_2]$  (Table 4), and by low  $[\text{Fe}]$ , undetectable  $\Sigma\text{S}(-\text{II})$  and  $[\text{CH}_4]$  and relatively high  $[\text{SO}_4^{2-}]$  in overlying water (Lazzaretti et al., 1992; Lazzaretti-Ulmer and Hanselmann, 1999). Despite this, the COS values determined for the two sites of Lake Lugano appear realistic and consistent with those calculated for Lakes Tantaré Basin B, Bédard and Jacks. This disparity between Lake Tantaré Basin A and Lake Lugano could be explained by the presence of benthic organisms in the former (Hare et al., 1994) but their absence in the latter, as shown by the presence of varves (Lazzaretti et al., 1992) and the absence of benthos remains in the recent sediments of Lake Lugano (Niessen et al., 1992).”

***Originality:*** Much of the work is an update on the results of Clayer et al. 2018. The text should clearly distinguish the novel aspects, especially how (or if) the difference in conclusions is more than just refinement of the numbers from that previous work. For example, a statement on lines 58-60 reads: “Based on the observation that methanogenesis produced  $\text{CH}_4$  three times faster than  $\text{CO}_2$  . . . Clayer et al. (2018) concluded that the fermenting OM had a markedly negative COS value of  $-1.9$ ”. This parallels the statement in the Abstract, which presumably should highlight the results from this work: “we calculate, from  $\text{CH}_4$  and DIC production rates. . .COS below  $-0.9$ ”. This seems to convey the same information.

We agree. There is some overlap with the results of Clayer et al., 2018, although new datasets are presented and additional data from published work is re interpreted.

We have modified the abstract, introduction and conclusions (see our response to comments “Conclusions” and “Line 454” for changes in the conclusion) to better highlight the novel aspect of the present study.

L. **14-28** (13-24) now read:

“To test the validity of this assumption, we modeled using reaction-transport equations vertical profiles of the concentration and isotopic composition ( $\delta^{13}\text{C}$ ) of  $\text{CH}_4$  and DIC in the top 25 cm of the sediment column from two lake basins, one whose hypolimnion is perennially oxygenated and one with seasonal anoxia. Furthermore,

we modeled solute porewater profiles reported in the literature for four other seasonally anoxic lake basins. A total of seventeen independent porewater datasets are analysed. CH<sub>4</sub> and DIC production rates associated with methanogenesis at the five seasonally anoxic sites collectively show that the fermenting OM has a mean ( $\pm$ SD) carbon oxidation state (COS) value of  $-1.4 \pm 0.3$ . This value is much lower than the value of zero expected from carbohydrates fermentation. We conclude that carbohydrates do not adequately represent the fermenting OM in hypolimnetic sediments and propose to include the COS in the formulation of OM fermentation in models applied to lake sediments to better quantify sediment CH<sub>4</sub> outflux. This study highlights the potential of mass balancing the products of OM mineralization to characterize labile substrates undergoing fermentation in sediments.”

And L. **139-151**(68-74):

“In this study, the approach described in Clayer et al. (2018), combining concentration and  $\delta^{13}\text{C}$  inverse modeling, is applied to the two newly acquired datasets. These datasets include centimeter-scale vertical porewater profiles of the concentrations and of the stable carbon isotope ratios ( $\delta^{13}\text{C}$ ) of CH<sub>4</sub> and dissolved inorganic carbon (DIC), as well as those of the concentrations of EAs from hypolimnetic sediments of two boreal lake basins showing contrasted O<sub>2</sub> dynamics: one whose hypolimnion remains perennially oxygenated and the other whose hypolimnion becomes anoxic for several months annually. This procedure enables us to constrain the effective rates of OM mineralization reactions and calculate, using a mass balance equation, the COS of the substrates fermenting in the sediments in these two lake basins. In addition, we modelled solute porewater profiles gathered from the scientific literature or from our data repository for four other seasonally anoxic lake basins to estimate, using the mass balance equation, the COS of the substrates fermenting in these sediments. A total of seventeen independent datasets are analysed to provide additional insight into the COS of the fermenting OM in boreal lakes and the associated mineralization pathways.”

**Justifying the inclusion or omission of processes: The coupling with the sulfur cycle seems particularly suspect. The cryptic oxidation of sulfide coupled to iron oxides is used as an important pathway for H<sub>2</sub> production. While this reaction is commonly considered (but can be written in various stoichiometries), it is rarely the only reaction that is considered from the complicated network of reactions that comprise the sedimentary Fe and S cycling. Puzzlingly, the modeled SO<sub>4</sub> and Fe profiles are not shown (line235). These absolutely need to be shown. The sulfur cycle in this system seems highly unusual. For example (Line 201 and Fig. 2), “SO<sub>4</sub><sup>2-</sup> concentrations reach a minimum between SWI and 5 cm depth, and increase below”. These highly unusual features need to be discussed. How can SO<sub>4</sub> be produced in anoxic sediment? Does oxidation of H<sub>2</sub>S by Fe(III) somehow proceed faster than sulfate reduction? What about precipitation of iron sulfides? Similarly, precipitation of CaCO<sub>3</sub> does not seem to be considered as a CO<sub>2</sub> sink, while Line 380 mentions that it had to be considered by the used datasets. Were the saturation indexes negative for the study sites?**

We agree that the description of the reactions was lacking some rigor in section 2.3.

Unraveling the complex Fe and S cycling is, however, out of the scope of this study, we now refer to Couture et al. (2016). Nonetheless, note that these features described at L. 201 are discussed at L. 353-360 which have been modified following the comment of another reviewer as described below. Regarding the precipitation of iron sulfides we now clarify that iron sulfide are currently experiencing dissolution, hence precipitation could be neglected (see below).

As stated L. **236** (144), “the precipitation of carbonates (*can be neglected*) whose saturation index values are negative ( $\text{SI} \leq -1.5$ ) except for siderite (r7) in Lake Bédard ( $\text{SI} = 0.0$  to  $0.7$  below 10 cm depth)”

Finally, we added the modelled Fe and SO<sub>4</sub> profiles into an additional figure in the supplementary information Fig. S3. and refer to it in the text:

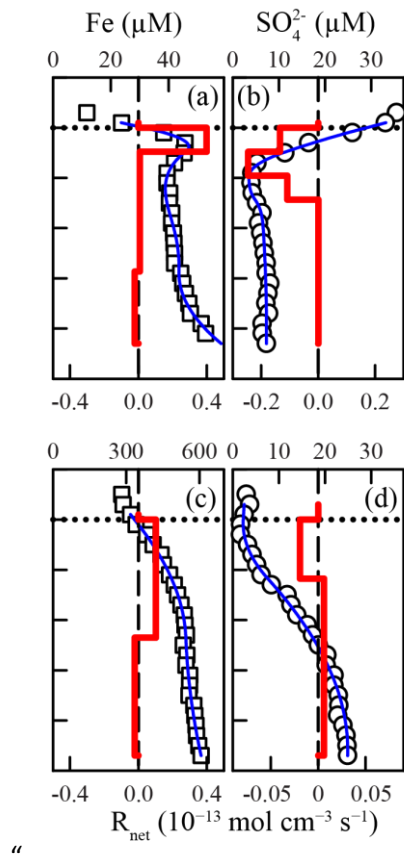


**Figure S3: Comparison of the modeled (blue lines) and average ( $n = 3$ ) measured (symbols) concentration profiles of  $\text{SO}_4$  (a and c) and Fe (b and d) in Lakes Tantaré Basin A (a–b) and Bédard (c–d). The horizontal dotted line indicates the sediment-water interface. The thick red lines represent the net solute reaction rate ( $R_{\text{net}}^{\text{solute}}$ )."**

Regarding reducing Fe and S cycling, it now reads (237-243):

"Lastly, sulfide oxidation by iron oxides (r8), which can be a source of  $\text{SO}_4^{2-}$  and  $\text{H}_2$  (Clayer et al., 2018; Holmkvist et al., 2011), is also considered. Note that iron sulfide enrichments formed during past decades of elevated atmospheric  $\text{SO}_4$  deposition are presently dissolving in Lake Tantaré Basin A (Couture et al., 2016). This process also occurs in the seasonally anoxic Basin B of Lake Tantaré (Couture et al., 2016) and is likely to also occur in Lake Bédard. Hence, other reactions involving reduced S and Fe species, such as pyrite precipitation, are believed to be insignificant for C cycling in the present study and are thus ignored."

L. 602-610 (353-360) now read:

"The progressive downward increases in dissolved Fe and  $\text{SO}_4^{2-}$  (Fig. 2e, f, m and n) below ~5 cm depth and decrease in  $\Sigma\text{S}(-\text{II})$  (Fig. 2n) observed in the porewaters suggest a net production of  $\text{H}_2$  from r8 in both lakes. However, in the  $Z_1$  and  $Z_2$  of Lake Tantaré Basin A, the rate of solid Fe(III) reduction ( $<3 \text{ fmol cm}^{-3} \text{ s}^{-1}$ ; calculated from Liu et al. 2015) is much lower than that required from r8 (i.e., 1 to 2 times the additional  $\text{H}_2$  production of  $4R_4 - 2R_1$ ;  $70\text{--}424 \text{ fmol cm}^{-3} \text{ s}^{-1}$ ) to produce sufficient amounts of  $\text{H}_2$  to sustain the additional hydrogenotrophy. The net production rates of dissolved Fe ( $<10 \text{ fmol cm}^{-3} \text{ s}^{-1}$ ) and  $\text{SO}_4^{2-}$  ( $<1 \text{ fmol cm}^{-3} \text{ s}^{-1}$ ) and the net consumption rate of  $\Sigma\text{S}(-\text{II})$  ( $<1 \text{ fmol cm}^{-3} \text{ s}^{-1}$ ) are also consistent with this assertion (Fig. S3)."



***Discussing implications:* If the organic matter used in methanogenesis had negative COS, what happened to the rest of the C pool? Is oxidized OM not mineralized? Or is it mineralized preferentially earlier, in the water column? What are the implications, e.g. for burial, signature of OM in rock record, etc.? The statement on line 450 seems to address it somewhat, but the statement is not clear.**

The implications of our study are now better described although we believe it does not influence burial or the signature of OM in rock record since only a very small fraction of the C pool is mineralized (see below).

Statement on line **788-790** (450) has been clarified as follows:

“the most labile compounds are mineralized during OM downward migration in the water column and at the sediment surface leaving mainly reduced organic compounds to fuel methanogenesis in the sediments”

L. **546-551** (334) the following sentences were added regarding the rest of the C pool:

“Considering the sediment accumulation rate and sediment  $C_{org}$  content given in section 2.1, we calculate an average accumulation rate of  $C_{org}$  of  $4.7 \times 10^{-11}$  to  $1.0 \times 10^{-10}$  and  $2.9 \times 10^{-11}$  to  $7.6 \times 10^{-10}$  mol C cm<sup>-2</sup> s<sup>-1</sup> for lakes Tantaré Basin A and Bédard, respectively. Hence, the total sediment OM degradation rate ( $\Sigma R_1 + \Sigma R_2 + \Sigma R_6$ ) of  $1.3 \times 10^{-12}$  and  $1.4 \times 10^{-12}$  reported in this study for lakes Tantaré Basin A and Bédard, respectively, would involve only 1.2–2.8% and 0.2–4.8% of the total  $C_{org}$  deposited. Given that the remaining 95.2–99.8% of the deposited  $C_{org}$  is preserved in the sediment, it is not surprising that the sediment  $C_{org}$  concentration is constant with depth (Fig. 2).”

**It would also help to discuss how special or typical these lakes are, given that the implications seem to include global extrapolations. For example, diagenesis in Lake Tantaré (or is it Lake Bédard? – see below) seems to lack contributions from terminal electron acceptors. How different would this be from a “typical” boreal forest lake?**

To be able to better assess how “typical” our case study lakes are, we added some background information on the sediment OM in Section 2.1. In addition, we included a brief discussion to which degree they are representative of boreal forest lakes.

We added a figure (Fig. 2) and some information on the sediment OM in section 2.1 as follows:

L. **164-171**

“The sediment accumulation rates are 4.0–7.3 and 2.4–46.8 mg cm<sup>-2</sup> yr<sup>-1</sup> at the deepest sites of Lake Tantaré Basin A and Lake Bédard, respectively (Couture et al., 2010). The relatively constant organic C ( $C_{org}$ ) content ( $20 \pm 2\%$ ; Fig. 2b), the elevated  $\{C_{org}\}:\{N\}$  molar ratio ( $17 \pm 2$ ; Fig. 2b), the  $\delta^{13}C$  ( $-29\%$ ; Joshani, 2015) and  $\delta^{15}N$  ( $+0.5\%$  to  $-2.5\%$ ; Joshani, 2015) values reported for the sediment OM over the top 30 cm in Lake Tantaré Basin A are typical of terrestrial humic substances (Botrel et al., 2014; Francioso et al., 2005). The  $C_{org}$  content ( $21 \pm 2.7\%$ ; Fig. 2a) and  $\{C_{org}\}:\{N\}$  molar ratio ( $14 \pm 1.9$ ; Fig. 2a) reported over the top 30 cm of Lake Bédard sediments show slightly more variation with depth, but are also typical of terrestrial OM. In addition, the  $\{C_{org}\}:\{S\}$  ratios of both lake basin sediments (50–200) are typical of those reported for soil OM ( $\sim 125$ ; Buffle, 1988).

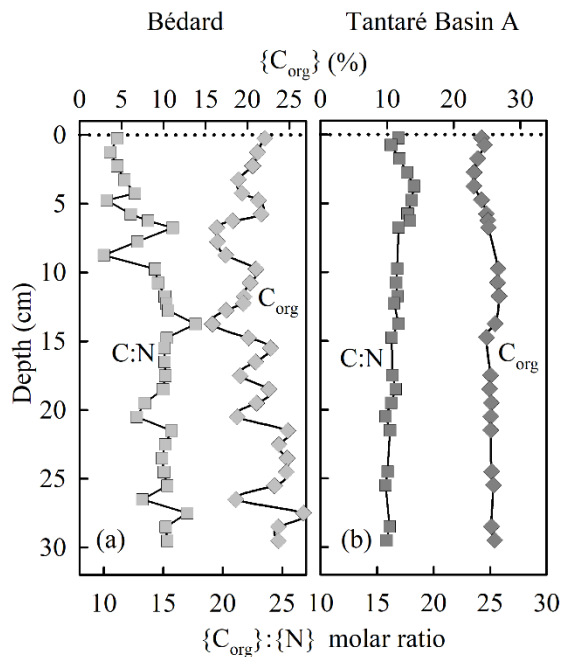


Figure 2: Depth profiles of the organic C concentrations and of the C : N molar ratio in sediment cores collected at the deepest sites of Lake Bédard (a) and Lake Tantaré Basin A (b).”

L. **784-790** (450 – 453) now read:

“The OM in the sediment of the three boreal lakes, as well as their O<sub>2</sub> seasonal dynamics, are typical of boreal forest lakes. While Lake Bédard experiences prolonged episodes of extended hypolimnetic anoxia, Lake Tantaré Basin B and Jacks Lake show more moderate seasonal anoxia, where some years the hypolimnion of Lake Tantaré Basin B is only hypoxic (Clayer et al., 2016; Carignan et al., 1991). Hence, the selective mineralization of OM described by Clayer et al. (2018), involving that the most labile compounds are mineralized during OM downward migration in the water column and at the sediment surface leaving mainly reduced organic compounds to fuel methanogenesis in the sediments, likely applies to a large portion of boreal lakes.”

**Other criticisms and suggestions:**

**Conclusions:** “fermentation and methanogenesis represent . . .100% of OM mineralization . . . in Lake Tantaré” – Methanogenesis can be fermentation. More importantly, why are there no contributions from terminal electron acceptors? Is it really 100%? Confusingly, Fig. 2 shows that sulfate reduction is clearly active in Lake Tantaré, whereas contributions of terminal electron acceptors are likely smaller in Lake Bédard.

We apologize, this is a mistake, it should be the other way around. The correct sentence now reads:

L. **773-775**

“Our results show that fermentation and methanogenesis represent about 50% and 100% of OM mineralization in the top 25 cm of the sediments at the hypolimnetic sites in Lake Tantaré Basin A and Bédard, respectively”

**One of the main results seems to be expressed by Eq. 15. Given the range of COS values (-1.4+-0.3), it might be helpful to state the range in the stoichiometric coefficients explicitly.**

Response to reviewers

Agreed, we have added a sentence L. **801-803** (460)

“Introducing the average COS values reported in this study ( $-1.4 \pm 0.3$ ) into Eq. 14, the coefficients  $a$  and  $b$  would take values of  $2.7 \pm 0.15$  and  $0.65 \pm 0.125$ , respectively, and the  $\text{CH}_4$  and  $\text{CO}_2$  stoichiometric coefficients would be  $0.68 \pm 0.04$  and  $0.32 \pm 0.04$ , respectively.”

**Line 284: “i) when labile OM is depleted, ii) with increasing sediment depth” – aren’t these two statements in practice the same?**

The first statement refers to OM depletion across time, while the other is across space.

**Line 454: “misestimating  $\text{CH}_4$  and  $\text{CO}_4$  production” – not sure what this means. Underestimating the amounts? But early diagenetic models generally work okay and can reproduce measured profiles. Are the differences small enough that they are within uncertainties?**

Early diagenetic models are rarely validated against both  $\text{CH}_4$  and DIC profiles at the same time. Below we also better describe how significant our findings could be for  $\text{CH}_4$  sediment fluxes and oxidant consumption rates.

To better clarify, we modified L. **791-794** (454) as follows:

“Hence, the current representation of the fermenting OM, i.e.,  $\text{CH}_2\text{O}$ , in process-based biogeochemical models entails a significant risk of underestimating sedimentary  $\text{CH}_4$  production and release to the bottom water and, to a certain extent, of its evasion to the atmosphere under transient environmental scenarios.”

Added the following text L. **801-807** (460):

“Introducing the average COS values reported in this study ( $-1.4 \pm 0.3$ ) into Eq. 14, the coefficients  $a$  and  $b$  would take values of  $2.7 \pm 0.15$  and  $0.65 \pm 0.125$ , respectively, and the  $\text{CH}_4$  and  $\text{CO}_2$  stoichiometric coefficients would be  $0.68 \pm 0.04$  and  $0.32 \pm 0.04$ , respectively. Note that the same stoichiometric formulation would be obtained with any possible combination of acetoclasty and hydrogenotrophy. Under these conditions, fermentation ( $r_1$ ) coupled to methanogenesis ( $r_4$ ) yields  $2.2 \pm 0.4$  times more  $\text{CH}_4$  than DIC for the studied lake sediments. Ignoring the implications of the present study regarding the COS of the fermenting OM could lead to the underestimation of  $\text{CH}_4$  sediment outflux or of the rate of oxidant consumption required to mitigate this efflux by a factor of up to 2.6.”

### **Reviewer 3:**

**Anonymous Referee #3 Received and published: 22 April 2020**

**In this paper, Clayer et al. found the average carbon oxidation state (COS) is negative COS values by modelling solute pore-water profiles. They concluded that carbohydrates do not adequately represent the fermenting OM and that the COS should be included in the formulation of OM fermentation in models. It is an interesting work and the results can guide new biogeochemical model for OM degradation. However, the manuscript needs substantial improvement of the presentation before it can be recommended for publication.**

We are thankful to the reviewer for constructive and rigorous comments. We believe that it helped improve the manuscript.

**The main issues is the lack of the OM and mobile labile information. There are no data for the deposition/sedimentation rate of OM, the chemical composition of OM (C,H,O,N,S,P,..), d13C distribution of OM et al. The results of COS from modelling solute pore-water profiles have not been validated. Even in the solute model there are too many fitting parameters and the conclusion is not convincing.**

Agreed, background information on OM was lacking.

As we understand it, the reviewer would also have appreciated to see chemical composition data on single organic compounds that corroborate our COS estimations. However, we do not dispose of such analytical methods nor of any additional samples to perform these analyses. We agree that it could have been an interesting complement. However, we believe that the strength of our demonstration resides is the consistency among the COS estimations reported for the seasonally anoxic basins. See also our response to your comment #5 below.

Regarding the solute model, we now have re-organized the methods description to better describe our approach in a convincing way. While the robustness of the net reaction rates obtained with PROFILE is clearly highlighted L. 226-232. Extracts of the method sections now reads

“L. **245-247**(148)

Considering the net reaction rates obtained by inverse modelling, a realistic range of values can be given for each of the effective reaction rates  $R_i$  in each depth interval using the general equations described below (Eqs. 3, 4 and 5). The detailed calculations for each  $R_i$  at both study sites are described in section S2.

(...)

L. **291-296**(160)

Once the range of values have been determined for each of the effective rates  $R_i$  (see Table S2), they can be used in another reaction-transport equation to model the  $\delta^{13}\text{C}$  profiles of  $\text{CH}_4$  and DIC. Only sets of  $R_i$  values that yield acceptable modeled  $\delta^{13}\text{C}$  profiles, i.e., which fall within one standard deviation of the measured  $\delta^{13}\text{C}$  profiles (grey area fills in Fig. 4), were kept for COS calculation below (section 2.8). The  $\delta^{13}\text{C}$  modeling procedure is summarized below and described in detail in Section S.2. This procedure takes into account the effect of diffusion, bioirrigation (in Lake Tantaré Basin A) and the isotopic fractionation effect of each reaction  $r_i$ .

(...)

L. **334-342**(176)

## 2.8 COS calculation

Considering the complete fermentation of metabolizable OM of general formula  $\text{C}_x\text{H}_y\text{O}_z$ , and making two assumptions, described below for clarity, the COS of the fermenting molecule is given by (combining Eq. S8 and S15; see Section S2 for details):

$$\text{COS} = -4 \left( \frac{R_{\text{net}}^{\text{CH}_4} - R_{\text{net}}^{\text{DIC}} - R_{\text{net}}^{\text{Ox}} + R_2}{R_{\text{net}}^{\text{CH}_4} + R_{\text{net}}^{\text{DIC}} + (1 - \chi_M)R_{\text{net}}^{\text{Ox}} - R_2} \right) \quad (9)$$

where  $\chi_M$  is the fraction of oxidants consumed by methanotrophy. Equation (9) is only valid if i)  $r_1$  is the only source of substrates for hydrogenotrophy and acetoclasty (this assumption is discussed in Section 4.2 below); and that ii) siderite precipitation ( $r_7$ ) is negligible (Saturation Index for siderite are negative except below 10 cm depth in the sediment of Lake Bédard, this case is considered in Section S2.1.2.2). With values of  $R_{\text{net}}^{\text{CH}_4}$  and  $R_{\text{net}}^{\text{Ox}}$  obtained from PROFILE (section 2.4), values of  $R_2$ ,  $\chi_H$  and  $\chi_M$  constrained by  $\delta^{13}\text{C}$  modeling (section 2.7), Eq. (9) can be used to calculate the COS of the fermenting molecule.”

We added a figure (Fig. 2) and some information on the sediment OM as follows:

#### L. 164-171

“The sediment accumulation rates are 4.0–7.3 and 2.4–46.8  $\text{mg cm}^{-2} \text{yr}^{-1}$  at the deepest sites of Lake Tantaré Basin A and Lake Bédard, respectively (Couture et al., 2010). The relatively constant organic C ( $C_{\text{org}}$ ) content ( $20 \pm 2\%$ ; Fig. 2b), the elevated  $\{C_{\text{org}}\}:\{N\}$  molar ratio ( $17 \pm 2$ ; Fig. 2b), the  $\delta^{13}\text{C}$  ( $-29\%$ ; Joshani, 2015) and  $\delta^{15}\text{N}$  ( $+0.5\%$  to  $-2.5\%$ ; Joshani, 2015) values reported for the sediment OM over the top 30 cm in Lake Tantaré Basin A are typical of terrestrial humic substances (Botrel et al., 2014; Francioso et al., 2005). The  $C_{\text{org}}$  content ( $21 \pm 2.7\%$ ; Fig. 2a) and  $\{C_{\text{org}}\}:\{N\}$  molar ratio ( $14 \pm 1.9$ ; Fig. 2a) reported over the top 30 cm of Lake Bédard sediments show slightly more variation with depth, but are also typical of terrestrial OM. In addition, the  $\{C_{\text{org}}\}:\{S\}$  ratios of both lake basin sediments (50–200) are typical of those reported for soil OM ( $\sim 125$ ; Buffle, 1988).

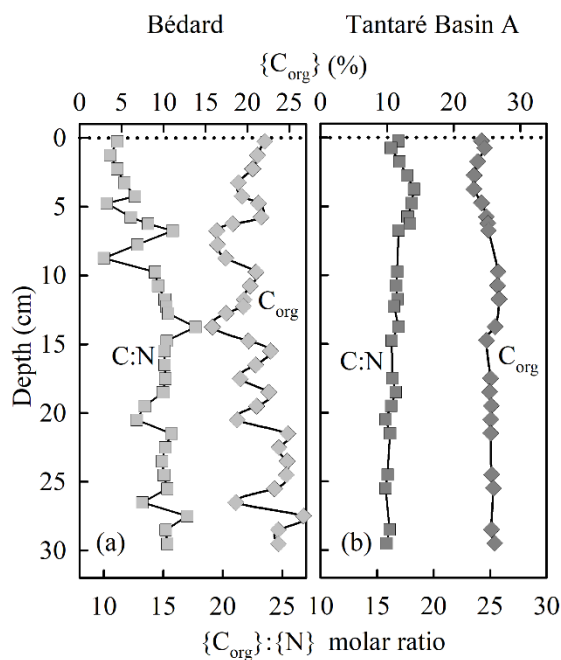


Figure 2: Depth profiles of the organic C concentrations and of the C : N molar ratio in sediment cores collected at the deepest sites of Lake Bédard (a) and Lake Tantaré Basin A (b).”

Here are some details:

**1. Reactions:** Since the reactions the precipitation of siderite ( $r_7$ ) and sulfide oxidation by iron oxides ( $r_8$ ) were taken into account, the pyrite formation by  $\text{Fe}^{2+}$  and  $\text{H}_2\text{S}$  should be considered, too. The hydrogen  $\text{H}_2$  in eq. ( $r_8$ ) is usually consumed easily by sulphate reducer

**bacteria rather than CO<sub>2</sub> reduction. The authors used general oxidant instead of O<sub>2</sub>, Fe(III) and SO<sub>4</sub>, which could have different oxidation rates, especially for CH<sub>4</sub> oxidation (r5).**

We agree that the description of the reactions was lacking some rigor in section 2.3. Regarding reducing Fe and S cycling, it now reads (**237-243**):

“Lastly, sulfide oxidation by iron oxides (r8), which can be a source of SO<sub>4</sub><sup>2-</sup> and H<sub>2</sub> (Clayer et al., 2018; Holmkvist et al., 2011), is also considered. Note that iron sulfide enrichments formed during past decades of elevated atmospheric SO<sub>4</sub> deposition are presently dissolving in Lake Tantaré Basin A (Couture et al., 2016). This process also occurs in the seasonally anoxic Basin B of Lake Tantaré (Couture et al., 2016) and is likely to also occur in Lake Bédard. Hence, other reactions involving reduced S and Fe species, such as pyrite precipitation, are believed to be insignificant for C cycling in the present study and are thus ignored.”

Concerning the consumption of H<sub>2</sub> by sulphate reducer, it possibly occurs in the top 5 cm in Lake Tantaré Basin A, but considering the low SO<sub>4</sub> concentrations, this process is likely negligible. Note that we have added a figure in the supplementary information showing modelled SO<sub>4</sub> profiles and reaction rates. This figure shows net SO<sub>4</sub> production below 5-7 cm depth at a very low rate.

Note that the various oxidation state of the oxidants are taken into account as now stressed

L. **279-299** / 153 and thereafter

“R<sub>net</sub><sup>Ox</sup> is the net reaction rate of all relevant oxidants consumption, i.e., O<sub>2</sub>, Fe(III) and SO<sub>4</sub><sup>2-</sup> only because NO<sub>3</sub><sup>-</sup> and Mn(IV) are negligible (see above). For simplicity, R<sub>net</sub><sup>Ox</sup> is expressed in equivalent moles of O<sub>2</sub> consumption rate, taking into account that SO<sub>4</sub><sup>2-</sup> and Fe(III) have twice and one quarter the oxidizing capacity of O<sub>2</sub>, respectively. In practice, the value of R<sub>net</sub><sup>Ox</sup> was calculated by adding those of R<sub>net</sub><sup>O<sub>2</sub></sup>,  $\frac{1}{4}$ R<sub>net</sub><sup>Fe(III)}</sup> and 2R<sub>net</sub><sup>SO<sub>4</sub><sup>2-</sup></sup> where R<sub>net</sub><sup>O<sub>2</sub></sup>, R<sub>net</sub><sup>Fe(III)}</sup> and R<sub>net</sub><sup>SO<sub>4</sub><sup>2-</sup></sup> were estimated with PROFILE. In this calculation, we assumed that all dissolved Fe is in the form of Fe(II), and that the rate of Fe(II) consumption through reactions r7 is negligible compared to those associated with reactions r5 and r6. Under these conditions, R<sub>net</sub><sup>Fe(III)}</sup> = -R<sub>net</sub><sup>Fe</sup>. It should be noted that using R<sub>net</sub><sup>O<sub>2</sub></sup>, -R<sub>net</sub><sup>Fe</sup> and R<sub>net</sub><sup>SO<sub>4</sub><sup>2-</sup></sup> to calculate R<sub>net</sub><sup>Ox</sup>, we indirectly take into account the re-oxidation of reduced S and Fe(II), respectively, to SO<sub>4</sub><sup>2-</sup> and Fe(III) by O<sub>2</sub>. Indeed, with this procedure, we underestimate the terms  $\frac{1}{4}$ R<sub>net</sub><sup>Fe(III)}</sup> and 2R<sub>net</sub><sup>SO<sub>4</sub><sup>2-</sup></sup> because re-oxidation reactions are ignored, but we overestimate by the same amount the term R<sub>net</sub><sup>O<sub>2</sub></sup>. In other words, omission of these re-oxidation reactions affects only the relative consumption rates of individual oxidants and not the value of R<sub>net</sub><sup>Ox</sup>, which is of interest here.”

New figure:

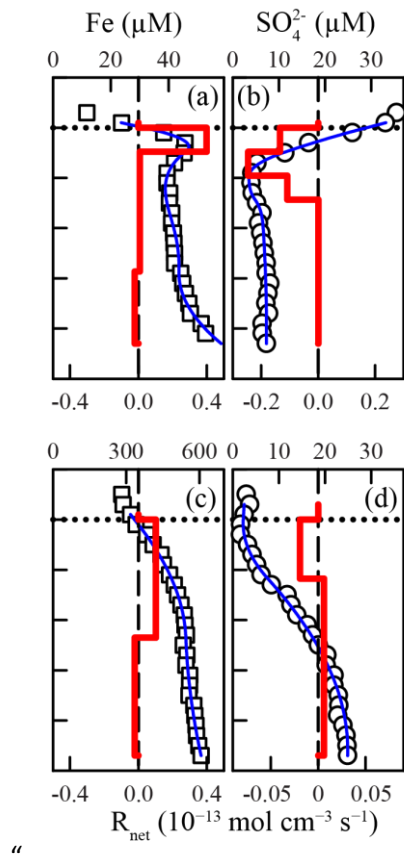


Figure S3: Comparison of the modeled (blue lines) and average ( $n = 3$ ) measured (symbols) concentration profiles of  $\text{SO}_4$  (a and c) and Fe (b and d) in Lakes Tantaré Basin A (a–b) and Bédard (c–d). The horizontal dotted line indicates the sediment-water interface. The thick red lines represent the net solute reaction rate ( $R_{\text{net}}^{\text{solute}}$ )."

**2. Rate calculation:** The reaction rate were calculated by computer code PROFILE. This rates obtained from PROFILE were very rough. It is better to use reactiontransport model to calculate the rate by considering OM deposition and degradation.

We agree with the reviewer that a limitation of inverse modeling methods is that the predicted rate profiles may not be unique. However, we are confident that the depth distributions of the net reaction rates that we present in Fig. 3g, h, o and p for  $[\text{CH}_4]$  and DIC are robust. Indeed, as stated L. 226-232 the statistical F-testing implemented in PROFILE allows to objectively select, among all the possible solutions, the one that gives the simplest rate profile while providing a satisfying explanation of the averaged solute concentration profile. Also, as can be seen in Fig. S1, using another inverse modeling code, i.e., Rate Estimation from Concentrations (REC, Lettmann et al., 2012), produces consistent results with those obtained with the code PROFILE. Moreover, the values of the net rates are of similar magnitude. Note that REC uses the Tikhonov regularization technique. This statistical method implies the adjustment of one discrete parameter (i.e., the smoothing parameter  $\lambda$ ) and, in contrast to PROFILE, does not suggest a given number of zones.

After having seriously considered the suggestion of the reviewer, we decided to keep our inverse modeling approach since we believe it is reliable as described above. To our knowledge, a non-steady state model is not necessarily better suited to interpret the concentration profiles because it

requires a high number of adjustable parameters (e.g., the flux of labile organic carbon and of dissolved oxygen and other oxidants, the rate constants for each reaction of OM degradation) which is not the case for the inverse model. In addition, using a forward model would imply making additional subjective choices regarding the rate expressions and boundary conditions, e.g., parametrizing the O<sub>2</sub> sediment flux.

**3. The bioirrigation term was shown in the equation (2) but the bioirrigation depth and coefficient were not clear. How does the bioirrigation affect COS estimation was also not clear. General once bioirrigation is strong, bioturbation should be considered, too. The solid phase (OM, iron oxides) in the bioturbation zone is well mixed, which strongly affect OM degradation.**

Agreed, there was some information lacking regarding biological processes. Bioturbation has been shown previously to be negligible compared to diffusion or bioirrigation (e.g. Clayer et al., 2016; Couture et al., 2008) This is now fixed as follows (in section 2.3):

L. **212-215** (124)

“The values of  $\alpha_{\text{Irrigation}}$  in Lake Tantaré Basin A were calculated as in Clayer et al. (2016), considering that  $\alpha_{\text{Irrigation}}$  varies linearly from  $\alpha_{0\_Irrigation}$  at the SWI (calculated according to Boudreau 1984 based on an inventory of benthic animals Hare et al., 1994) to 0 at 10 cm depth (the maximum depth at which chironomids are found in lake sediments; Matisoff and Wang 1998), and were assumed to be 0 in Lake Bédard since its bottom water was anoxic (Fig. 1).”

L. 122-123 “considering steady state and negligible solute transport by bioturbation and advection. The validity of these assumptions has been previously demonstrated for the study sites (Couture et al., 2008; Couture et al., 2010; Clayer et al., 2016).”

To describe the sensitivity of COS values to the bioirrigation term we added the following sentence:

L. **696-699** (422)

“Clayer et al. (2016) provided evidences that sediment irrigation by benthic animals is effective in Lake Tantaré Basin A and that reaction rates are sensitive to the bioirrigation coefficient. Nevertheless, additional simulations show that changing the bioirrigation coefficient by a factor of 2 (increased and decreased) did not result in significant changes in COS values (<0.2).”

**4. I don't understand why the acetoclastic methanogenesis was absent here. Generally acetoclastic methanogenesis dominates in lake sediment and hydrogenotrophic methanogenesis in sea sediment. The two pathways generate different d13C-CH<sub>4</sub> and d13-DIC pattern. Diffusion and birrigation will also change this pattern. The authors should prove it.**

Here, we clearly show that methanogenesis is 100% hydrogenotrophic at both study sites using a reactive-transport modeling approach considering diffusion and bioirrigation.

L. **294-296** (242-244):

“The  $\delta^{13}\text{C}$  modeling procedure is summarized below and described in detail in Section S.2. This procedure takes into account the effect of diffusion, bioirrigation (in Lake Tantaré Basin A) and the isotopic fractionation effect of each reaction  $r_i$ .”

As stated L. **496-499** (284-287):



“hydrogenotrophy becomes an increasingly important CH<sub>4</sub> production pathway: i) when labile OM is depleted (Chasar et al., 2000; Hornibrook et al., 2000; Whitticar et al., 1986), ii) with increasing sediment/soil depth (Conrad et al., 2009; Hornibrook et al., 1997), or iii) with decreasing rates of primary production in aquatic environments (Galand et al., 2010; Wand et al., 2006)”

We also replaced l. **468-471** (269-279):

“Modeled  $\delta^{13}\text{C}$  profiles were considered acceptable only when they fell within one standard deviation of the measured  $\delta^{13}\text{C}$  profiles (grey area fills in Fig. 4). Acceptable modeled  $\delta^{13}\text{C}$  profiles were obtained only when methanogenesis was 100% hydrogenotrophic, i.e., when  $R_3 = 0$  (see section S2.2.2.1).”

**5. The chemical composition of individual molecules in OM pools can be detected from various state-of-the-art instrumentation including GC-MS, LC-MS/MS, HPLC-MS, NMR, Orbitrap MS, and Fourier transform ion cyclotron resonance (FTICR-MS). By combining a suite of previously developed thermodynamic theories ( Kleerebezem and Van Loosdrecht, 2010; LaRowe and Van Cappellen, 2011), one can calculate COS. If the results are consistent, the paper method is more convincing.**

Agreed, presenting data from state-of-the-art analytical methods on the composition of organic molecules could have been convincing, if we were able to isolate the compounds of interest. Indeed, the fraction of the organic C that is degraded in the sediment only represents <5% of the total C<sub>org</sub> deposited. It could be challenging to isolate the compounds of interest that we believe are undergoing fermentation. This could well be the subject of a future study.

Nonetheless, fatty acids and alcohols, which are believed to be at the origin of methanogenesis here, are widespread compounds in lake sediments, and are major component of plant organic material (Cranwell, 1981; Matsumoto, 1989).

To better appreciate the point that only a insignificant fraction of C<sub>org</sub> was degraded in the sediment we added the following text in section 4.1:

L. **546-551**

“Considering the sediment accumulation rate and sediment C<sub>org</sub> content given in section 2.1, we calculate an average accumulation rate of C<sub>org</sub> of  $4.7 \times 10^{-11}$  to  $1.0 \times 10^{-10}$  and  $2.9 \times 10^{-11}$  to  $7.6 \times 10^{-10}$  mol C cm<sup>-2</sup> s<sup>-1</sup> for lakes Tantaré Basin A and Bédard, respectively. Hence, the total sediment OM degradation rate ( $\Sigma R_1 + \Sigma R_2 + \Sigma R_6$ ) of  $1.3 \times 10^{-12}$  and  $1.4 \times 10^{-12}$  reported in this study for lakes Tantaré Basin A and Bédard, respectively, would involve only 1.2–2.8% and 0.2–4.8% of the total C<sub>org</sub> deposited. Given that the remaining 95.2–99.8% of the deposited C<sub>org</sub> is preserved in the sediment, it is not surprising that the sediment C<sub>org</sub> concentration is constant with depth (Fig. 2).”

**6. d13C-CH4 in Lake Tantaré Basin A (Fig.3) is very negative (-107.0). Is there some explanation?**

A common explanation given in the literature is the intertwined hydrogenotrophy and methanotrophy. This process is also shown here to produce this local 13C depletion. See L. **473-483** (305-317).

**REFs:**

Botrel, M., Gregory-Eaves, I. & Maranger, R. Defining drivers of nitrogen stable isotopes ( $\delta^{15}\text{N}$ ) of surface sediments in temperate lakes. *Journal of Paleolimnology* 52, 419-433 (2014).

Clayer, F., Gobeil, C. and Tessier, A.: Rates and pathways of sedimentary organic matter mineralization in two basins of a boreal lake: Emphasis on methanogenesis and methanotrophy: Methane cycling in boreal lake sediments, *Limnology and Oceanography*, 61(S1), S131–S149, doi:10.1002/lno.10323, 2016.

Conrad, R. (1999). Contribution of hydrogen to methane production and control of hydrogen concentrations in methanogenic soils and sediments. *FEMS Microbiology Ecology*, 28(3), 193–202. <https://doi.org/10.1111/j.1574-6941.1999.tb00575.x>

Couture, R.-M., Gobeil, C. and Tessier, A.: Chronology of Atmospheric Deposition of Arsenic Inferred from Reconstructed Sedimentary Records, *Environ. Sci. Technol.*, 42(17), 6508–6513, doi:10.1021/es800818j, 2008.

Cranwell P. A. (1981) Diagenesis of free and bound lipids in terrestrial detritus deposited in a lacustrine sediment. *Org. Geochem.* 3, 79–89.

Francioso, O., Montecchio, D., Gioacchini, P., and Ciavatta, C. Thermal analysis (TG–DTA) and isotopic characterization ( $^{13}\text{C}$ – $^{15}\text{N}$ ) of humic acids from different origins (2005) *Applied Geochemistry* 20(3), 537-544

Matsumoto G. I. (1989) Biogeochemical study of organic substances in Antarctic lakes. *Hydrobiologia* 172, 265–289.

# Mineralization of organic matter in boreal lake sediments: Rates, pathways and nature of the fermenting substrates

François Clayer<sup>1,3,\*</sup>, Yves Gélinas<sup>2,3</sup>, André Tessier<sup>1</sup>, Charles Gobeil<sup>1,3</sup>

<sup>1</sup>INRS-ETE, Université du Québec, 490 rue de la Couronne, Québec (QC), Canada G1K 9A9

5 <sup>2</sup>Concordia University, Department of Chemistry and Biochemistry, 7141 Sherbrooke Street West, Montreal (QC), Canada H4B 1R6

<sup>3</sup>Geotop, Interuniversity research and training centre in geosciences, 201 Président-Kennedy Ave., Montréal (QC), Canada H2X 3Y7

\*Present address: Norwegian Institute for Water Research (NIVA), Gaustadalléen 21, 0349 Oslo, Norway

10 *Correspondence to:* François Clayer (francois.clayer@niva.no)

**Abstract.** The complexity of organic matter (OM) degradation mechanisms represents a significant challenge for developing biogeochemical models to quantify the role of aquatic sediments in the climate system. The common representation of OM by carbohydrates formulated as CH<sub>2</sub>O in models comes with the assumption that its degradation by fermentation produces equimolar amounts of methane (CH<sub>4</sub>) and dissolved inorganic carbon (DIC). To test the validity of this assumption, we modeled using reaction-transport equations vertical profiles of the concentration and isotopic composition ( $\delta^{13}\text{C}$ ) of CH<sub>4</sub> and DIC in the top 25 cm of the sediment column from two lake basins, one whose hypolimnion is perennially oxygenated and one with seasonal anoxia. ~~Our results reveal that methanogenesis only occurs via hydrogenotrophy in both basins.~~ Furthermore, we ~~calculate, from modeled solute porewater profiles reported in the literature for four other seasonally anoxic lake basins. A total of seventeen independent porewater datasets are analysed.~~ CH<sub>4</sub> and DIC production rates associated with methanogenesis, ~~at the five seasonally anoxic sites collectively show~~ that the fermenting OM has ~~an average a mean ( $\pm$ SD)~~ carbon oxidation state (COS) ~~below  $-0.9$ . Modeling solute porewater profiles reported in the literature for four other seasonally anoxic lake basins also yields negative COS values. Collectively, the mean ( $\pm$ SD) COS value of  $-1.4 \pm 0.3$  for all the seasonally anoxic sites. This value~~ is much lower than the value of zero expected from carbohydrates fermentation. We conclude that carbohydrates do not adequately represent the fermenting OM ~~in hypolimnetic sediments~~ and ~~that propose to include~~ the COS ~~should be included~~ in the formulation of OM fermentation in models applied to lake sediments- ~~to better quantify sediment CH<sub>4</sub> outflux.~~ This study highlights the ~~need to better potential of mass balancing the products of OM mineralization to characterize the labile OM substrates undergoing mineralization to interpret present day greenhouse gases cycling and predict its alteration under environmental changes~~ fermentation in sediments.

## 1 Introduction

30 Significant proportions of atmospheric methane (CH<sub>4</sub>) and carbon dioxide (CO<sub>2</sub>), two powerful greenhouse gases, are thought to originate from freshwater lake sediments (Bastviken et al., 2004; Turner et al., 2015; Wuebbles and Hayhoe, 2002), but

large uncertainties remain concerning their contribution to the global CO<sub>2</sub> and CH<sub>4</sub> budgets (Saunois et al., 2016). The role of these waterbodies in the global carbon (C) budget has been acknowledged for more than a decade (Cole et al., 2007). Especially in the lake-rich boreal region, lakes are hotspots of CO<sub>2</sub> and CH<sub>4</sub> release (Hastie et al., 2018; Wallin et al., 2018) and intensive sites of terrestrial C processing (Holgerson and Raymond, 2016; Staehr et al., 2012). Using high-resolution satellite imagery, Verpoorter et al. (2014) estimated to about 27 million the number of lakes larger than 0.01 km<sup>2</sup> on Earth and reported that the highest lake concentration and surface area are found in boreal regions. Boreal lakes, which are typically small and shallow, are known to store large amounts of organic C, to warm up quickly, and to develop anoxic hypolimnia in the warm season (Sabrekov et al., 2017; Schindler et al., 1996). Owing to the great abundance of boreal lakes, their sensitivity to climate change and foreseen important role in the global C cycle, there is a need to further develop process-based models to better quantify C processing reactions in these lakes and their alteration under warming (Saunois et al., 2016).

In aquatic environments, CH<sub>4</sub> is mainly produced (methanogenesis) in the sediment along with CO<sub>2</sub> at depths where most electron acceptors (EAs) are depleted (Conrad, 1999; Corbett et al., 2013). During its upward migration to the atmosphere, CH<sub>4</sub> is partly aerobically or anaerobically oxidized to CO<sub>2</sub> (methanotrophy) in the upper strata of the sediments and in the water column (Bastviken et al., 2008; Beal et al., 2009; Egger et al., 2015; Ettwig et al., 2010; Raghoebarsing et al., 2006). The oxidation of organic matter (OM) by EAs such as O<sub>2</sub>, NO<sub>3</sub><sup>-</sup>, Fe(III), Mn(IV), SO<sub>4</sub><sup>2-</sup> and humic substances, as well as the partial fermentation of high molecular weight organic matter (HMW OM) into lower molecular weight organic matter (LMW OM) are also potential sources of CO<sub>2</sub> in the sedimentary environment (Corbett et al., 2015). Predicting fluxes of CH<sub>4</sub> and CO<sub>2</sub> from the aquatic sediments and water column to the atmosphere is challenging considering the various transport processes and chemical and microbially-mediated reactions implicated and the complexity of natural OM which serves as substrate (Natchimuthu et al., 2017).

Process-based geochemical models taking into account both the numerous biogeochemical reactions involving C and transport processes are powerful tools able to interpret present-day sediment, porewater and water-column profiles of C species and offer a great potential to forecast changes in cycling of this element under variable environmental scenarios (Arndt et al., 2013; Paraska et al., 2014; Saunois et al., 2016; Wang and Van Cappellen, 1996). Nonetheless, the performance of these models depends on the correct formulation of the complete OM mineralization reactions, e.g., OM decomposition to DIC, phosphate, ammonium and CH<sub>4</sub> through oxidation and fermentation reactions (Burdige 1991), particularly in terms of the metabolizable organic compounds involved. Up to now, carbohydrates, represented as the simple chemical formula CH<sub>2</sub>O (or C<sub>6</sub>H<sub>12</sub>O<sub>6</sub>), whose average carbon oxidation state (COS) is zero, are commonly assumed to be representative of the bulk of metabolizable OM, including the substrates involved in fermentation reactions (e.g., Arndt et al., 2013; Arning et al., 2016; Paraska et al., 2014 and references therein). The capacity of CH<sub>2</sub>O to represent adequately the ensemble of labile organic compounds is, nevertheless, becoming increasingly questioned in the literature given the variety and complexity of organic molecules present in the environment (Alperin et al., 1994; Burdige and Komada, 2011; Clayer et al., 2016; Jørgensen and Parkes, 2010). Based on the observation that methanogenesis produced CH<sub>4</sub> three times faster than CO<sub>2</sub> in the sediments of a boreal, sporadically anoxic lake basin, Clayer et al. (2018) concluded that the fermenting OM had a markedly negative COS value of -1.9. This

COS value corresponds more closely to a mixture of fatty acids and fatty alcohols than to carbohydrates (e.g., CH<sub>2</sub>O), which would have yielded equivalent CH<sub>4</sub> and CO<sub>2</sub> production rates. The low COS value of metabolizable OM in the sediment layer where methanogenesis occurred in this lake has been attributed to the nearly complete consumption of the most labile organic components (e.g., carbohydrates, proteins) during its downward transport through the water column and the upper sediment layers, thus leaving only material of lower lability such as fatty acids and fatty alcohols available for methanogenesis. Such interpretation, however, must be validated by investigating other lakes before revising the formulation of the fermenting OM used in diagenetic models in order to improve model predictions of C cycling, including greenhouse gases production and emission from these environments.

~~In this study.~~ In this study, the approach described in Clayer et al. (2018), combining concentration and  $\delta^{13}\text{C}$  inverse modeling, is applied to the two newly acquired datasets. These datasets include centimeter-scale vertical porewater profiles of the concentrations and of the stable carbon isotope ratios ( $\delta^{13}\text{C}$ ) of CH<sub>4</sub> and dissolved inorganic carbon (DIC), as well as those of the concentrations of EAs ~~were obtained in the~~ from hypolimnetic sediments of two ~~additional~~ boreal lake basins showing contrasted O<sub>2</sub> dynamics: one whose hypolimnion remains perennially oxygenated and the other whose hypolimnion becomes anoxic for several months annually. ~~Reaction-transport equations are used~~ This procedure enables us to quantify/constrain the effective rates of ~~each~~ OM mineralization pathway/reactions and ~~estimate/calculate, using a mass balance equation,~~ the COS of the substrates fermenting in the sediments. ~~Additional insight into the COS of the fermenting OM in lakes is also provided by applying in these equations to similar~~ two lake basins. In addition, we modelled solute porewater solute concentration profiles gathered from the scientific literature or from our data repository for four other seasonally anoxic lake basins to estimate, using the mass balance equation, the COS of the substrates fermenting in these sediments. A total of seventeen independent datasets are analysed to provide additional insight into the COS of the fermenting OM in boreal lakes and the associated mineralization pathways.

## 2 Materials and Methods

### 2.1 ~~Sites and sample collection~~ Study sites

This study was carried out in two small, dimictic, oligotrophic and headwater lakes located within 50 km from Québec City, Eastern Canada and having fully forested and uninhabited watersheds (Fig. 1). Lake Tantaré (47°04'N, 71°32'W) is part of the Tantaré Ecological Reserve and has four basins connected by shallow channels and a total surface area of 1.1 km<sup>2</sup>. Lake Bédard (47°16'N, 71°07'W), lying in the protected Montmorency Forest, comprises only one small (0.05 km<sup>2</sup>) basin. The samples for this study were collected at the deepest sites of Lake Bédard (10 m) and of the westernmost basin of Lake Tantaré (15 m), thereafter referred to as Basin A of Lake Tantaré to remain consistent with our previous studies (e.g., Clayer et al., 2016; Couture et al., 2008). These two sampling sites were selected based on their contrasting O<sub>2</sub> regimes (Fig. 1): Lake Bédard develops an anoxic hypolimnion early in the summer (D'arcy, 1993), whereas the hypolimnion of Lake Tantaré Basin A is

perennially oxygenated (Couture et al., 2008). The O<sub>2</sub> diffusion depth in the sediments of Lake Tantaré Basin A, as measured with a microelectrode, does not exceed 4 mm (Couture et al., 2016).

The sediment accumulation rates are 4.0–7.3 and 2.4–46.8 mg cm<sup>-2</sup> yr<sup>-1</sup> at the deepest sites of Lake Tantaré Basin A and Lake Bédard, respectively (Couture et al., 2010). The relatively constant organic C (C<sub>org</sub>) content (20 ± 2%; Fig. 2b), the elevated {C<sub>org</sub>}: {N} molar ratio (17 ± 2; Fig. 2b), the δ<sup>13</sup>C (-29‰; Joshani, 2015) and δ<sup>15</sup>N (+0.5‰ to -2.5‰; Joshani, 2015) values reported for the sediment OM over the top 30 cm in Lake Tantaré Basin A are typical of terrestrial humic substances (Botrel et al., 2014; Francioso et al., 2005). The C<sub>org</sub> content (21 ± 2.7%; Fig. 2a) and {C<sub>org</sub>}: {N} molar ratio (14 ± 1.9; Fig. 2a) reported over the top 30 cm of Lake Bédard sediments show slightly more variation with depth, but are also typical of terrestrial OM. In addition, the {C<sub>org</sub>}: {S} ratios of both lake basin sediments (50–200) are typical of those reported for soil OM (~125; Buffle, 1988).

## 2.2 Sample collection

Sediment porewater samples were acquired by *in situ* dialysis in October 2015 with peepers (Carignan et al., 1985; Hesslein, 1976) deployed by divers within a 25-m<sup>2</sup> area at the deepest site of each lake basin. Bottom water O<sub>2</sub> concentrations were ~2.5 and < 0.1 mg L<sup>-1</sup> in Lake Tantaré Basin A and in Lake Bédard, respectively. The acrylic peepers comprised two columns of 4-mL cells, filled with ultrapure water, and covered by a 0.2-µm Gelman HT-200 polysulfone membrane, which allowed porewater sampling from about 23–25 cm below the sediment-water interface (SWI) to 5 cm above this interface (thereafter referred to as overlying water) at a 1-cm depth resolution. Oxygen was removed from the peepers prior to their deployment, as described by Laforte et al. (2005). Four peepers were left in the sediments of each lake basin for at least 15 d, i.e., a longer time period than that required for solute concentrations in the peeper cells to reach equilibrium with those in the porewater (5–10 d; Carignan et al., 1985; Hesslein, 1976). At least three independent porewater profiles of pH, of the concentrations of CH<sub>4</sub>, DIC, acetate, NO<sub>3</sub><sup>-</sup>, SO<sub>4</sub><sup>2-</sup>, Fe and Mn, and of the δ<sup>13</sup>C of CH<sub>4</sub> and DIC were generated for the two sampling sites. In Lake Bédard, samples were also collected to determine three porewater profiles of sulfide concentrations (ΣS(-II)). After peeper retrieval, samples (0.9–1.9 mL) for CH<sub>4</sub> and DIC concentrations and δ<sup>13</sup>C measurements were collected within 5 minutes from the peeper cells with He-purged polypropylene syringes. They were injected through rubber septa into He-purged 3.85-mL exetainers (Labco Limited), after removal of a volume equivalent to that of the collected porewater. The exetainers were preacidified with 40–80 µL of HCl 1N to reach a final pH ≤ 2. The protocols used to collect and preserve water samples for the other solutes are given by Laforte et al. (2005).

## 2.2.3 Analyses

Concentrations and carbon isotopic composition of CH<sub>4</sub> and DIC were measured as described by Clayer et al. (2018). Briefly, the concentrations were analyzed within 24 h of peeper retrieval by gas chromatography with a precision better than 4 % and detection limits (DL) of 2 µM and 10 µM for CH<sub>4</sub> and DIC, respectively. The <sup>13</sup>C/<sup>12</sup>C abundance ratios of CH<sub>4</sub> and CO<sub>2</sub> were

determined by Mass Spectrometry with a precision of  $\pm 0.2 \text{ ‰}$  when 25  $\mu\text{mol}$  of an equimolar mixture of  $\text{CH}_4$  and  $\text{CO}_2$  was injected, and results are reported as:

$$\delta^{13}\text{C} = 1000 \left( \frac{\left( \frac{^{13}\text{C}_{\text{solute}}}{^{12}\text{C}_{\text{solute}}} \right)_{\text{sample}}}{\left( \frac{^{13}\text{C}}{^{12}\text{C}} \right)_{\text{standard}}} - 1 \right) \quad (1)$$

195 where the subscript solute stands for  $\text{CH}_4$  or DIC and the reference standard is Vienna Pee Dee Belemnite (VPDB). Acetate concentration was determined by ion chromatography (DL of 1.4  $\mu\text{M}$ ) and those of Fe, Mn,  $\text{NO}_3^-$ ,  $\text{SO}_4^{2-}$  and  $\Sigma\text{S}(-\text{II})$ , as given by Laforte et al. (2005).

### 2.34 Modeling of porewater solutes and the reaction network

200 The computer program WHAM 6 (Tipping, 2002) was used, as described by Clayer et al. (2016), to calculate the speciation of porewater cations and anions. The solute activities thus obtained, together with solubility products ( $K_s$ ), were used to calculate saturation index values ( $\text{SI} = \log \text{IAP}/K_s$ , where IAP is the ion activity product).

The following one-dimensional mass-conservation equation (Boudreau, 1997):

$$\frac{\partial}{\partial x} \left( \varphi D_s \frac{\partial [\text{solute}]}{\partial x} \right) + \varphi \alpha_{\text{Irrigation}} ([\text{solute}]_{\text{tube}} - [\text{solute}]) + R_{\text{net}}^{\text{solute}} = 0 \quad (2)$$

205 was used to model the porewater profiles of  $\text{CH}_4$ , DIC,  $\text{O}_2$ , Fe and  $\text{SO}_4^{2-}$ , assuming considering steady state and negligible solute transport by bioturbation and advection. The validity of these assumptions has been previously demonstrated for the study sites (Couture et al., 2008; Couture et al., 2010; Clayer et al., 2016). In this equation,  $[\text{solute}]$  and  $[\text{solute}]_{\text{tube}}$  denote a solute concentration in the porewater and in the animal tubes (assumed to be identical to that in the overlying water), respectively,  $x$  is depth (positive downward),  $\varphi$  is porosity,  $D_s$  is the solute effective diffusion coefficient in sediments,  $\alpha_{\text{Irrigation}}$  is the bioirrigation coefficient, and  $R_{\text{net}}^{\text{solute}}$  (in  $\text{mol cm}^{-3}$  of wet sediment  $\text{s}^{-1}$ ) is the solute net production rate (or consumption rate if  $R_{\text{net}}^{\text{solute}}$  is negative).  $D_s$  was assumed to be  $\varphi^2 D_w$  (Ullman and Aller, 1982), where  $D_w$  is the solute tracer diffusion coefficient in water. The values of  $D_w$ , corrected for in situ temperature (Clayer et al., 2018), were  $9.5 \times 10^{-6} \text{ cm}^2 \text{ s}^{-1}$ ,  $6.01 \times 10^{-6} \text{ cm}^2 \text{ s}^{-1}$  and  $1.12 \times 10^{-5}$ ,  $5.81 \times 10^{-6}$ ,  $3.19 \times 10^{-6}$ ,  $1.17 \times 10^{-5}$   $\text{cm}^2 \text{ s}^{-1}$  for  $\text{CH}_4$ ,  $\text{HCO}_3^-$  and  $\text{CO}_2$ ,  $\text{SO}_4^{2-}$ , Fe and  $\text{O}_2$ , respectively. The values of  $\alpha_{\text{Irrigation}}$  in Lake Tantaré Basin A were calculated as in Clayer et al. (2016), considering that  $\alpha_{\text{Irrigation}}$  varies linearly from  $\alpha_{0, \text{Irrigation}}$  at the SWI (calculated according to Boudreau, 1984 based on an inventory of benthic animals (Hare et al., 1994); to 0 at 10 cm depth (the maximum depth at which chironomids are found in lake sediments; Matisoff and Wang, 1998), and were assumed to be 0 in Lake Bédard since its bottom water was anoxic (Fig. 1).

215 The  $R_{\text{net}}^{\text{solute}}$  values were determined from the average ( $n = 3$  or 4) solute concentration profiles by numerically solving Eq. (2) with the computer code PROFILE (Berg et al., 1998). The boundary conditions were the solute concentrations at the top and at the base of the porewater profiles. In situ porewater  $\text{O}_2$  profiles were not measured in Lake Tantaré Basin A. For modeling this solute with PROFILE, we assumed that the  $[\text{O}_2]$  in the overlying water was identical to that measured in the lake bottom

220 water and equal to 0 below 0.5 cm (based on O<sub>2</sub> penetration depth; Couture et al., 2016). This procedure provides a rough estimate of R<sub>net</sub><sup>O<sub>2</sub></sup> at the same vertical resolution as for the other solutes. The code PROFILE yields a discontinuous profile of discrete R<sub>net</sub><sup>solute</sup> values over depth intervals (zones) which are objectively selected by using the least square criterion and statistical F-testing (Berg et al., 1998). ~~The fluxes of solute transport across the SWI due to diffusion and bioirrigation are also estimated by PROFILE.~~ In order to estimate the variability in R<sub>net</sub><sup>solute</sup> related to heterogeneity within the 25-m<sup>2</sup> sampling area, 225 additional R<sub>net</sub><sup>solute</sup> values were obtained by modeling the average profiles whose values were increased or decreased by one standard deviation. This variability generally ranges between 2 and 10 fmol cm<sup>-3</sup> s<sup>-1</sup>.

## 2.5 Reaction network

The main reactions retained in this study to describe carbon cycling in the sediments of the two lake basins are shown in Table 1. ~~R<sub>i</sub> and α<sub>i</sub> denote, respectively, the effective (or gross) reaction rate and the carbon isotopic fractionation factor associated with each reaction r<sub>i</sub> (Table 1).~~ Once oxidants are depleted, fermentation of metabolizable OM ~~(+)~~of general formula C<sub>x</sub>H<sub>y</sub>O<sub>z</sub> can yield acetate, CO<sub>2</sub> and H<sub>2</sub> ~~(r1)~~. ~~The coefficient v<sub>1</sub> in r1 constrains the relative contribution of acetoclasty and hydrogenotrophy.~~ The partial degradation of high molecular weight OM (HMW OM) into lower molecular weight OM (LMW OM) can also produce CO<sub>2</sub> (r2, Corbett et al., 2013; Corbett et al., 2015). Acetoclasty (r3) and hydrogenotrophy (r4) yield CH<sub>4</sub>. Moreover, CH<sub>4</sub> (r5) and OM (r6) can be oxidized to CO<sub>2</sub> when electron acceptors such as O<sub>2</sub>, Fe(III) and SO<sub>4</sub><sup>2-</sup> are present. Note that the electron acceptors (EAs) NO<sub>3</sub><sup>-</sup> and Mn oxyhydroxides ~~can~~~~were shown to be neglected~~~~negligible~~ in these two lake basins (Clayer et al., 2016; Feyte et al., 2012) as well as the precipitation of ~~metal~~ carbonates whose saturation index values are negative (SI ≤ -1.5) except for siderite (r7) in Lake Bédard (SI = 0.0 to 0.7 below 10 cm depth). Lastly, sulfide oxidation by iron oxides (r8), which can be a source of SO<sub>4</sub><sup>2-</sup> and H<sub>2</sub> (Clayer et al., 2018; Holmkvist et al., 2011), is also considered. Note that iron sulfide enrichments formed during past decades of elevated atmospheric SO<sub>4</sub> deposition are presently dissolving in Lake Tantaré Basin A (Couture et al., 2016). This process also occurs in the seasonally anoxic Basin B of Lake Tantaré (Couture et al., 2016) and is likely to also occur in Lake Bédard. Hence, other reactions involving reduced S and Fe species, such as pyrite precipitation, are believed to be insignificant for C cycling in the present study and are thus ignored.

## 2.6 Determining realistic ranges for effective reaction rates

245 Considering the net reaction rates obtained by inverse modelling, a realistic range of values can be given for each of the effective reaction rates R<sub>i</sub> in each depth interval using the general equations described below. The detailed calculations for each R<sub>i</sub> at both study sites are described in section S2.

From Table 1, the net rate of CH<sub>4</sub> production, R<sub>net</sub><sup>CH<sub>4</sub></sup>, in the sediments is:

$$R_{\text{net}}^{\text{CH}_4} = R_3 + R_4 - R_5 \quad (3)$$



where  $R_3$  and  $R_4$  are the rates of acetoclastic ( $r_3$ ) and hydrogenotrophic ( $r_4$ ) production of  $\text{CH}_4$ , respectively, and  $R_5$  is the rate of DIC production due to  $\text{CH}_4$  oxidation ( $r_5$ ). The net rate of DIC production,  $R_{\text{net}}^{\text{DIC}}$ , can be expressed as:

$$R_{\text{net}}^{\text{DIC}} = R_1 + R_2 + R_3 - R_4 + R_5 + R_6 - R_7 \quad (4)$$

where  $R_1$ ,  $R_2$  and  $R_6$  are the rates of DIC production due to complete fermentation of labile OM ( $r_1$ ), partial fermentation of HMW OM ( $r_2$ ) and OM oxidation ( $r_6$ ), respectively, and  $R_7$  is the rate of DIC removal by siderite precipitation ( $r_7$ ). It can also be written that:

$$R_{\text{net}}^{\text{Ox}} = -2R_5 - R_6 \quad (5)$$

where  $R_{\text{net}}^{\text{Ox}}$  is the net reaction rate of all ~~the relevant~~ oxidants (~~consumption, i.e.,  $\text{O}_2$ , Fe(III) and  $\text{SO}_4^{2-}$~~ ) ~~consumption only~~ because  $\text{NO}_3^-$  and Mn(IV) are negligible (see above). For simplicity,  $R_{\text{net}}^{\text{Ox}}$  is expressed in equivalent moles of  $\text{O}_2$  consumption rate, taking into account that  $\text{SO}_4^{2-}$  and Fe(III) have twice and one quarter the oxidizing capacity of  $\text{O}_2$ , respectively. In practice, the value of  $R_{\text{net}}^{\text{Ox}}$  was calculated by adding those of  $R_{\text{net}}^{\text{O}_2}$ ,  $\frac{1}{4}R_{\text{net}}^{\text{Fe(III)}}$  and  $2R_{\text{net}}^{\text{SO}_4^{2-}}$  where  $R_{\text{net}}^{\text{O}_2}$ ,  $R_{\text{net}}^{\text{Fe(III)}}$  and  $R_{\text{net}}^{\text{SO}_4^{2-}}$  were estimated with PROFILE. In this calculation, we assumed that all dissolved Fe is in the form of Fe(II), and that the rate of Fe(II) consumption through reactions  $r_7$  is negligible compared to those associated with reactions  $r_5$  and  $r_6$ . Under these conditions,  $R_{\text{net}}^{\text{Fe(III)}} = -R_{\text{net}}^{\text{Fe}}$ . ~~It should be noted that using  $R_{\text{net}}^{\text{O}_2}$ ,  $-R_{\text{net}}^{\text{Fe}}$  and  $R_{\text{net}}^{\text{SO}_4^{2-}}$  to calculate  $R_{\text{net}}^{\text{Ox}}$ , we indirectly take into account the re-oxidation of reduced S and Fe(II), respectively, to  $\text{SO}_4^{2-}$  and Fe(III) by  $\text{O}_2$ . Indeed, with this procedure, we underestimate the terms  $\frac{1}{4}R_{\text{net}}^{\text{Fe(III)}}$  and  $2R_{\text{net}}^{\text{SO}_4^{2-}}$  because re-oxidation reactions are ignored, but we overestimate by the same amount the term  $R_{\text{net}}^{\text{O}_2}$ . In other words, omission of these re-oxidation reactions affects only the relative consumption rates of individual oxidants and not the value of  $R_{\text{net}}^{\text{Ox}}$ , which is of interest here.~~

## 2.4 Modeling7 Constraining effective reaction rates with $\delta^{13}\text{C}$ modeling

Once the range of values have been determined for each of the effective rates  $R_i$  (see Table S2), they can be used in another reaction-transport equation to model the  $\delta^{13}\text{C}$  profiles of  $\text{CH}_4$  and DIC. Only sets of  $R_i$  values that yield acceptable modeled  $\delta^{13}\text{C}$  profiles, i.e., which fall within one standard deviation of the measured  $\delta^{13}\text{C}$  profiles (grey area fills in Fig. 4), were kept for COS calculation below (section 2.8). The  $\delta^{13}\text{C}$  modeling procedure is summarized below and described in detail in Section S.2. This procedure takes into account the effect of diffusion, bioirrigation (in Lake Tantaré Basin A) and the isotopic fractionation effect of each reaction  $r_i$ .

~~The~~ Briefly, the  $\delta^{13}\text{C}$  profiles of  $\text{CH}_4$  ( $\delta^{13}\text{C}\text{-CH}_4$ ) and DIC ( $\delta^{13}\text{C}\text{-DIC}$ ) were simulated with a modified version of Eq. 1 (Clayer et al., 2018):

$$\delta^{13}\text{C} = 1000 \left( \frac{\left( \frac{[^{13}\text{C}]}{[\text{C}]} \right)_{\text{sample}}}{\left( \frac{^{13}\text{C}}{^{12}\text{C}} \right)_{\text{standard}}} - 1 \right) \quad (6)$$

320 where [C] is the total CH<sub>4</sub> or DIC concentration ([<sup>12</sup>C] can be replaced by [C] since ~99% of C is <sup>12</sup>C), and [<sup>13</sup>C] is the isotopically heavy CH<sub>4</sub> or DIC concentration. Equation 6 allows calculating a δ<sup>13</sup>C profile once the depth distributions of [<sup>13</sup>C] and [C] are known. This information is obtained by solving the mass-conservation equations of C and <sup>13</sup>C for CH<sub>4</sub> and DIC. The one-dimensional mass-conservation of [C] is given by Eq. 2 where [solute] is replaced by [C], whereas that for [<sup>13</sup>C] is the following modified version of Eq. 2 (Clayer et al., 2018):

$$\frac{\partial}{\partial x} \left( \varphi \frac{D_s}{f} \frac{\partial [^{13}\text{C}]}{\partial x} \right) + \varphi \alpha_{\text{Irrigation}} ([^{13}\text{C}]_{\text{tube}} - [^{13}\text{C}]) + \sum_{i=1}^5 \frac{R_i}{\alpha_i} \left( \frac{\delta^{13}\text{C}_i^{\text{reactant}}}{1000} + 1 \right) \left( \frac{^{13}\text{C}}{^{12}\text{C}} \right)_{\text{standard}} = 0 \quad (7)$$

325 where f, the molecular diffusivity ratio, is the diffusion coefficient of the regular solute divided by that of the isotopically heavy solute, α<sub>i</sub> is the isotope fractionation factor in reaction r<sub>i</sub>, and δ<sup>13</sup>C<sub>i</sub><sup>reactant</sup> is the δ<sup>13</sup>C of the reactant leading to the formation of the solute (CH<sub>4</sub> or DIC) in reaction r<sub>i</sub>. Input and boundary conditions used to numerically solve Eqs 2 and 7 for [C] and [<sup>13</sup>C], respectively, via the bvp5c function of MATLAB<sup>®</sup> are described in section 3.4 and in section S2 of the Supporting Information (SI).

330 The goodness of fit of the model was assessed with the norm of residuals (N<sub>res</sub>):

$$N_{\text{res}} = \sqrt{\sum_{x=0.5}^{22.5} (\delta^{13}\text{C}_m - \delta^{13}\text{C}_s)^2} \quad (8)$$

where δ<sup>13</sup>C<sub>m</sub> and δ<sup>13</sup>C<sub>s</sub> are the measured and simulated δ<sup>13</sup>C values, respectively. The norm of residuals (N<sub>res</sub>) varies between 0 and infinity with smaller numbers indicating better fits.

## 2.8 COS calculation

335 Considering the complete fermentation of metabolizable OM of general formula C<sub>x</sub>H<sub>y</sub>O<sub>z</sub>, and making two assumptions, described below for clarity, the COS of the fermenting molecule is given by (combining Eq. S8 and S15; see Section S2 for details):

$$\text{COS} = -4 \left( \frac{R_{\text{net}}^{\text{CH}_4} - R_{\text{net}}^{\text{DIC}} - R_{\text{net}}^{\text{Ox}} + R_2}{R_{\text{net}}^{\text{CH}_4} + R_{\text{net}}^{\text{DIC}} + (1 - \chi_M) R_{\text{net}}^{\text{Ox}} - R_2} \right) \quad (9)$$

340 where χ<sub>M</sub> is the fraction of oxidants consumed by methanotrophy. Equation 9 is only valid if i) r1 is the only source of substrates for hydrogenotrophy and acetoclasty (this assumption is discussed in Section 4.2 below); and that ii) siderite precipitation (r7) is negligible (Saturation Index for siderite are negative except below 10 cm depth in the sediment of Lake Bédard, this case is considered in Section S2.1.2.2). With values of R<sub>net</sub><sup>CH<sub>4</sub></sup> and R<sub>net</sub><sup>Ox</sup> obtained from PROFILE (section 2.4),

values of  $R_2$  and  $\chi_M$  constrained by  $\delta^{13}C$  modeling (section 2.7), Eq. 9 can be used to calculate the COS of the fermenting molecule.

## **2.9 Data treatment of other data sets**

To better assess the COS of the fermenting OM in lakes, relevant sets of porewater concentration profiles ( $CH_4$ , DIC, EAs, Ca) available from the literature or from our data repository have been modeled with the code PROFILE, as described in section 2.3, to extract their  $R_{net}^{CH_4}$ ,  $R_{net}^{DIC}$  and  $R_{net}^{Ox}$  profiles. These porewater datasets, described in section S3 of the SI, had been generated by sampling porewater in the hypolimnetic sediments of: i) Lake Bédard and Basin A of Lake Tantaré, at other dates than for this study (Clayer et al, 2016); ii) Basin B of Lake Tantaré (adjacent to Basin A; Fig 1), on four occasions (Clayer et al., 2016; 2018); iii) Williams Bay of Jacks Lake (44°41' N, 78°02' W), located in Ontario, Canada, on the edge of the Canadian Shield (Carignan and Lean, 1991); iv) the southern basin of the alpine Lake Lugano (46°00'N, 3°30'E) located in Switzerland, on two occasions (Lazzaretti-Ulmer and Hanselmann, 1999). All lake basins, except Basin A of Lake Tantaré develop an anoxic hypolimnion.

## **3 Results**

### **3.1 Solute concentration profiles**

Differences among the replicate profiles of  $CH_4$ , DIC,  $SO_4^{2-}$ ,  $\Sigma S(-II)$  and Fe (Fig. 23) at the two sampling sites are generally small (except perhaps those of  $SO_4^{2-}$  in Lake Bédard) and should be mainly ascribed to spatial variability within the 25-m<sup>2</sup> sampling area. Indeed, the main vertical variations in the profiles are defined by several data points without the sharp discontinuities expected from sampling and handling artifacts. Note that the acetate concentrations, which were consistently low ( $< 2 \mu M$ ), are not shown.

The low Fe ( $< 5 \mu M$ ; Fig. 23f) and  $CH_4$  ( $< 2 \mu M$ ; Fig. 23a) concentrations as well as the relatively high  $SO_4^{2-}$  concentrations ( $36 \pm 2.1 \mu M$ ; Fig. 32e) in the sediment overlying water of Lake Tantaré Basin A are all consistent with the  $[O_2]$  ( $\sim 2.5 \text{ mg L}^{-1}$ ) measured in the bottom water and are indicative of oxic conditions at the sediment surface. The sharp Fe gradients near the SWI indicate an intense recycling of Fe oxyhydroxides (Fig. 2f3f; Clayer et al., 2016) and the concave-down curvatures in the  $SO_4^{2-}$  profiles (Fig. 2e3e) reveal  $SO_4^{2-}$  reduction near the SWI. In contrast to Lake Tantaré Basin A, high Fe ( $> 200 \mu M$ ), measurable  $CH_4$  ( $> 200 \mu M$ ) low  $SO_4^{2-}$  ( $2.7 \pm 1.4 \mu M$ ) and detectable  $\Sigma S(-II)$  concentrations in the overlying waters of Lake Bédard (Fig. 2i3i, m and n) are consistent with anoxic conditions at the sediment surface. The absence of a sharp Fe gradient at the SWI in Lake Bédard suggests that Fe oxyhydroxides were not recycled in these sediments when porewater sampling occurred.

In the two lake basins,  $SO_4^{2-}$  concentrations reach a minimum between the SWI and 5 cm depth (Fig. 2e-3e and m), and increase below these depths. Alongside, all Fe profiles show a slight increase downward (Fig. 2f-3f and n) indicating that solid Fe(III)

is reduced to produce dissolved Fe. In Lake Bédard, the  $\Sigma\text{S}(-\text{II})$  concentrations decrease from the SWI to ~10 cm depth and remain relatively constant below that depth at  $0.08 \pm 0.06 \mu\text{M}$  for two of the profiles and at  $0.71 \pm 0.18 \mu\text{M}$  for the other one (grey filled triangles in Fig. 2a3n).

375 The concentrations of  $\text{CH}_4$  ( $< 1.5 \text{ mM}$ ; Fig. 23a and i) are well below saturation at  $4^\circ\text{C}$  and *in situ* pressure (4.4–5.5 mM; Duan and Mao, 2006), implying that  $\text{CH}_4$  ebullition is a negligible  $\text{CH}_4$  transport process. The  $\text{CH}_4$  values increases from  $< 2 \mu\text{M}$  in the overlying water to 0.18–0.20 mM at the base of the Lake Tantaré Basin A profiles (Fig. 2a3a), and from 0.2–0.5 mM to 1.0–1.4 mM in those of Lake Bédard (Fig. 2i3i). The three  $\text{CH}_4$  profiles from Lake Tantaré Basin A (Fig. 2a3a) show a modest concave-up curvature in their upper part, close to the SWI, indicative of a net  $\text{CH}_4$  consumption, and a convex-up curvature in their lower part, typical of a net  $\text{CH}_4$  production. Such trends, however, are not observed in Lake Bédard sediments. The  $\text{CH}_4$  profiles from this lake exhibit a convex-up curvature over the whole sediment column, although more pronounced in its upper part (Fig. 2i3i).

380 The DIC concentrations consistently increase from 0.27–0.32 mM and 1.2–1.5 mM in the sediment overlying water to 0.76–0.83 mM and 3.5–4.3 mM at the bottom of the profiles in Lake Tantaré Basin A and Lake Bédard, respectively (Fig. 2e3c and k). All DIC profiles show a similar shape with a slight concave-up curvature in their lower segment and a convex-up curvature in their upper portions.

### 3.2 Modeled $\text{CH}_4$ and DIC concentration profiles

The modeled  $[\text{CH}_4]$  and DIC profiles accurately fit the average ( $n = 3$  or  $4$ ) data points ( $r^2 > 0.996$  and  $r^2 > 0.998$  for  $\text{CH}_4$  and DIC, respectively; Fig. 2e3g,h,o and p). The  $R_{\text{net}}^{\text{CH}_4}$  profiles reveal three zones in each lake basin numbered  $Z_1$ ,  $Z_2$  and  $Z_3$  from the sediment surface whose boundaries match those defined by the  $R_{\text{net}}^{\text{DIC}}$  profiles. For Lake Tantaré Basin A,  $Z_1$  corresponds to a net  $\text{CH}_4$  consumption and  $Z_2$  and  $Z_3$  to net  $\text{CH}_4$  production, with the highest rate in  $Z_2$  (Fig. 32g). In contrast, the three zones in Lake Bédard show net  $\text{CH}_4$  production with the highest rate in  $Z_1$  and the lowest in  $Z_3$  (Fig. 32o). The  $R_{\text{net}}^{\text{DIC}}$  profiles in both lake basins show a zone of net DIC consumption below two zones of net DIC production with the highest rate values in the  $Z_1$  and  $Z_2$  for Lake Tantaré Basin A and Lake Bédard, respectively.

395 The  $R_{\text{net}}^{\text{CH}_4}$  and  $R_{\text{net}}^{\text{DIC}}$  profiles displayed in Figure 2-3 are, among all the possible solutions, the ones that give the simplest rate profile while providing a satisfying explanation of the averaged solute concentration profile as determined by statistical F-testing implemented in the code PROFILE (P value  $\leq 0.001$  except for the  $R_{\text{net}}^{\text{DIC}}$  profile in Lake Bédard whose P value is  $\leq 0.005$ ). As an additional check of the robustness of the depth distribution of  $R_{\text{net}}^{\text{CH}_4}$  and  $R_{\text{net}}^{\text{DIC}}$  provided by PROFILE, we used another inverse model, i.e., Rate Estimation from Concentrations (REC; Lettmann et al., 2012) to model the average  $\text{CH}_4$  and DIC profiles. Note that the statistical method, implemented in REC to objectively select the depth distribution of the net reaction rates, i.e., the Tikhonov regularization technique, differs from that of PROFILE. Figure S1 (SI) shows that the two codes predicted mutually consistent  $R_{\text{net}}^{\text{CH}_4}$  and  $R_{\text{net}}^{\text{DIC}}$  profiles, with rate values of similar magnitude. PROFILE was also used ~~in~~ **this study** to estimate  $R_{\text{net}}^{\text{SO}_4^{2-}}$ ,  $R_{\text{net}}^{\text{Fe}}$  and  $R_{\text{net}}^{\text{O}_2}$  in order to calculate the value of  $R_{\text{net}}^{\text{Ox}}$  in each zone at both sampling sites (see

section 2.3 for details). The modeled  $[\text{SO}_4^{2-}]$  and  $[\text{Fe}]$  profiles ~~are not shown but, again, they~~ accurately fit the data points ( $r^2 > 0.983$ ; Fig. S3). As expected from the contrasting  $\text{O}_2$  regimes of the two lake basins,  $R_{\text{net}}^{\text{Ox}}$  values for Lake Tantaré Basin A were one to two orders of magnitude higher than those for Lake Bédard. ~~Note that  $R_{\text{net}}^{\text{O}_2}$  was by far the highest contributor to the value of  $R_{\text{net}}^{\text{Ox}}$  in Lake Tantaré Basin A with values of  $-290$  and  $-72 \text{ fmol cm}^{-3} \text{ s}^{-1}$  in the  $Z_1$  and  $Z_2$ , respectively.~~ The values of  $R_{\text{net}}^{\text{CH}_4}$ ,  $R_{\text{net}}^{\text{DIC}}$  and  $R_{\text{net}}^{\text{Ox}}$  estimated in each zone of each lake basins are reported in Table 2.

### 3.3 ~~The Measured~~ $\delta^{13}\text{C}$ profiles

The  $\delta^{13}\text{C}$ -DIC values increase from  $-28.2 \pm 0.4 \text{ ‰}$  and  $-17.2 \pm 0.7 \text{ ‰}$  in the overlying water to  $-5.1 \pm 1.0 \text{ ‰}$  and  $3.6 \pm 1.7 \text{ ‰}$  at the base of the profiles in Lake Tantaré Basin A and Lake Bédard, respectively (Fig. ~~2d-3d~~ and l). Similarly, the  $\delta^{13}\text{C}$ - $\text{CH}_4$  values in Lake Bédard increase steadily from  $-82.5 \pm 3.3 \text{ ‰}$  in the overlying water to  $-74.0 \pm 1.5 \text{ ‰}$  at 24.5 cm depth (Fig. ~~2j-3j~~). Regarding Lake Tantaré Basin A, the  $\text{CH}_4$  concentrations above 1.5 cm depth were too low for their  $^{13}\text{C}/^{12}\text{C}$  ratio to be determined. Starting at 1.5 cm depth, the  $\delta^{13}\text{C}$ - $\text{CH}_4$  values first decrease from  $-91.1 \pm 11.1 \text{ ‰}$  to  $-107.0 \pm 6.8 \text{ ‰}$  at 2.5 cm depth and then increase progressively to  $-83.5 \pm 1.6 \text{ ‰}$  at the base of the profiles (Fig. ~~2b-3b~~). Note that a shift toward more positive  $\delta^{13}\text{C}$ - $\text{CH}_4$  values upward, generally attributed to the oxidation of  $\text{CH}_4$  (Chanton et al., 1997; Norđi et al., 2013), is only observed in the profiles of Lake Tantaré Basin A (Fig. ~~2b-3b~~).

As shown in Fig. S2 (SI), the isotopic signatures of nearly all samples from the two lake basins fall within the ranges reported for hydrogenotrophic methanogenesis, i.e.,  $\text{CO}_2$  reduction, in a  $\delta^{13}\text{C}$ - $\text{CO}_2$  vs  $\delta^{13}\text{C}$ - $\text{CH}_4$  graph similar to that proposed by Whiticar (1999). Indeed, the values of  $\delta^{13}\text{C}$ - $\text{CH}_4$  which are lower than  $-70 \text{ ‰}$  over the whole profiles in the two lake basins, and the large difference (67 to 92 ‰) between the  $\delta^{13}\text{C}$  of gaseous  $\text{CO}_2$  ( $\delta^{13}\text{C}$ - $\text{CO}_2$ ) and  $\delta^{13}\text{C}$ - $\text{CH}_4$ , strongly contrast with the typical  $\delta^{13}\text{C}$ - $\text{CH}_4$  values ( $-68$  to  $-50 \text{ ‰}$ ) and with the difference between  $\delta^{13}\text{C}$ - $\text{CO}_2$  and  $\delta^{13}\text{C}$ - $\text{CH}_4$  (39 to 58 ‰) reported for acetoclasty (Whiticar, 1999). The  $\delta^{13}\text{C}$  results reported previously for another basin of Lake Tantaré (Basin B; Clayer et al., 2018) show also in the hydrogenotrophy domain in Fig. S2.

### 3.4 Modeled $\delta^{13}\text{C}$ profiles

In order to model the  $\delta^{13}\text{C}$  profiles with Eq. 6, accurate profiles of  $[\text{C}]$  and  $[\text{C}]^{13}$  need first to be determined by numerically solving Eqs. 2 and 7, respectively. The modeled profiles of  $[\text{CH}_4]$  and DIC obtained with Eq. 2 replicated ~~well perfectly~~ the measured profiles of these two solutes ~~when the depth distributions of  $R_{\text{net}}^{\text{CH}_4}$  or  $R_{\text{net}}^{\text{DIC}}$  provided by PROFILE (Table 2) and those of  $D_s$ ,  $\alpha_{\text{irrigation}}$  and  $\phi$  were used as inputs in Eq. 2, and when measured  $\text{CH}_4$  or DIC concentrations at the top and bottom of the profiles were imposed as boundary conditions.~~ Getting a truthful profile of  $[\text{C}]^{13}$  with Eq. 7 requires, ~~however,~~ accurate values of  $\delta^{13}\text{C}_i^{\text{reactant}}$ ,  $\alpha_i$ , and  $R_i$  for each of the reactions given in Table 1, and of  $f$  for both  $\text{CH}_4$  ( $f\text{-CH}_4$ ) and DIC ( $f\text{-DIC}$ ). The multi-step procedure ~~followed~~ to obtain the best  $[\text{C}]^{13}$  profiles for  $\text{CH}_4$  and DIC is described in section S2 (SI). ~~This modeling exercise revealed that  $R_3 = 0$  for all) and allowed us to constrain the zones in the sediments of both lake basins, thus confirming that practically all  $\text{CH}_4$  is produced through hydrogenotrophy, as inferred above from the  $\delta^{13}\text{C}_f$ ,  $\chi_M$ ,  $\alpha_i$  and  $R_i$  values.~~

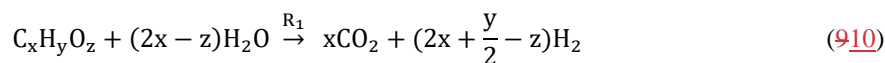
The best fits between the simulated and measured  $\delta^{13}\text{C}$  profiles of  $\text{CH}_4$  and DIC for Lake Tantaré Basin A and Lake Bédard (red lines in Fig. 34) were obtained with the  $f$ ,  $\alpha_i$  and  $R_i$  values displayed in Table 3. The optimal  $\alpha_i$  and  $f$  values were within the ranges reported in the literature for both lake basins, and similar to those reported in our previous study on Lake Tantaré Basin B (Clayer et al., 2018), except for the lower-than-expected value of  $\alpha_2$  (0.984) in the  $Z_2$  of Lake Bédard. Note that  $\alpha_3$  is not given in Table 3 since the modeling of the Modeled  $\delta^{13}\text{C}$  profiles of  $\text{CH}_4$  and DIC indicates that  $R_3 = 0$  were considered acceptable only when they fell within one standard deviation of the measured  $\delta^{13}\text{C}$  profiles (grey area fills in Fig. 4). Acceptable modeled  $\delta^{13}\text{C}$  profiles were obtained only when methanogenesis was 100% hydrogenotrophic, i.e., when  $R_3 = 0$  (see section S2.2.2.1 in the SI). Optimal values for  $\alpha_4$ ,  $\alpha_5$  and  $f$   $\text{CH}_4$  for both lake basins were also similar to those reported in our previous study on Lake Tantaré Basin B (Clayer et al., 2018).

The sharp upward depletion in  $^{13}\text{C}\text{-CH}_4$  leading to a minimum  $\delta^{13}\text{C}\text{-CH}_4$  value at 2.5 cm depth in Lake Tantaré Basin A sediments (Fig. 4a) was unanticipated since it occurs in the methanotrophic zone, i.e., where the remaining  $\text{CH}_4$  is expected to be  $^{13}\text{C}$ -enriched as a result of  $\text{CH}_4$  oxidation. Marked  $^{13}\text{C}\text{-CH}_4$  depletions at the base of the sulfate-methane transition zone, where  $\text{CH}_4$  is consumed via  $\text{SO}_4^{2-}$  reduction, have often been observed in marine sediments (Burdige et al., 2017 and references therein). Such features are generally attributed to the production of  $\text{CH}_4$  by hydrogenotrophy from the  $^{13}\text{C}$ -depleted DIC resulting from the anaerobic  $\text{CH}_4$  oxidation, a process referred to as intertwined methanotrophy and hydrogenotrophy (e.g., Borowski et al., 1997; Burdige et al., 2017; Pohlman et al., 2008). Here the modelled  $\delta^{13}\text{C}\text{-CH}_4$  profile captured the minimum in  $\delta^{13}\text{C}\text{-CH}_4$  in the  $Z_1$  by simply assuming concomitant hydrogenotrophy and methanotrophy in this zone and an upward-increasing  $\alpha_4$  value from 1.085 in the  $Z_3$  to 1.094 in the  $Z_1$  (section S2.2.1 of the SI). A small variation with sediment depth in the fractionation factor  $\alpha_4$  is arguably possible since its value depends on the types of microorganisms producing  $\text{CH}_4$  (Conrad, 2005).

## 4 Discussion

### 4.1 Organic matter mineralization pathways at the sampling sites

The porewater data as well as the combined modeling of carbon isotopes and concentration profiles, allows to highlight key OM mineralization mechanisms and to quantify the relative contribution of methanogenesis and fermentation to OM degradation at both sampling sites. The  $^{13}\text{C}$  isotopic signatures, i.e., highly negative values of  $\delta^{13}\text{C}\text{-CH}_4$  and large differences between  $\delta^{13}\text{C}\text{-CO}_2$  and  $\delta^{13}\text{C}\text{-CH}_4$  (section 3.3 and Fig. S2 in the SI), as well as the modeling of the  $\delta^{13}\text{C}\text{-CO}_2$  and  $\delta^{13}\text{C}\text{-CH}_4$  profiles (section S2.2.2.1 and Fig S4a and b in the SI) all point to hydrogenotrophy as being the only pathway for methanogenesis in the two lake basins. The dominance of hydrogenotrophy is consistent also with the finding that acetate concentrations were close to or below DL in the porewater samples. Under the condition that ~~acetocalsty~~ acetoclasty is negligible (i.e.,  $x = \nu_1$ ), reaction r1 from Table 1 becomes:



495 Methanogenesis was also reported to be essentially hydrogenotrophic in the sediments of Basin B of Lake Tantaré (Clayer et al 2018). The absence of acetoclasty in the sediments of the oligotrophic lakes Bédard and Tantaré is consistent with the consensus that hydrogenotrophy becomes an increasingly important CH<sub>4</sub> production pathway: i) when labile OM is depleted (Chasar et al., 2000; Hornibrook et al., 2000; Whiticar et al., 1986), ii) with increasing sediment/soil depth (Conrad et al., 2009; Hornibrook et al., 1997), or iii) with decreasing rates of primary production in aquatic environments (Galand et al., 2010; Wand et al., 2006).

500 The modelling of concentrations and  $\delta^{13}\text{C}$  profiles revealed that oxidative processes occurred essentially in the upper 7 cm of the sediments of the perennially oxygenated Lake Tantaré Basin A, i.e., mainly in the Z<sub>1</sub> and, to a lesser extent, in the Z<sub>2</sub> (Table 3 and sections S2.1.2.1 and S2.1.2.2 of the SI). Moreover, it showed that methanotrophy was the dominant oxidative reaction in these sediment layers since 75% of the oxidants were consumed through r5 (section S2.2.2.2 of the SI). This outcome is consistent with several studies showing that methanotrophy occurs at higher rates than OM oxidation at low EA concentrations (Kankaala et al., 2013; Pohlman et al., 2013; Sivan et al., 2007; Thottathil et al., 2019). Methanotrophy is also evidenced in 505 the Z<sub>1</sub> of this lake basin by the negative R<sub>net</sub><sup>CH<sub>4</sub></sup> value and by a shift of the  $\delta^{13}\text{C}$ -CH<sub>4</sub> profiles to more positive values in their upper part (Fig. 2b-3b and g). Use of Eq. 2 to model the EAs profiles with the code PROFILE predicts that O<sub>2</sub> was by far the main EA involved either directly, or indirectly via the coupling with the Fe or S cycles, in the oxidative processes. Indeed, comparing the values of R<sub>net</sub><sup>O<sub>2</sub></sup> and R<sub>net</sub><sup>Ox</sup> (see Section 3.2 and Table 2) shows that O<sub>2</sub> accounts for 87% and 70% of the oxidants 510 consumed in the Z<sub>1</sub> and Z<sub>2</sub> of Lake Tantaré Basin A, respectively. Since O<sub>2</sub> penetration in the sediment by molecular diffusion is limited to ~4-mm, a significant amount of O<sub>2</sub> is predicted by Eq. 2 to be transported deeper in the sediment through bioirrigation. The predominance of O<sub>2</sub> among the EAs consumed in the sediments is consistent with our previous study in this basin of Lake Tantaré (Clayer et al., 2016). Given that methanotrophy is the dominant oxidative process and that O<sub>2</sub> is the main oxidant consumed, it is probable that aerobic oxidation of methane prevails over its anaerobic counterpart in this lake 515 basin. This is in line with the common thinking that CH<sub>4</sub> oxidation in freshwater lake sediments is carried out by methanotrophs essentially in the uppermost oxic sediment layer (Bastviken et al., 2008 and references therein).

~~The sharp upward depletion in <sup>13</sup>C-CH<sub>4</sub> leading to a minimum  $\delta^{13}\text{C}$ -CH<sub>4</sub> value at 2.5 cm depth in Lake Tantaré Basin A sediments (Fig. 3a) was unanticipated since, according to the modeling with the code PROFILE, it occurs in the methanotrophic zone, i.e., where the remaining CH<sub>4</sub> is expected to be <sup>13</sup>C enriched as a result of CH<sub>4</sub> oxidation. Marked <sup>13</sup>C-CH<sub>4</sub> depletions at 520 the base of the sulfate-methane transition zone, where CH<sub>4</sub> is consumed via SO<sub>4</sub><sup>2-</sup> reduction, have often been observed in marine sediments (Burdige et al., 2017 and references therein). Such features are generally attributed to the production of CH<sub>4</sub> by hydrogenotrophy from the <sup>13</sup>C depleted DIC resulting from the anaerobic CH<sub>4</sub> oxidation, a process referred to as intertwined methanotrophy and hydrogenotrophy (e.g., Borowski et al., 1997; Burdige et al., 2017; Pohlman et al., 2008). Here the modelled  $\delta^{13}\text{C}$ -CH<sub>4</sub> profile captured the minimum in  $\delta^{13}\text{C}$ -CH<sub>4</sub> in the Z<sub>1</sub> by simply assuming concomitant hydrogenotrophy and methanotrophy in this zone and an upward increasing  $\alpha_4$  value from 1.085 in the Z<sub>2</sub> to 1.094 in the Z<sub>1</sub> (section S2.2.1 of the SI). These  $\alpha_4$  values remain within the range reported for this isotope fractionation factor (Table S1 in the SI). A small 525 variation with sediment depth in the fractionation factor  $\alpha_4$  is arguably possible since its value depends on the types of~~

~~microorganisms producing CH<sub>4</sub> (Conrad, 2005). The possibility that a depth variation in this isotope fractionation factor could explain some of the minima in δ<sup>13</sup>C-CH<sub>4</sub> reported in other studies should be considered.~~

- 530 In the Z<sub>2</sub> of Lake Bédard, the net rate of DIC production (i.e., 167 fmol cm<sup>-3</sup> s<sup>-1</sup>) was more than 3 times that of CH<sub>4</sub> production (50 fmol cm<sup>-3</sup> s<sup>-1</sup>; Table 2). Given that the R<sub>net</sub><sup>OX</sup> was negligible in this zone (i.e., R<sub>5</sub> = R<sub>6</sub> = 0), we obtain from Eqs 3 and 4 and Table 2 that R<sub>net</sub><sup>CH<sub>4</sub></sup> = R<sub>4</sub> = 50 fmol cm<sup>-3</sup> s<sup>-1</sup> and R<sub>net</sub><sup>DIC</sup> = R<sub>1</sub> + R<sub>2</sub> - R<sub>4</sub> = 167 fmol cm<sup>-3</sup> s<sup>-1</sup> (see section S2.1.2.2 of the SI). Should we assume that DIC production by r2 is negligible, i.e., R<sub>2</sub> = 0, a R<sub>1</sub>/R<sub>4</sub> ratio of 4.3 would be obtained. This high ratio indicates that DIC was not produced by ~~hydrogenotrophy (r4) coupled to~~ fermentation (r1) alone in the Z<sub>2</sub> of this lake.
- 535 Indeed, methanogenesis through the coupling of ~~these two reactions r1 and r4~~ yields a R<sub>1</sub>/R<sub>4</sub> ratio of 2 if the fermenting substrate is carbohydrates (COS of 0) and lower than 2 if the fermenting substrate has a negative COS value. We thus attributed the production of the additional DIC to the partial fermentation of HMW OM, an assumed non-fractionating process reported to occur in wetlands (Corbett et al., 2015). The better fitting of the δ<sup>13</sup>C-DIC profile when α<sub>2</sub> is set to 0.980–0.984 rather than to 1.000 in the Z<sub>2</sub> (compare the blue and red lines in Fig. 4b) suggests that C fractionates during this partial fermentation process.
- 540 Table 3 displays the depth-integrated reaction rates (ΣR<sub>i</sub>) over the top 21cm of the sediment column which are given by:

$$\Sigma R_i = \sum_{j=1}^3 \Delta x_j R_i \quad (4011)$$

- where Δx<sub>j</sub> (cm) is the thickness of the zone Z<sub>j</sub>. In this calculation, we assume that other zones of CH<sub>4</sub> or DIC production are absent below 21 cm. Values of ΣR<sub>i</sub> clearly show that anaerobic carbon mineralization reactions (fermentation and methanogenesis) are important contributors to the overall OM mineralization in the two studied lake basins. Indeed, the sum of the rates of CH<sub>4</sub> production (ΣR<sub>4</sub>), DIC production due to ~~fermentation associated with~~ CH<sub>4</sub> formation (ΣR<sub>1</sub> - ΣR<sub>4</sub>) and
- 545 HMW OM partial fermentation (ΣR<sub>2</sub>) represents ~~49.54%~~ and 100% of the total OM degradation rate (ΣR<sub>1</sub> + ΣR<sub>2</sub> + ~~ΣR<sub>5</sub> + ΣR<sub>6</sub>~~) in the sediment of lakes Tantaré Basin A and Bédard, respectively. ~~Considering the sediment accumulation rate and sediment C<sub>org</sub> content given in section 2.1, we calculate an average accumulation rate of C<sub>org</sub> of 4.7×10<sup>-11</sup> to 1.0×10<sup>-10</sup> and 2.9×10<sup>-11</sup> to 7.6×10<sup>-10</sup> mol C cm<sup>-2</sup> s<sup>-1</sup> for lakes Tantaré Basin A and Bédard, respectively. Hence, the total sediment OM degradation rate (ΣR<sub>1</sub> + ΣR<sub>2</sub> + ΣR<sub>6</sub>) of 1.3×10<sup>-12</sup> and 1.4×10<sup>-12</sup> reported in this study for lakes Tantaré Basin A and Bédard, respectively, would~~
- 550 ~~involve only 1.2–2.8% and 0.2–4.8% of the total C<sub>org</sub> deposited. Given that the remaining 95.2–99.8% of the deposited C<sub>org</sub> is preserved in the sediment, it is not surprising that the sediment C<sub>org</sub> concentration is constant with depth (Fig. 2).~~

- The contribution of anaerobic mineralization for Lake Tantaré Basin A is about 1.68 times higher than the average of 30% reported for this lake basin in a previous study (Clayer et al., 2016). This significant discrepancy arises because these authors, in the absence of isotopic data to adequately constrain the R<sub>i</sub> values, assumed that R<sub>4</sub> = 0 in the net methanotrophic zone Z<sub>1</sub>.
- 555 Should we make the same assumption in the present study, we would also estimate that fermentation and methanogenesis represent only 30% of the total rate of OM degradation in the oxygenated Lake Tantaré Basin A and we would thus underestimate the importance of methanogenesis. The inclusion of δ<sup>13</sup>C data in the present modeling study thus allowed to



better constrain the effective rates of CH<sub>4</sub> production (R<sub>4</sub>). Indeed, a value of R<sub>4</sub> = 119 fmol cm<sup>-3</sup>s<sup>-1</sup> was required in Eq. 7 to produce an acceptable δ<sup>13</sup>C-CH<sub>4</sub> profile (Table 3 and Fig. S3).

## 590 4.2 Organic substrates for methanogenesis at the sampling sites

Table 3 indicates that hydrogenotrophy (r<sub>4</sub>) coupled to the complete fermentation of OM (r<sub>1</sub>) produces CH<sub>4</sub> at higher rates (R<sub>4</sub>) than DIC (R<sub>1</sub> - R<sub>4</sub>) in the Z<sub>1</sub> and Z<sub>2</sub> of both lake basins. This outcome is inconsistent with the equimolar production of CH<sub>4</sub> and DIC expected from the fermentation of glucose (C<sub>6</sub>H<sub>12</sub>O<sub>6</sub>), the model molecule used to represent labile OM in diagenetic models (Paraska et al., 2014), thus suggesting that the fermentation of this compound is not the exclusive source of  
 595 the H<sub>2</sub> required for hydrogenotrophy. Had OM been represented by C<sub>6</sub>H<sub>12</sub>O<sub>6</sub> in r<sub>1</sub>, the rate of H<sub>2</sub> production by this reaction would have been twice that of CO<sub>2</sub>, i.e., 2R<sub>1</sub>. For its part, the rate of H<sub>2</sub> consumption through hydrogenotrophy is four times that of the CH<sub>4</sub> production, i.e., 4R<sub>4</sub>. Hence, an additional H<sub>2</sub> production at rates of up to 212 and 70 fmol cm<sup>-3</sup> s<sup>-1</sup>, i.e., 4R<sub>4</sub> - 2R<sub>1</sub>, is needed to balance the H<sub>2</sub> production rate expected from the fermentation of C<sub>6</sub>H<sub>12</sub>O<sub>6</sub> and the H<sub>2</sub> consumption rate by hydrogenotrophy observed in the sediments of Lake Tantaré Basin A and Lake Bédard, respectively. As discussed by Clayer  
 600 et al. (2018), this additional production rate of H<sub>2</sub> could be provided by a cryptic Fe-S cycle such as r<sub>8</sub> (Table1), or by the production of CH<sub>4</sub> via the fermentation of organic substrates more reduced than glucose.

The progressive downward increases in dissolved Fe and SO<sub>4</sub><sup>2-</sup> (Fig. 23e, f, m and n) below ~5 cm depth and decrease in ΣS(-II) (Fig. 2a3n) observed in the porewaters support suggest a net production of H<sub>2</sub> from r<sub>8</sub> in both lakes. However, modeling the appropriate solute profiles with the code PROFILE indicates that the production rates of dissolved Fe (<10 fmol cm<sup>-3</sup>s<sup>-1</sup>) and SO<sub>4</sub><sup>2-</sup> (<1 fmol cm<sup>-3</sup>s<sup>-1</sup>) and the consumption rate of ΣS(-II) (<1 fmol cm<sup>-3</sup>s<sup>-1</sup>) are about one order of magnitude too low to explain the missing H<sub>2</sub> production rate in both basins. Moreover, in the Z<sub>1</sub> and Z<sub>2</sub> of Lake Tantaré Basin A, the rate of solid Fe(III) reduction (<3 fmol cm<sup>-3</sup> s<sup>-1</sup>; calculated from Liu et al. 2015) is much lower than that required from r<sub>8</sub> (i.e., 1 to 2 times the additional H<sub>2</sub> production of 4R<sub>4</sub> - 2R<sub>1</sub>; 70–424 fmol cm<sup>-3</sup> s<sup>-1</sup>) to produce sufficient amounts of H<sub>2</sub> to sustain the additional hydrogenotrophy. The net production rates of dissolved Fe (<10 fmol cm<sup>-3</sup> s<sup>-1</sup>) and SO<sub>4</sub><sup>2-</sup> (<1 fmol cm<sup>-3</sup> s<sup>-1</sup>) and the net  
 610 consumption rate of ΣS(-II) (<1 fmol cm<sup>-3</sup> s<sup>-1</sup>) are also consistent with this assertion (Fig. S3). Given these results, we submit that a cryptic Fe-S cycle, if present, would contribute only minimally to the missing rate of H<sub>2</sub> production, and that the fermentation of reduced organic compounds could provide a better explanation to the imbalance between the H<sub>2</sub> production and consumption rates.

Since CH<sub>4</sub> is produced by hydrogenotrophy in the two lake basins (χ<sub>H</sub> = 1), Eqn. S15 (section S2.2.2. of the SI) describing the COS of the fermenting organic substrate C<sub>x</sub>H<sub>y</sub>O<sub>z</sub> simplifies as:

$$\text{COS} = -4 \left( \frac{2 \left( R_{\text{net}}^{\text{CH}_4} - \frac{1}{2} \chi_{\text{M}} R_{\text{net}}^{\text{Ox}} \right) - R_{\text{F}}}{R_{\text{F}}} \right) \quad (11)$$

where χ<sub>M</sub> is the fraction of oxidants consumed through methanotrophy. Combining Eqs. S7 and S5 of the SI with Eq. 11, we obtain:

$$\text{COS} = -4 \left( \frac{R_{\text{net}}^{\text{CH}_4} - R_{\text{net}}^{\text{DIC}} - R_{\text{net}}^{\text{Ox}} + R_2}{R_{\text{net}}^{\text{DIC}} + R_{\text{net}}^{\text{CH}_4} + (1 - \chi_M) R_{\text{net}}^{\text{Ox}} - R_2} \right) \quad (12)$$

Introducing the values of  $R_{\text{net}}^{\text{CH}_4}$ ,  $R_{\text{net}}^{\text{DIC}}$ ,  $R_{\text{net}}^{\text{Ox}}$ ,  $\chi_M$  and  $R_2$  (Table 2 and 3) into Eq. 12, we calculate COS values of  $-3.2$  and  $-0.9$  for the  $Z_1$  and  $Z_2$  of Lake Tantaré Basin A, respectively, and of  $-1.0$  to  $-1.1$  for the  $Z_1$  of Lake Bédard, respectively. Note that we were unable to constrain with Eq. 12 the COS for the  $Z_2$  of Lake Bédard since we had to assume a COS value to estimate  $R_2$  (the  $R_2$ ) and the COS has no influence of the modelled  $\delta^{13}\text{C}$  profiles (section S2.2.2.3 of the SI). Negative COS values between  $-0.9$  and  $-1.1$  suggest that fermenting OM in the sediments of the two lake basins would be better represented by a mixture of fatty acids and fatty alcohols than by carbohydrates, as suggested by Clayer et al. (2018) for the sporadically anoxic Lake Tantaré Basin B. For its part, the highly negative COS value of  $-3.2$  calculated for the  $Z_1$  of Lake Tantaré Basin A is unreasonable, and the inaccuracy of the COS determination in this lake basin is discussed in section 4.3.

### 4.3 Reduced organic compounds as methanogenic substrates in lake sediments

In order to better appraise the COS of the fermenting OM in lakes, relevant datasets of porewater solute concentration profiles were gathered from our data repository and from a thorough literature search. To be able to obtain by reactive-transport modeling the  $R_{\text{net}}^{\text{solute}}$  required to calculate the COS with Eq. 12, the datasets had to: (i) comprise porewater concentration profiles of  $\text{CH}_4$  and DIC and, ideally, those of the EAs; (ii) reveal a net methanogenesis zone, and (iii) enable the estimation of the carbonate precipitation/dissolution contribution to the DIC concentrations to be estimated,  $R_{\text{net}}^{\text{DIC}}$ . Detailed information on the origin and processing of the 17 selected datasets, acquired in 6 different lake basins from one sub-alpine and three boreal lakes sampled at various dates and/or depths, is given in section S3 of the SI. The  $\text{CH}_4$  and DIC porewater profiles determined at hypolimnetic sites of these lake basins and their modeling with the code PROFILE are shown in Fig. 45, whereas the  $R_{\text{net}}^{\text{CH}_4}$ ,  $R_{\text{net}}^{\text{DIC}}$  and  $R_{\text{net}}^{\text{Ox}}$  values determined from this modeling are regrouped in Table 4. The COS values displayed in Table 4 for all lake basins and dates were calculated by substituting the appropriate  $R_{\text{net}}^{\text{CH}_4}$ ,  $R_{\text{net}}^{\text{DIC}}$  and  $R_{\text{net}}^{\text{Ox}}$  and  $R_2$  values in Eq. 12 and assuming that  $R_2 = 0$ . This latter assumption was not required varying  $\chi_M$  between 0 and 1, except for Lake Tantaré Basin A (October 2015) and Lake Bédard (October 2015) for which  $R_2$  values were known,  $\chi_M = 0.75$  (Table 4-3). When the value for  $R_2$  was not available, we assumed that  $R_2 = 0$ . Equation 12 indicates that any DIC contribution from  $R_2 > 0$ , would yield lower COS values than those reported in Table 4. The value of  $\chi_M$  was assumed to be alternately 0 and 1 to provide a range of COS values. The only exception was Lake Tantaré Basin A in October 2015 for which  $\chi_M$  is known to be 0.75 (section S2.2.2.2 of the SI). Note that although Eq. 12 was derived with the assumption that methanogenesis was hydrogenotrophic ( $\chi_H = 1$ ), assuming that  $\text{CH}_4$  was produced by acetoclasty ( $\chi_H = 0$ ) would yield the same expression.

According to Table 4 the COS values are systematically negative at all dates for Lake Tantaré Basin B, Lake Bédard, Jacks Lake and the two sites of Lake Lugano, and they vary generally between  $-0.9$  and  $-1.9$ , with the exception of a value of  $-2.5$  obtained for Lake Tantaré Basin B in July 2007. This latter value is likely too low to be representative of fermenting material and should be rejected. The mean ( $\pm$  SD) COS values are  $-1.7 \pm 0.4$  for Lake Tantaré Basin B,  $-1.4 \pm 0.4$  for Lake Bédard,

680  $-1.4 \pm 0.2$  for Jacks Lake and  $-1.4 \pm 0.3$  for Lake Lugano. These COS values, representative of a mixture of fatty acids (COS of  $-1.0$  for C4-fatty acids to about  $-1.87$  for C32-fatty acids) and of fatty alcohols (COS =  $-2.00$ ), strongly supports the idea that methanogenesis in oligotrophic boreal lakes sediments, ~~as well as in the sediments of and possibly~~ other lake types of lakes, is fueled by more reduced organic compounds than glucose. Lipids such as fatty acids and fatty alcohols with similar COS are naturally abundant in sediments to sustain the estimated rates of CH<sub>4</sub> and DIC production during fermentation (Burdige, 2007; Cranwell, 1981; Hedges and Oades, 1997; Matsumoto, 1989). As discussed by Clayer et al. (2018) the most labile organic compounds (i.e., proteins and carbohydrates) can be rapidly degraded during their transport through the water column and in the uppermost sediment layer, leaving mainly lipids as metabolizable substrates at depths where fermentation and methanogenesis occurs. This interpretation is consistent with thermodynamic and kinetic evidences that proteins and carbohydrates are more labile and are degraded faster than lipids (LaRowe and Van Cappellen, 2011).

685 The COS values determined for the perennially oxygenated Basin A of Lake Tantaré (mean of  $-0.6 \pm 1.1$ ; range of  $-3.2$  to  $2.1$ ; Table 4) are much more variable than for the five other seasonally anoxic lake basins ~~which undergo seasonal anoxia. Moreover, the COS values estimated including unrealistic values~~ for October 2015 in the Z<sub>1</sub> ( $-3.2$ ), September 2016 ( $0.4$ – $0.6$ ) and October 2005 ( $1.8$ – $2.1$ ) ~~are unrealistic.~~ Indeed, the very negative value of  $-3.2$  does not correspond to any degradable compound under anoxic conditions, whereas the positive values of  $0.4$ – $0.6$  and  $1.8$ – $2.1$  would involve either amino acids and nucleotides which are very labile (Larowe and Van Cappellen 2011) and tend to be degraded in the water column (Burdige 2007), or oxidized compounds, such as ketones, aldehydes and esters, known to be quickly reduced to alcohols. Possible sources of uncertainty in the COS estimation include mis-quantification of bioirrigation and DIC production through HMW OM fermentation (reaction r2; Corbett et al. 2013). Clayer et al. (2016) provided evidences that sediment irrigation by benthic animals is effective in Lake Tantaré Basin A and that reaction rates are sensitive to the bioirrigation coefficient. Nevertheless, additional simulations show that changing the bioirrigation coefficient by a factor of 2 (increased and decreased) did not result in significant changes in COS values (<0.2). Bioirrigation might also be mis-represented. Indeed, the term used in Eq. 2 to

690 calculate this contribution, i.e.,  $\phi\alpha_{\text{irrigation}}([\text{solute}]_{\text{tube}} - [\text{solute}])$ , is indeed an approximation of intricate 3-D processes variable in space and time (Meile et al., 2005; Boudreau and Marinelli, 1994; Forster and Graf, 1995; Gallon et al., 2008; Riisgård and Larsen, 2005). On the other hand, DIC production through HMW OM fermentation (reaction r2; Corbett et al. 2013) was constrained by default in Lake Tantaré Basin A (Table 4). Indeed, fitting with Eq. 7 the experimental  $\delta^{13}\text{C}$  data does not allow partitioning the production of DIC between r1 and r2 given that both processes share the same fractionation factor ( $\alpha_1 = \alpha_2 = 1.000$ ). Equation 9 indicates that to obtain negative COS values for Lake Tantaré Basin A in September 2006 and October 2005,  $R_2$  should be  $>11 \text{ fmol cm}^{-2} \text{ s}^{-1}$  and  $>110 \text{ fmol cm}^{-2} \text{ s}^{-1}$ , respectively. These  $R_2$  values correspond to transferring  $>9\%$  and  $>44\%$  of the rate of DIC production from  $R_1$  to  $R_2$  for September 2006 and October 2005, respectively. ~~These observations indicate that the COS determination in this lake basin is unreliable. The misestimation of the COS can probably not be explained by the presence of O<sub>2</sub> itself at the sediment surface of Lake Tantaré Basin A. Indeed, Hence, owing to the~~

700 imperfection in the COS estimations for Lake Tantaré Basin A, COS values estimated for this site should be treated with caution. Note that the sediment surface was also oxic at the sites Melide and Figino of Lake Lugano in March 1989 (Table 4)

710

as revealed by detectable bottom water [O<sub>2</sub>] (Table 4), and by low [Fe], undetectable ΣS(-II) and [CH<sub>4</sub>] and relatively high [SO<sub>4</sub><sup>2-</sup>] in overlying water (Lazzaretti et al., 1992; Lazzaretti-Ulmer and Hanselmann, 1999). Despite this, the COS values determined for the two sites of Lake Lugano appear ~~to be realistic and coherent~~ consistent with those calculated for Lakes Tantaré Basin B, Bédard and Jacks. ~~However, we know that benthic organisms are present in~~ This disparity between Lake Tantaré Basin A and Lake Lugano could be explained by the presence of benthic organisms in the former (Hare et al., 1994) but ~~lacking at their absence in the two sites of Lake Lugano latter~~, as shown by the presence of varves (Lazzaretti et al., 1992) and the absence of benthos remains in the recent sediments at these sites of Lake Lugano (Niessen et al., 1992). ~~Clayer et al. (2016) provided evidences that sediment irrigation by benthic animals is effective in Lake Tantaré Basin A and that it should be taken into account in modeling the porewater solutes profiles. However, these authors also point out the difficulty to properly estimate the magnitude of solute transport by bioirrigation. The term used in Eq. 2 to calculate this contribution, i.e.,  $\phi_{\text{irrigation}}([\text{solute}]_{\text{tube}} - [\text{solute}])$ , is indeed an approximation of intricate 3-D processes (Meile et al., 2005). And, in the conceptualization of this bioirrigation term, it was notably assumed that benthic animals continuously irrigate their tubes to maintain solute concentrations in their biogenic structures ( $[\text{solute}]_{\text{tube}}$ ) identical to those in the water overlying the sediments. But~~ microbenthic animals are generally reported to irrigate the sediments in a discontinuous manner and the solute concentrations in their biogenic structures may be highly variable with time (Boudreau and Marinelli, 1994; Forster and Graf, 1995; Gallon et al., 2008; Riisgård and Larsen, 2005). Hence, owing to the imperfection of the representation of bioirrigation in Eq. 2, COS values estimated for the sediment of Lake Tantaré Basin A should be treated with caution, especially in the Z<sub>1</sub> where the bioirrigation coefficient takes the highest value. Another potential bias in the estimation of COS values for the oxygenated basin is the possibility of DIC production through HMW OM fermentation (reaction r<sub>2</sub>; Corbett et al. 2013). Note that fitting with Eq. 6 the experimental δ<sup>13</sup>C data does not allow partitioning the production of DIC between r<sub>1</sub> and r<sub>2</sub> since the two processes share the same value of fractionation factor (α<sub>1</sub> = α<sub>2</sub> = 1.000). It was possible to attribute unequivocally the excess of DIC production rate over that of CH<sub>4</sub> production in the Z<sub>2</sub> of Lake Bédard in October 2015 (Table 4 and Section S2.1.2.2 of the SI) to HMW OM fermentation merely because R<sub>net</sub><sup>Ox</sup> was negligible compared to R<sub>net</sub><sup>CH<sub>4</sub></sup> and R<sub>net</sub><sup>DIC</sup>, which is not the case for Lake Tantaré Basin A (Table 4). Equation 12 indicates that to obtain negative COS values for Lake Tantaré Basin A in September 2006 and October 2005, R<sub>2</sub> should be >11 fmol cm<sup>-2</sup> s<sup>-1</sup> and >110 fmol cm<sup>-2</sup> s<sup>-1</sup>, respectively. These R<sub>2</sub> values correspond to transferring >9% and >44% of the rate of DIC production from R<sub>1</sub> to R<sub>2</sub> for September 2006 and October 2005, respectively. The above discussion underlines several factors that can explain the unreliability in the actual COS estimation for the perennially oxic Lake Tantaré Basin A, and further research is needed to better assess the importance of these factors.

740 ~~However, it does not dismiss that the substrate for methanogenesis in this lake basin may have a negative COS value.~~

## 5 Conclusions

~~Our results show that fermentation and methanogenesis represent nearly 50% and 100% of OM mineralization in the top 25 cm of the sediments at the hypolimnetic sites in Lake Bédard and in Basin A of Lake Tantaré, respectively and that methane~~

is produced only by hydrogenotrophy at these two sites. An earlier study reached similar conclusions about the pathways of methanogenesis and the contribution of this process in OM mineralization in Basin B of Lake Tantaré (Our results show that fermentation and methanogenesis represent about 50% and 100% of OM mineralization in the top 25 cm of the sediments at the hypolimnetic sites in Lake Tantaré Basin A and Bédard, respectively, that methane is produced only by hydrogenotrophy and fermentation substrates have a negative COS at these two sites. The association of hydrogenotrophy with the fermentation of reduced OM (COS < -0.9; implying that labile compounds are depleted) in the studied lake sediments is consistent with the fact that hydrogenotrophy becomes increasingly important when labile OM is depleted (Chasar et al., 2000; Hornibrook et al., 2000; Whiticar et al., 1986).

~~Clayer et al., 2018).~~

Reactive-transport modelling of twelve datasets of porewater solutes profiles from three boreal lakes, i.e., Bédard, Tantaré (Basin B) and Jacks, as well as of the sub-alpine Lake Lugano (Melide and Figino sites) consistently showed that the main substrates for sediment methanogenesis at deep seasonally anoxic hypolimnetic sites have a mean COS value of  $-1.4 \pm 0.3$ .

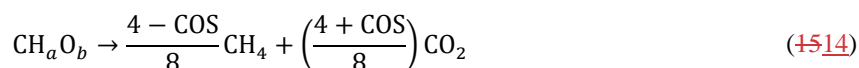
~~Mineralization~~ The OM in the sediment of the three boreal lakes, as well as their O<sub>2</sub> seasonal dynamics, are typical of boreal forest lakes. While Lake Bédard experiences prolonged episodes of extended hypolimnetic anoxia, Lake Tantaré Basin B and Jacks Lake show more moderate seasonal anoxia, where some years the hypolimnion of Lake Tantaré Basin B is only hypoxic (Clayer et al., 2016; Carignan et al., 1991). Hence, the selective mineralization of OM described by Clayer et al. (2018), involving that the most labile compounds are mineralized during OM downward migration in the water column and ~~in~~ the uppermost-sediment layers likely explains why surface leaving mainly reduced organic compounds to fuel methanogenesis in these the sediments-, likely applies to a large portion of boreal lakes.

~~The~~ Hence, the current representation of the fermenting OM, i.e., CH<sub>2</sub>O, in process-based biogeochemical models entails a significant risk of ~~misestimating~~ underestimating sedimentary CH<sub>4</sub> and CO<sub>2</sub> production and release to the bottom water and, to a certain extent, of ~~mispredicting its~~ evasion of these greenhouse gases to the atmosphere under transient environmental scenarios. To better constrain CH<sub>4</sub> and CO<sub>2</sub> production within sediments, we suggest taking specifically into account the COS of the fermenting OM in formulating the reactions of methanogenesis associated with fermentation in these models. For example, the rates of CH<sub>4</sub> (R<sup>CH<sub>4</sub></sup>) and DIC (R<sup>DIC</sup>) production during fermentation coupled to hydrogenotrophy can be expressed as:

$$R^{\text{CH}_4} = R_4 = \frac{4 - \text{COS}}{8} R_1 \quad (4312)$$

$$R^{\text{DIC}} = R_1 - R_4 = R_1 \left( 1 - \frac{4 - \text{COS}}{8} \right) \quad (4413)$$

Given these rate expressions, the stoichiometric formulation of a typical fermentation reaction producing ~~methane~~ CH<sub>4</sub> becomes:



800 where  $a = 2 - \frac{\text{COS}}{2}$ ,  $b = 1 + \frac{\text{COS}}{4}$ . ~~Note that the same stoichiometric formulation would be obtained for acetoclastic~~  
~~methanogenesis.~~ Introducing the average COS values reported in this study ( $-1.4 \pm 0.3$ ) into Eq. 14, the coefficients  $a$  and  $b$   
would take values of  $2.7 \pm 0.15$  and  $0.65 \pm 0.125$ , respectively, and the  $\text{CH}_4$  and  $\text{CO}_2$  stoichiometric coefficients would be  
 $0.68 \pm 0.04$  and  $0.32 \pm 0.04$ , respectively. Note that the same stoichiometric formulation would be obtained with any possible  
combination of acetoclasty and hydrogenotrophy. Under these conditions, fermentation (r1) coupled to methanogenesis (r4)  
805 yields  $2.2 \pm 0.4$  times more  $\text{CH}_4$  than DIC for the studied lake sediments. Ignoring the implications of the present study regarding  
the COS of the fermenting OM could lead to the underestimation of  $\text{CH}_4$  sediment outflux or of the rate of oxidant consumption  
required to mitigate this efflux by a factor of up to 2.6.

The approach used to estimate the COS of the fermenting OM, although successful for the seasonally anoxic basins, failed to  
produce reliable COS values when applied to the perennially oxygenated Basin A of Lake Tantaré. We attribute this peculiarity  
810 to a misestimation and/or misrepresentation of the benthic irrigation and to the impossibility to partition the DIC production  
between reactions r1 and r2 which share the same fractionation factor value. Similar problems would likely be encountered  
also in other lake ecosystems such as epilimnetic sediments and wetlands where solute transport processes remain ill-known.  
Indeed, these shallow aquatic environments are subject to enhanced benthic activity (Hare, 1995), to plant-mediated transport  
of  $\text{CH}_4$  and  $\text{O}_2$  (Chanton et al., 1989; Wand et al., 2006), as well as to turbulence (Poindexter et al., 2016) which complicates  
815 the estimation of  $\text{CH}_4$  and  $\text{CO}_2$  production and consumption rates. Hence, the remaining challenge resides in the robust  
estimations the COS of the fermenting OM in epilimnetic sediments and shallow freshwater environments (e.g., ponds,  
wetlands), since these environments were shown to be the main contributors to freshwater  $\text{CH}_4$  release to the atmosphere  
(Bastviken et al., 2008; DelSontro et al., 2016). One potential solution is to investigate trends in the oxygen isotope signatures  
in the sedimentary DIC in addition to  $\delta^{13}\text{C}$  values since it is also influenced by the source of the OM undergoing degradation  
820 (e.g., Sauer et al., 2001).

#### **Data availability:**

Upon acceptance, readers will be able to access the data at this url:  
<https://www.hydroshare.org/resource/38e069761d7b4cf4abe3cbcaaac06016/>. A proper reference with a DOI will be made  
available to cite this dataset if the present paper is accepted.

#### 825 **Author contribution:**

Conceptualization: FC, AT, and CG. Data curation: FC and AT. Formal analysis: FC and AT. Funding acquisition: CG, YG  
and AT. Investigation: FC and YG. Methodology: AT, CG, YG and FC. Project administration: CG. Resources: CG and YG.  
Software: FC. Supervision: CG, AT and YG. Validation: AT. Writing – original draft: FC and AT. Writing – review & editing:  
All.

## Competing interests:

The authors declare that they have no conflict of interest.

## Acknowledgments

865 We thank P. Boissinot, L. Rancourt, P. Girard, J.-F. Dutil, S. Duval, A. Royer-Lavallée, A. Laberge and A. Barber for research and field work assistance. We are also thankful to J.-F. Hélie, from the Laboratoire de géochimie des isotopes stables légers (UQÀM), who graciously calibrated our  $\delta^{13}\text{C}$  internal standard. This work was supported by grants to C.G., A.T. and Y.G. from the Natural Sciences and Engineering Research Council of Canada and the Fonds de Recherche Québécois – Nature et Technologies. Permission from the Québec Ministère du Développement durable, de l'Environnement et de la Lutte contre les  
870 changements climatiques to work in the Tantaré Ecological Reserve is gratefully acknowledged.

## References

- Alperin, M. J., Albert, D. B. and Martens, C. S.: Seasonal variations in production and consumption rates of dissolved organic carbon in an organic-rich coastal sediment, *Geochimica et Cosmochimica Acta*, 58(22), 4909–4930, doi:10.1016/0016-7037(94)90221-6, 1994.
- 875 Arndt, S., Jørgensen, B. B., LaRowe, D. E., Middelburg, J. J., Pancost, R. D. and Regnier, P.: Quantifying the degradation of organic matter in marine sediments: A review and synthesis, *Earth-Science Reviews*, 123, 53–86, doi:10.1016/j.earscirev.2013.02.008, 2013.
- Arning, E. T., van Berk, W. and Schulz, H.-M.: Fate and behaviour of marine organic matter during burial of anoxic sediments: Testing  $\text{CH}_2\text{O}$  as generalized input parameter in reaction transport models, *Marine Chemistry*, 178, 8–21, doi:10.1016/j.marchem.2015.12.002, 2016.
- 880 Bastviken, D., Cole, J., Pace, M. and Tranvik, L.: Methane emissions from lakes: Dependence of lake characteristics, two regional assessments, and a global estimate: LAKE METHANE EMISSIONS, *Global Biogeochemical Cycles*, 18(4), n/a-n/a, doi:10.1029/2004GB002238, 2004.
- Bastviken, D., Cole, J. J., Pace, M. L. and Van de Bogert, M. C.: Fates of methane from different lake habitats: Connecting whole-lake budgets and  $\text{CH}_4$  emissions: FATES OF LAKE METHANE, *Journal of Geophysical Research: Biogeosciences*, 113(G2), n/a-n/a, doi:10.1029/2007JG000608, 2008.
- 885 Beal, E. J., House, C. H. and Orphan, V. J.: Manganese- and iron-dependent marine methane oxidation, *Science*, 325(5937), 184–187, doi:10.1126/science.1169984, 2009.
- Berg, P., Risgaard-Petersen, N. and Rysgaard, S.: Interpretation of measured concentration profiles in sediment pore water, *Limnology and Oceanography*, 43(7), 1500–1510, doi:10.4319/lo.1998.43.7.1500, 1998.
- 890 Borowski, W. S., Paull, C. K. and Ussler, W.: Carbon cycling within the upper methanogenic zone of continental rise sediments: An example from the methane-rich sediments overlying the Blake Ridge gas hydrate deposits, *Marine Chemistry*, 57(3), 299–311, doi:10.1016/S0304-4203(97)00019-4, 1997.

- 895 [Botrel, M., Gregory-Eaves, I. and Maranger, R.: Defining drivers of nitrogen stable isotopes \( \$\delta^{15}\text{N}\$ \) of surface sediments in temperate lakes, \*J Paleolimnol\*, 52\(4\), 419–433, doi:10.1007/s10933-014-9802-6, 2014.](#)
- [Boudreau, B. P.: On the equivalence of nonlocal and radial-diffusion models for porewater irrigation, \*Journal of Marine Research\*, 42\(3\), 731–735, doi:10.1357/002224084788505924, 1984.](#)
- [Boudreau, B. P.: Diagenetic models and their implementation: modelling transport and reactions in aquatic sediments, Springer., 1997.](#)
- 900 [Buffle, J.: Complexation reactions in aquatic systems: An analytical approach, Ellis Horwood Limited., 1988.](#)
- [Burdige, D., Komada, T., Magen, C. and Chanton, J. P.: Methane dynamics in Santa Barbara Basin \(USA\) sediments as examined with a reaction-transport model, \*Journal of Marine Research\*, 74, 277–313, 2017.](#)
- [Burdige, D. J.: Preservation of Organic Matter in Marine Sediments: Controls, Mechanisms, and an Imbalance in Sediment Organic Carbon Budgets?, \*Chem. Rev.\*, 107\(2\), 467–485, doi:10.1021/cr050347q, 2007.](#)
- 905 [Burdige, D. J. and Komada, T.: Anaerobic oxidation of methane and the stoichiometry of remineralization processes in continental margin sediments, \*Limnology and Oceanography\*, 56\(5\), 1781–1796, doi:10.4319/lo.2011.56.5.1781, 2011.](#)
- [Carignan, R. and Lean, D. R. S.: Regeneration of dissolved substances in a seasonally anoxic lake: The relative importance of processes occurring in the water column and in the sediments, \*Limnology and Oceanography\*, 36\(4\), 683–707, doi:10.4319/lo.1991.36.4.0683, 1991.](#)
- 910 [Carignan, R., Rapin, F. and Tessier, A.: Sediment porewater sampling for metal analysis: A comparison of techniques, \*Geochimica et Cosmochimica Acta\*, 49\(11\), 2493–2497, doi:10.1016/0016-7037\(85\)90248-0, 1985.](#)
- [Chanton, J. P., Martens, C. S. and Kelley, C. A.: Gas transport from methane-saturated, tidal freshwater and wetland sediments, \*Limnology and Oceanography\*, 34\(5\), 807–819, doi:10.4319/lo.1989.34.5.0807, 1989.](#)
- 915 [Chanton, J. P., Whiting, G. J., Blair, N. E., Lindau, C. W. and Bollich, P. K.: Methane emission from rice: Stable isotopes, diurnal variations, and CO<sub>2</sub> exchange, \*Global Biogeochemical Cycles\*, 11\(1\), 15–27, doi:10.1029/96GB03761, 1997.](#)
- [Chasar, L. S., Chanton, J. P., Glaser, P. H., Siegel, D. I. and Rivers, J. S.: Radiocarbon and stable carbon isotopic evidence for transport and transformation of dissolved organic carbon, dissolved inorganic carbon, and CH<sub>4</sub> in a northern Minnesota peatland, \*Global Biogeochemical Cycles\*, 14\(4\), 1095–1108, doi:10.1029/1999GB001221, 2000.](#)
- 920 [Clayer, F., Gobeil, C. and Tessier, A.: Rates and pathways of sedimentary organic matter mineralization in two basins of a boreal lake: Emphasis on methanogenesis and methanotrophy: Methane cycling in boreal lake sediments, \*Limnology and Oceanography\*, 61\(S1\), S131–S149, doi:10.1002/lno.10323, 2016.](#)
- [Clayer, F., Moritz, A., G elinas, Y., Tessier, A. and Gobeil, C.: Modeling the carbon isotope signatures of methane and dissolved inorganic carbon to unravel mineralization pathways in boreal lake sediments, \*Geochimica et Cosmochimica Acta\*, 229, 36–52, doi:10.1016/j.gca.2018.02.012, 2018.](#)
- 925 [Cole, J. J., Prairie, Y. T., Caraco, N. F., McDowell, W. H., Tranvik, L. J., Striegl, R. G., Duarte, C. M., Kortelainen, P., Downing, J. A., Middelburg, J. J. and Melack, J.: Plumbing the Global Carbon Cycle: Integrating Inland Waters into the Terrestrial Carbon Budget, \*Ecosystems\*, 10\(1\), 172–185, doi:10.1007/s10021-006-9013-8, 2007.](#)



- Conrad, R.: Contribution of hydrogen to methane production and control of hydrogen concentrations in methanogenic soils and sediments, FEMS Microbiology Ecology, 28(3), 193–202, doi:10.1111/j.1574-6941.1999.tb00575.x, 1999.
- 965 Conrad, R.: Quantification of methanogenic pathways using stable carbon isotopic signatures: a review and a proposal, Organic Geochemistry, 36(5), 739–752, doi:10.1016/j.orggeochem.2004.09.006, 2005.
- Conrad, R., Claus, P. and Casper, P.: Characterization of stable isotope fractionation during methane production in the sediment of a eutrophic lake, Lake Dagow, Germany, Limnology and Oceanography, 54(2), 457–471, doi:10.4319/lo.2009.54.2.0457, 2009.
- 970 Corbett, J. E., Tfaily, M. M., Burdige, D. J., Cooper, W. T., Glaser, P. H. and Chanton, J. P.: Partitioning pathways of CO<sub>2</sub> production in peatlands with stable carbon isotopes, Biogeochemistry, 114, 327–340, 2013.
- Corbett, J. E., Tfaily, M. M., Burdige, D. J., Glaser, P. H. and Chanton, J. P.: The relative importance of methanogenesis in the decomposition of organic matter in northern peatlands, Journal of Geophysical Research: Biogeosciences, 120(2), 280–293, doi:10.1002/2014JG002797, 2015.
- 975 Couture, R.-M., Gobeil, C. and Tessier, A.: Chronology of Atmospheric Deposition of Arsenic Inferred from Reconstructed Sedimentary Records, Environ. Sci. Technol., 42(17), 6508–6513, doi:10.1021/es800818j, 2008.
- Couture, R.-M., Gobeil, C. and Tessier, A.: Arsenic, iron and sulfur co-diagenesis in lake sediments, Geochimica et Cosmochimica Acta, 74(4), 1238–1255, doi:10.1016/j.gca.2009.11.028, 2010.
- 980 Couture, R.-M., Fischer, R., Van Cappellen, P. and Gobeil, C.: Non-steady state diagenesis of organic and inorganic sulfur in lake sediments, Geochimica et Cosmochimica Acta, 194, 15–33, doi:10.1016/j.gca.2016.08.029, 2016.
- Cranwell, P. A.: Diagenesis of free and bound lipids in terrestrial detritus deposited in a lacustrine sediment, Organic Geochemistry, 3(3), 79–89, doi:10.1016/0146-6380(81)90002-4, 1981.
- D'arcy, P.: Relations entre les propriétés du bassin versant, la morphométrie du lac et la qualité des eaux, INRS-ETE, Université du Québec, Québec City, Québec, Canada., 1993.
- 985 DelSontro, T., Boutet, L., St-Pierre, A., del Giorgio, P. A. and Prairie, Y. T.: Methane ebullition and diffusion from northern ponds and lakes regulated by the interaction between temperature and system productivity: Productivity regulates methane lake flux, Limnology and Oceanography, 61(S1), S62–S77, doi:10.1002/lno.10335, 2016.
- 990 Egger, M., Rasigraf, O., Sapart, C. J., Jilbert, T., Jetten, M. S. M., Röckmann, T., van der Veen, C., Bândă, N., Kartal, B., Ettwig, K. F. and Slomp, C. P.: Iron-Mediated Anaerobic Oxidation of Methane in Brackish Coastal Sediments, Environ. Sci. Technol., 49(1), 277–283, doi:10.1021/es503663z, 2015.
- 995 Ettwig, K. F., Butler, M. K., Le Paslier, D., Pelletier, E., Mangenot, S., Kuypers, M. M. M., Schreiber, F., Dutilh, B. E., Zedelius, J., de Beer, D., Gloerich, J., Wessels, H. J. C. T., van Alen, T., Luesken, F., Wu, M. L., van de Pas-Schoonen, K. T., Op den Camp, H. J. M., Janssen-Megens, E. M., Francoijs, K.-J., Stunnenberg, H., Weissenbach, J., Jetten, M. S. M. and Strous, M.: Nitrite-driven anaerobic methane oxidation by oxygenic bacteria, Nature, 464(7288), 543–548, doi:10.1038/nature08883, 2010.
- Feyte, S., Gobeil, C., Tessier, A. and Cossa, D.: Mercury dynamics in lake sediments, Geochimica et Cosmochimica Acta, 82, 92–112, doi:10.1016/j.gca.2011.02.007, 2012.

- 1000 Francioso, O., Montecchio, D., Gioacchini, P. and Ciavatta, C.: Thermal analysis (TG–DTA) and isotopic characterization (13C–15N) of humic acids from different origins, Applied Geochemistry, 20(3), 537–544, doi:10.1016/j.apgeochem.2004.10.003, 2005.
- Galand, P. E., Yrjälä, K. and Conrad, R.: Stable carbon isotope fractionation during methanogenesis in three boreal peatland ecosystems, Biogeosciences, 7(11), 3893–3900, doi:https://doi.org/10.5194/bg-7-3893-2010, 2010.
- Hare, L.: Sediment Colonization by Littoral and Profundal Insects, Journal of the North American Benthological Society, 14, 315, doi:10.2307/1467783, 1995.
- 1005 Hare, L., Carignan, R. and Huerta-Diaz, M. A.: A field study of metal toxicity and accumulation by benthic invertebrates: implications for the acid-volatile sulfide (AVS) model, Limnology and Oceanography, 39(7), 1653–1668, doi:10.4319/lo.1994.39.7.1653, 1994.
- 1010 Hastie, A., Lauerwald, R., Weyhenmeyer, G., Sobek, S., Verpoorter, C. and Regnier, P.: CO<sub>2</sub> evasion from boreal lakes: Revised estimate, drivers of spatial variability, and future projections, Global Change Biology, 24(2), 711–728, doi:10.1111/gcb.13902, 2018.
- Hedges, J. I. and Oades, J. M.: Comparative organic geochemistries of soils and marine sediments, Organic Geochemistry, 27(7), 319–361, doi:10.1016/S0146-6380(97)00056-9, 1997.
- Hesslein, R. H.: An in situ sampler for close interval pore water studies<sup>1</sup>, Limnology and Oceanography, 21(6), 912–914, doi:10.4319/lo.1976.21.6.0912, 1976.
- 1015 Holgerson, M. A. and Raymond, P. A.: Large contribution to inland water CO<sub>2</sub> and CH<sub>4</sub> emissions from very small ponds, Nature Geoscience, 9(3), 222–226, doi:10.1038/ngeo2654, 2016.
- Holmkvist, L., Ferdelman, T. G. and Jørgensen, B. B.: A cryptic sulfur cycle driven by iron in the methane zone of marine sediment (Aarhus Bay, Denmark), Geochimica et Cosmochimica Acta, 75(12), 3581–3599, doi:10.1016/j.gca.2011.03.033, 2011.
- 1020 Hornibrook, E. R. C., Longstaffe, F. J. and Fyfe, W. S.: Spatial distribution of microbial methane production pathways in temperate zone wetland soils: Stable carbon and hydrogen isotope evidence, Geochimica et Cosmochimica Acta, 61(4), 745–753, doi:10.1016/S0016-7037(96)00368-7, 1997.
- Hornibrook, E. R. C., Longstaffe, F. J. and Fyfe, W. S.: Evolution of stable carbon isotope compositions for methane and carbon dioxide in freshwater wetlands and other anaerobic environments, Geochimica et Cosmochimica Acta, 64(6), 1013–1027, doi:10.1016/S0016-7037(99)00321-X, 2000.
- 1025 Jørgensen, B. B. and Parkes, R. J.: Role of sulfate reduction and methane production by organic carbon degradation in eutrophic fjord sediments (Limfjorden, Denmark), Limnology and Oceanography, 55(3), 1338–1352, doi:10.4319/lo.2010.55.3.1338, 2010.
- 1030 Joshani, A.: Investigating organic matter preservation through complexation with iron oxides in Lake Tantaré, masters, Concordia University, 1 September. [online] Available from: <https://spectrum.library.concordia.ca/980434/> (Accessed 12 December 2019), 2015.
- Kankaala, P., Huotari, J., Tulonen, T. and Ojala, A.: Lake-size dependent physical forcing drives carbon dioxide and methane effluxes from lakes in a boreal landscape, Limnology and Oceanography, 58(6), 1915–1930, doi:10.4319/lo.2013.58.6.1915, 2013.

- 1035 [Laforte, L., Tessier, A., Gobeil, C. and Carignan, R.: Thallium diagenesis in lacustrine sediments, \*Geochimica et Cosmochimica Acta\*, 69\(22\), 5295–5306, doi:10.1016/j.gca.2005.06.006, 2005.](#)
- [LaRowe, D. E. and Van Cappellen, P.: Degradation of natural organic matter: A thermodynamic analysis, \*Geochimica et Cosmochimica Acta\*, 75\(8\), 2030–2042, doi:10.1016/j.gca.2011.01.020, 2011.](#)
- 1040 [Lazzaretti, M. A., Hanselmann, K. W., Brandl, H., Span, D. and Bachofen, R.: The role of sediments in the phosphorus cycle in Lake Lugano. II. Seasonal and spatial variability of microbiological processes at the sediment-water interface, \*Aquatic Science\*, 54\(3\), 285–299, doi:10.1007/BF00878142, 1992.](#)
- [Lazzaretti-Ulmer, M. A. and Hanselmann, K. W.: Seasonal variation of the microbially regulated buffering capacity at sediment-water interfaces in a freshwater lake, \*Aquat. Sci.\*, 61\(1\), 59–74, doi:10.1007/s000270050052, 1999.](#)
- 1045 [Matisoff, G. and Wang, X.: Solute transport in sediments by freshwater infaunal bioirrigators, \*Limnology and Oceanography\*, 43\(7\), 1487–1499, doi:10.4319/lo.1998.43.7.1487, 1998.](#)
- [Matsumoto, G. I.: Biogeochemical study of organic substances in Antarctic lakes, \*Hydrobiologia\*, 172\(1\), 265–299, doi:10.1007/BF00031627, 1989.](#)
- [Meile, C. D., Berg, P., Cappellen, P. S. J. and Tuncay, K.: Solute-specific pore water irrigation: Implications for chemical cycling in early diagenesis, \*Journal of Marine Research\*, 63, doi:10.1357/0022240054307885, 2005.](#)
- 1050 [Natchimuthu, S., Wallin, M. B., Klemedtsson, L. and Bastviken, D.: Spatio-temporal patterns of stream methane and carbon dioxide emissions in a hemiboreal catchment in Southwest Sweden, \*Scientific Reports\*, 7\(1\), doi:10.1038/srep39729, 2017.](#)
- [Niessen, F., Wick, L., Bonani, G., Chondrogianni, C. and Siegenthaler, C.: Aquatic system response to climatic and human changes: Productivity, bottom water oxygen status, and sapropel formation in Lake Lugano over the last 10 000 years, \*Aquatic Science\*, 54\(3\), 257–276, doi:10.1007/BF00878140, 1992.](#)
- 1055 [Norði, K. à, Thamdrup, B. and Schubert, C. J.: Anaerobic oxidation of methane in an iron-rich Danish freshwater lake sediment, \*Limnology and Oceanography\*, 58\(2\), 546–554, doi:10.4319/lo.2013.58.2.0546, 2013.](#)
- [Paraska, D. W., Hipsey, M. R. and Salmon, S. U.: Sediment diagenesis models: Review of approaches, challenges and opportunities, \*Environmental Modelling & Software\*, 61, 297–325, doi:10.1016/j.envsoft.2014.05.011, 2014.](#)
- 1060 [Pohlman, J. W., Ruppel, C., Hutchinson, D. R., Downer, R. and Coffin, R. B.: Assessing sulfate reduction and methane cycling in a high salinity pore water system in the northern Gulf of Mexico, \*Marine and Petroleum Geology\*, 25\(9\), 942–951, doi:10.1016/j.marpetgeo.2008.01.016, 2008.](#)
- [Pohlman, J. W., Riedel, M., Bauer, J. E., Canuel, E. A., Paull, C. K., Lapham, L., Grabowski, K. S., Coffin, R. B. and Spence, G. D.: Anaerobic methane oxidation in low-organic content methane seep sediments, \*Geochimica et Cosmochimica Acta\*, 108, 184–201, doi:10.1016/j.gca.2013.01.022, 2013.](#)
- 1065 [Poindexter, C. M., Baldocchi, D. D., Matthes, J. H., Knox, S. H. and Variano, E. A.: The contribution of an overlooked transport process to a wetland’s methane emissions, \*Geophysical Research Letters\*, 43\(12\), 6276–6284, doi:10.1002/2016GL068782, 2016.](#)
- 1070 [Raghoebarsing, A. A., Pol, A., van de Pas-Schoonen, K. T., Smolders, A. J. P., Ettwig, K. F., Rijpstra, W. I. C., Schouten, S., Damsté, J. S. S., Op den Camp, H. J. M., Jetten, M. S. M. and Strous, M.: A microbial consortium couples anaerobic methane oxidation to denitrification, \*Nature\*, 440\(7086\), 918–921, doi:10.1038/nature04617, 2006.](#)

- Sabrekov, A. F., Runkle, B. R. K., Glagolev, M. V., Terentieva, I. E., Stepanenko, V. M., Kotsyurbenko, O. R., Maksyutov, S. S. and Pokrovsky, O. S.: Variability in methane emissions from West Siberia's shallow boreal lakes on a regional scale and its environmental controls, *Biogeosciences*, 14(15), 3715–3742, doi:<https://doi.org/10.5194/bg-14-3715-2017>, 2017.
- 1075 [Sauer, P. E., Miller, G. H. and Overpeck, J. T.: Oxygen isotope ratios of organic matter in arctic lakes as a paleoclimate proxy: field and laboratory investigations, \*Journal of Paleolimnology\*, 25\(1\), 43–64, doi:10.1023/A:1008133523139, 2001.](#)
- 1080 [Saunois, M., Bousquet, P., Poulter, B., Peregon, A., Ciais, P., Canadell, J. G., Dlugokencky, E. J., Etiope, G., Bastviken, D., Houweling, S., Janssens-Maenhout, G., Tubiello, F. N., Castaldi, S., Jackson, R. B., Alexe, M., Arora, V. K., Beerling, D. J., Bergamaschi, P., Blake, D. R., Brailsford, G., Brovkin, V., Bruhwiler, L., Crevoisier, C., Crill, P., Covey, K., Curry, C., Frankenberg, C., Gedney, N., Höglund-Isaksson, L., Ishizawa, M., Ito, A., Joos, F., Kim, H.-S., Kleinen, T., Krummel, P., Lamarque, J.-F., Langenfelds, R., Locatelli, R., Machida, T., Maksyutov, S., McDonald, K. C., Marshall, J., Melton, J. R., Morino, I., Naik, V., O&apos;Doherty, S., Parmentier, F.-J. W., Patra, P. K., Peng, C., Peng, S., Peters, G. P., Pison, I., Prigent, C., Prinn, R., Ramonet, M., Riley, W. J., Saito, M., Santini, M., Schroeder, R., Simpson, I. J., Spahni, R., Steele, P., Takizawa, A., Thornton, B. F., Tian, H., Tohjima, Y., Viovy, N., Voulgarakis, A., van Weele, M., van der Werf, G. R., Weiss, R., Wiedinmyer, C., Wilton, D. J., Wiltshire, A., Worthy, D., Wunch, D., Xu, X., Yoshida, Y., Zhang, B., Zhang, Z. and Zhu, Q.: The global methane budget 2000–2012, \*Earth System Science Data\*, 8\(2\), 697–751, doi:10.5194/essd-8-697-2016, 2016.](#)
- 1085 [Schindler, D. W., Curtis, P. J., Parker, B. R. and Stainton, M. P.: Consequences of climate warming and lake acidification for UV-B penetration in North American boreal lakes, \*Nature\*, 379\(6567\), 705–708, doi:10.1038/379705a0, 1996.](#)
- [Sivan, O., Schrag, D. P. and Murray, R. W.: Rates of methanogenesis and methanotrophy in deep-sea sediments, \*Geobiology\*, 5\(2\), 141–151, doi:10.1111/j.1472-4669.2007.00098.x, 2007.](#)
- 1090 [Staeher, P. A., Testa, J. M., Kemp, W. M., Cole, J. J., Sand-Jensen, K. and Smith, S. V.: The metabolism of aquatic ecosystems: history, applications, and future challenges, \*Aquatic Sciences\*, 74\(1\), 15–29, doi:10.1007/s00027-011-0199-2, 2012.](#)
- [Thottathil, S. D., Reis, P. C. J. and Prairie, Y. T.: Methane oxidation kinetics in northern freshwater lakes, \*Biogeochemistry\*, 143\(1\), 105–116, doi:10.1007/s10533-019-00552-x, 2019.](#)
- [Tipping, E.: Cation binding by humic substances, Cambridge University Press., 2002.](#)
- 1095 [Turner, A. J., Jacob, D. J., Wecht, K. J., Maasackers, J. D., Lundgren, E., Andrews, A. E., Biraud, S. C., Boesch, H., Bowman, K. W., Deutscher, N. M., Dubey, M. K., Griffith, D. W. T., Hase, F., Kuze, A., Notholt, J., Ohyama, H., Parker, R., Payne, V. H., Sussmann, R., Sweeney, C., Velazco, V. A., Warneke, T., Wennberg, P. O. and Wunch, D.: Estimating global and North American methane emissions with high spatial resolution using GOSAT satellite data, \*Atmospheric Chemistry and Physics\*, 15\(12\), 7049–7069, doi:<https://doi.org/10.5194/acp-15-7049-2015>, 2015.](#)
- 1100 [Ullman, W. J. and Aller, R. C.: Diffusion coefficients in nearshore marine sediments1, \*Limnology and Oceanography\*, 27\(3\), 552–556, doi:10.4319/lo.1982.27.3.0552, 1982.](#)
- [Verpoorter, C., Kutser, T., Seekell, D. A. and Tranvik, L. J.: A global inventory of lakes based on high-resolution satellite imagery, \*Geophysical Research Letters\*, 41\(18\), 6396–6402, doi:10.1002/2014GL060641, 2014.](#)
- 1105 [Wallin, M. B., Campeau, A., Audet, J., Bastviken, D., Bishop, K., Kokic, J., Laudon, H., Lundin, E., Löfgren, S., Natchimuthu, S., Sobek, S., Teutschbein, C., Weyhenmeyer, G. A. and Grabs, T.: Carbon dioxide and methane emissions of Swedish low-order streams—a national estimate and lessons learnt from more than a decade of observations, \*Limnology and Oceanography Letters\*, 3\(3\), 156–167, doi:10.1002/lol2.10061, 2018.](#)

- 110 Wand, U., Samarkin, V. A., Nitzsche, H.-M. and Hubberten, H.-W.: Biogeochemistry of methane in the permanently ice-covered Lake Untersee, central Dronning Maud Land, East Antarctica, Limnology and Oceanography, 51(2), 1180–1194, doi:10.4319/lo.2006.51.2.1180, 2006.
- Wang, Y. and Van Cappellen, P.: A multicomponent reactive transport model of early diagenesis: Application to redox cycling in coastal marine sediments, Geochimica et Cosmochimica Acta, 60(16), 2993–3014, doi:10.1016/0016-7037(96)00140-8, 1996.
- 115 Whiticar, M. J.: Carbon and hydrogen isotope systematics of bacterial formation and oxidation of methane, Chemical Geology, 161(1), 291–314, doi:10.1016/S0009-2541(99)00092-3, 1999.
- Whiticar, M. J., Faber, E. and Schoell, M.: Biogenic methane formation in marine and freshwater environments: CO<sub>2</sub> reduction vs. acetate fermentation—Isotope evidence, Geochimica et Cosmochimica Acta, 50(5), 693–709, doi:10.1016/0016-7037(86)90346-7, 1986.
- 120 Wuebbles, D. J. and Hayhoe, K.: Atmospheric methane and global change, Earth-Science Reviews, 57(3), 177–210, doi:10.1016/S0012-8252(01)00062-9, 2002.
- Alperin, M. J., Albert, D. B. and Martens, C. S.: Seasonal variations in production and consumption rates of dissolved organic carbon in an organic rich coastal sediment, Geochimica et Cosmochimica Acta, 58(22), 4909–4930, doi:10.1016/0016-7037(94)90221-6, 1994.
- 125 Arndt, S., Jørgensen, B. B., LaRowe, D. E., Middelburg, J. J., Pancost, R. D. and Regnier, P.: Quantifying the degradation of organic matter in marine sediments: A review and synthesis, Earth Science Reviews, 123, 53–86, doi:10.1016/j.earseirev.2013.02.008, 2013.
- Arning, E. T., van Berk, W. and Schulz, H. M.: Fate and behaviour of marine organic matter during burial of anoxic sediments: Testing CH<sub>2</sub>O as generalized input parameter in reaction transport models, Marine Chemistry, 178, 8–21, doi:10.1016/j.marchem.2015.12.002, 2016.
- 130 Bastviken, D., Cole, J., Pace, M. and Tranvik, L.: Methane emissions from lakes: Dependence of lake characteristics, two regional assessments, and a global estimate: LAKE METHANE EMISSIONS, Global Biogeochemical Cycles, 18(4), n/a–n/a, doi:10.1029/2004GB002238, 2004.
- Bastviken, D., Cole, J. J., Pace, M. L. and Van de Bogert, M. C.: Fates of methane from different lake habitats: Connecting whole lake budgets and CH<sub>4</sub> emissions: FATES OF LAKE METHANE, Journal of Geophysical Research: Biogeosciences, 113(G2), n/a–n/a, doi:10.1029/2007JG000608, 2008.
- 135 Beal, E. J., House, C. H. and Orphan, V. J.: Manganese and iron dependent marine methane oxidation, Science, 325(5937), 184–187, doi:10.1126/science.1169984, 2009.
- Berg, P., Risgaard Petersen, N. and Rysgaard, S.: Interpretation of measured concentration profiles in sediment pore water, Limnology and Oceanography, 43(7), 1500–1510, doi:10.4319/lo.1998.43.7.1500, 1998.
- 140 Borowski, W. S., Paull, C. K. and Ussler, W.: Carbon cycling within the upper methanogenic zone of continental rise sediments: An example from the methane rich sediments overlying the Blake Ridge gas hydrate deposits, Marine Chemistry, 57(3), 299–311, doi:10.1016/S0304-4203(97)00019-4, 1997.
- Boudreau, B. and Marinelli, R.: A modeling study of discontinuous biological irrigation, Journal of Marine Research, 52, 947–968, doi:10.1357/0022240943076902, 1994.

- 145 Boudreau, B. P.: Diagenetic models and their implementation: modelling transport and reactions in aquatic sediments, Springer., 1997.
- Burdige, D., Komada, T., Magen, C. and Chanton, J. P.: Methane dynamics in Santa Barbara Basin (USA) sediments as examined with a reaction-transport model, *Journal of Marine Research*, 74, 277–313, 2017.
- 150 Burdige, D. J.: Preservation of Organic Matter in Marine Sediments: Controls, Mechanisms, and an Imbalance in Sediment Organic Carbon Budgets?, *Chem. Rev.*, 107(2), 467–485, doi:10.1021/cr050347q, 2007.
- Burdige, D. J. and Komada, T.: Anaerobic oxidation of methane and the stoichiometry of remineralization processes in continental margin sediments, *Limnology and Oceanography*, 56(5), 1781–1796, doi:10.4319/lo.2011.56.5.1781, 2011.
- 155 Carignan, R. and Lean, D. R. S.: Regeneration of dissolved substances in a seasonally anoxic lake: The relative importance of processes occurring in the water column and in the sediments, *Limnology and Oceanography*, 36(4), 683–707, doi:10.4319/lo.1991.36.4.0683, 1991.
- Carignan, R., Rapin, F. and Tessier, A.: Sediment porewater sampling for metal analysis: A comparison of techniques, *Geochimica et Cosmochimica Acta*, 49(11), 2493–2497, doi:10.1016/0016-7037(85)90248-0, 1985.
- Chanton, J. P., Martens, C. S. and Kelley, C. A.: Gas transport from methane-saturated, tidal freshwater and wetland sediments, *Limnology and Oceanography*, 34(5), 807–819, doi:10.4319/lo.1989.34.5.0807, 1989.
- 160 Chanton, J. P., Whiting, G. J., Blair, N. E., Lindau, C. W. and Bollich, P. K.: Methane emission from rice: Stable isotopes, diurnal variations, and CO<sub>2</sub> exchange, *Global Biogeochemical Cycles*, 11(1), 15–27, doi:10.1029/96GB03761, 1997.
- Chasar, L. S., Chanton, J. P., Glaser, P. H., Siegel, D. I. and Rivers, J. S.: Radiocarbon and stable carbon isotopic evidence for transport and transformation of dissolved organic carbon, dissolved inorganic carbon, and CH<sub>4</sub> in a northern Minnesota peatland, *Global Biogeochemical Cycles*, 14(4), 1095–1108, doi:10.1029/1999GB001221, 2000.
- 165 Clayer, F., Gobeil, C. and Tessier, A.: Rates and pathways of sedimentary organic matter mineralization in two basins of a boreal lake: Emphasis on methanogenesis and methanotrophy: Methane cycling in boreal lake sediments, *Limnology and Oceanography*, 61(S1), S131–S149, doi:10.1002/lno.10323, 2016.
- Clayer, F., Moritz, A., Gélinas, Y., Tessier, A. and Gobeil, C.: Modeling the carbon isotope signatures of methane and dissolved inorganic carbon to unravel mineralization pathways in boreal lake sediments, *Geochimica et Cosmochimica Acta*, 229, 36–52, doi:10.1016/j.gca.2018.02.012, 2018.
- 170 Cole, J. J., Prairie, Y. T., Caraco, N. F., McDowell, W. H., Tranvik, L. J., Striegl, R. G., Duarte, C. M., Kortelainen, P., Downing, J. A., Middelburg, J. J. and Melack, J.: Plumbing the Global Carbon Cycle: Integrating Inland Waters into the Terrestrial Carbon Budget, *Ecosystems*, 10(1), 172–185, doi:10.1007/s10021-006-9013-8, 2007.
- Conrad, R.: Contribution of hydrogen to methane production and control of hydrogen concentrations in methanogenic soils and sediments, *FEMS Microbiology Ecology*, 28(3), 193–202, doi:10.1111/j.1574-6941.1999.tb00575.x, 1999.
- 175 Conrad, R.: Quantification of methanogenic pathways using stable carbon isotopic signatures: a review and a proposal, *Organic Geochemistry*, 36(5), 739–752, doi:10.1016/j.orggeochem.2004.09.006, 2005.
- Conrad, R., Claus, P. and Casper, P.: Characterization of stable isotope fractionation during methane production in the sediment of a eutrophic lake, Lake Dagow, Germany, *Limnology and Oceanography*, 54(2), 457–471, doi:10.4319/lo.2009.54.2.0457, 2009.
- 180

- 1215 Corbett, J. E., Tfaily, M. M., Burdige, D. J., Cooper, W. T., Glaser, P. H. and Chanton, J. P.: Partitioning pathways of CO<sub>2</sub> production in peatlands with stable carbon isotopes, *Biogeochemistry*, 114, 327–340, 2013.
- Corbett, J. E., Tfaily, M. M., Burdige, D. J., Glaser, P. H. and Chanton, J. P.: The relative importance of methanogenesis in the decomposition of organic matter in northern peatlands, *Journal of Geophysical Research: Biogeosciences*, 120(2), 280–293, doi:10.1002/2014JG002797, 2015.
- 1220 Couture, R. M., Gobeil, C. and Tessier, A.: Chronology of Atmospheric Deposition of Arsenic Inferred from Reconstructed Sedimentary Records, *Environ. Sci. Technol.*, 42(17), 6508–6513, doi:10.1021/es800818j, 2008.
- Couture, R. M., Fischer, R., Van Cappellen, P. and Gobeil, C.: Non-steady state diagenesis of organic and inorganic sulfur in lake sediments, *Geochimica et Cosmochimica Acta*, 194, 15–33, doi:10.1016/j.gea.2016.08.029, 2016.
- 1225 Cranwell, P. A.: Diagenesis of free and bound lipids in terrestrial detritus deposited in a lacustrine sediment, *Organic Geochemistry*, 3(3), 79–89, doi:10.1016/0146-6380(81)90002-4, 1981.
- ~~D'arcy, P.: Relations entre les propriétés du bassin versant, la morphométrie du lac et la qualité des eaux, INRS ETE, Université du Québec, Québec City, Québec, Canada., 1993.~~
- 1230 DelSontro, T., Boutet, L., St-Pierre, A., del Giorgio, P. A. and Prairie, Y. T.: Methane ebullition and diffusion from northern ponds and lakes regulated by the interaction between temperature and system productivity: Productivity regulates methane lake flux, *Limnology and Oceanography*, 61(S1), S62–S77, doi:10.1002/lno.10335, 2016.
- Egger, M., Rasigraf, O., Sapart, C. J., Jilbert, T., Jetten, M. S. M., Röckmann, T., van der Veen, C., Bândă, N., Kartal, B., Ettwig, K. F. and Slomp, C. P.: Iron Mediated Anaerobic Oxidation of Methane in Brackish Coastal Sediments, *Environ. Sci. Technol.*, 49(1), 277–283, doi:10.1021/es503663z, 2015.
- 1235 Ettwig, K. F., Butler, M. K., Le Paslier, D., Pelletier, E., Mangenot, S., Kuypers, M. M. M., Schreiber, F., Dutilh, B. E., Zedelius, J., de Beer, D., Gloerich, J., Wessels, H. J. C. T., van Alen, T., Luesken, F., Wu, M. L., van de Pas-Schoonen, K. T., Op-den Camp, H. J. M., Janssen-Megens, E. M., Francoijs, K. J., Stunnenberg, H., Weissenbach, J., Jetten, M. S. M. and Strous, M.: Nitrite-driven anaerobic methane oxidation by oxygenic bacteria, *Nature*, 464(7288), 543–548, doi:10.1038/nature08883, 2010.
- 1240 Feyte, S., Gobeil, C., Tessier, A. and Cossa, D.: Mercury dynamics in lake sediments, *Geochimica et Cosmochimica Acta*, 82, 92–112, doi:10.1016/j.gea.2011.02.007, 2012.
- Forster, S. and Graf, G.: Impact of irrigation on oxygen flux into the sediment: intermittent pumping by *Callinassa subterranea* and “piston pumping” by *Lanice conchilega*, *Marine Biology*, 123(2), 335–346, doi:10.1007/BF00353625, 1995.
- Galand, P. E., Yrjälä, K. and Conrad, R.: Stable carbon isotope fractionation during methanogenesis in three boreal peatland ecosystems, *Biogeosciences*, 7(11), 3893–3900, doi:https://doi.org/10.5194/bg-7-3893-2010, 2010.
- 1245 Gallon, C., Hare, L. and Tessier, A.: Surviving in anoxic surroundings: how burrowing aquatic insects create an oxic microhabitat, *Journal of the North American Benthological Society*, 27(3), 570–580, doi:10.1899/07-132.1, 2008.
- Hare, L.: Sediment Colonization by Littoral and Profundal Insects, *Journal of the North American Benthological Society*, 14, 315, doi:10.2307/1467783, 1995.

- 1250 Hare, L., Carignan, R. and Huerta-Diaz, M. A.: A field study of metal toxicity and accumulation by benthic invertebrates: implications for the acid volatile sulfide (AVS) model, *Limnology and Oceanography*, 39(7), 1653–1668, doi:10.4319/lo.1994.39.7.1653, 1994.
- Hastie, A., Lauerwald, R., Weyhenmeyer, G., Sobek, S., Verpoorter, C. and Regnier, P.: CO<sub>2</sub> evasion from boreal lakes: Revised estimate, drivers of spatial variability, and future projections, *Global Change Biology*, 24(2), 711–728, doi:10.1111/geb.13902, 2018.
- 1255 Hedges, J. I. and Oades, J. M.: Comparative organic geochemistries of soils and marine sediments, *Organic Geochemistry*, 27(7), 319–361, doi:10.1016/S0146-6380(97)00056-9, 1997.
- Hesslein, R. H.: An in situ sampler for close interval pore water studies I, *Limnology and Oceanography*, 21(6), 912–914, doi:10.4319/lo.1976.21.6.0912, 1976.
- 1260 Holgerson, M. A. and Raymond, P. A.: Large contribution to inland water CO<sub>2</sub> and CH<sub>4</sub> emissions from very small ponds, *Nature Geoscience*, 9(3), 222–226, doi:10.1038/ngeo2654, 2016.
- Holmkvist, L., Ferdelman, T. G. and Jørgensen, B. B.: A cryptic sulfur cycle driven by iron in the methane zone of marine sediment (Aarhus Bay, Denmark), *Geochimica et Cosmochimica Acta*, 75(12), 3581–3599, doi:10.1016/j.gea.2011.03.033, 2011.
- 1265 Hornibrook, E. R. C., Longstaffe, F. J. and Fyfe, W. S.: Spatial distribution of microbial methane production pathways in temperate zone wetland soils: Stable carbon and hydrogen isotope evidence, *Geochimica et Cosmochimica Acta*, 61(4), 745–753, doi:10.1016/S0016-7037(96)00368-7, 1997.
- Hornibrook, E. R. C., Longstaffe, F. J. and Fyfe, W. S.: Evolution of stable carbon isotope compositions for methane and carbon dioxide in freshwater wetlands and other anaerobic environments, *Geochimica et Cosmochimica Acta*, 64(6), 1013–1027, doi:10.1016/S0016-7037(99)00321-X, 2000.
- 1270 Jørgensen, B. B. and Parkes, R. J.: Role of sulfate reduction and methane production by organic carbon degradation in eutrophic fjord sediments (Limfjorden, Denmark), *Limnology and Oceanography*, 55(3), 1338–1352, doi:10.4319/lo.2010.55.3.1338, 2010.
- 1275 Kankaala, P., Huotari, J., Tulonen, T. and Ojala, A.: Lake size dependent physical forcing drives carbon dioxide and methane effluxes from lakes in a boreal landscape, *Limnology and Oceanography*, 58(6), 1915–1930, doi:10.4319/lo.2013.58.6.1915, 2013.
- Laforte, L., Tessier, A., Gobeil, C. and Carignan, R.: Thallium diagenesis in lacustrine sediments, *Geochimica et Cosmochimica Acta*, 69(22), 5295–5306, doi:10.1016/j.gea.2005.06.006, 2005.
- LaRowe, D. E. and Van Cappellen, P.: Degradation of natural organic matter: A thermodynamic analysis, *Geochimica et Cosmochimica Acta*, 75(8), 2030–2042, doi:10.1016/j.gea.2011.01.020, 2011.
- 1280 Lazzaretti, M. A., Hanselmann, K. W., Brandl, H., Span, D. and Bachofen, R.: The role of sediments in the phosphorus cycle in Lake Lugano. II. Seasonal and spatial variability of microbiological processes at the sediment-water interface, *Aquatic Science*, 54(3), 285–299, doi:10.1007/BF00878142, 1992.
- Lazzaretti Ulmer, M. A. and Hanselmann, K. W.: Seasonal variation of the microbially regulated buffering capacity at sediment-water interfaces in a freshwater lake, *Aquat. Sci.*, 61(1), 59–74, doi:10.1007/s000270050052, 1999.



- 1285 Matsumoto, G. I.: Biogeochemical study of organic substances in Antarctic lakes, *Hydrobiologia*, 172(1), 265–299, doi:10.1007/BF00031627, 1989.
- Meile, C. D., Berg, P., Cappellen, P. S. J. and Tuncay, K.: Solute specific pore water irrigation: Implications for chemical cycling in early diagenesis, *Journal of Marine Research*, 63, doi:10.1357/0022240054307885, 2005.
- 1290 Natchimuthu, S., Wallin, M. B., Klemetsson, L. and Bastviken, D.: Spatio-temporal patterns of stream methane and carbon dioxide emissions in a hemiboreal catchment in Southwest Sweden, *Scientific Reports*, 7(1), doi:10.1038/srep39729, 2017.
- Niessen, F., Wick, L., Bonani, G., Chondrogianni, C. and Siegenthaler, C.: Aquatic system response to climatic and human changes: Productivity, bottom water oxygen status, and sapropel formation in Lake Lugano over the last 10 000 years, *Aquatic Science*, 54(3), 257–276, doi:10.1007/BF00878140, 1992.
- 1295 Norði, K. à, Thamdrup, B. and Schubert, C. J.: Anaerobic oxidation of methane in an iron-rich Danish freshwater lake sediment, *Limnology and Oceanography*, 58(2), 546–554, doi:10.4319/lo.2013.58.2.0546, 2013.
- Paraska, D. W., Hipsey, M. R. and Salmon, S. U.: Sediment diagenesis models: Review of approaches, challenges and opportunities, *Environmental Modelling & Software*, 61, 297–325, doi:10.1016/j.envsoft.2014.05.011, 2014.
- 1300 Pohlman, J. W., Ruppel, C., Hutchinson, D. R., Downer, R. and Coffin, R. B.: Assessing sulfate reduction and methane cycling in a high salinity pore water system in the northern Gulf of Mexico, *Marine and Petroleum Geology*, 25(9), 942–951, doi:10.1016/j.marpetgeo.2008.01.016, 2008.
- Pohlman, J. W., Riedel, M., Bauer, J. E., Canuel, E. A., Paull, C. K., Lapham, L., Grabowski, K. S., Coffin, R. B. and Spence, G. D.: Anaerobic methane oxidation in low-organic content methane seep sediments, *Geochimica et Cosmochimica Acta*, 108, 184–201, doi:10.1016/j.gca.2013.01.022, 2013.
- 1305 Poindexter, C. M., Baldocchi, D. D., Matthes, J. H., Knox, S. H. and Variano, E. A.: The contribution of an overlooked transport process to a wetland's methane emissions, *Geophysical Research Letters*, 43(12), 6276–6284, doi:10.1002/2016GL068782, 2016.
- Raghoebarsing, A. A., Pol, A., van de Pas-Schoonen, K. T., Smolders, A. J. P., Ettwig, K. F., Rijpstra, W. I. C., Schouten, S., Damsté, J. S. S., Op den Camp, H. J. M., Jetten, M. S. M. and Strous, M.: A microbial consortium couples anaerobic methane oxidation to denitrification, *Nature*, 440(7086), 918–921, doi:10.1038/nature04617, 2006.
- 1310 Riisgård, H. U. and Larsen, P. S.: Water pumping and analysis of flow in burrowing zoobenthos: an overview, *Aquat Ecol*, 39(2), 237–258, doi:10.1007/s10452-004-1916-x, 2005.
- Sabrekov, A. F., Runkle, B. R. K., Glagolev, M. V., Terentieva, I. E., Stepanenko, V. M., Kotsyurbenko, O. R., Maksyutov, S. S. and Pokrovsky, O. S.: Variability in methane emissions from West Siberia's shallow boreal lakes on a regional scale and its environmental controls, *Biogeosciences*, 14(15), 3715–3742, doi:https://doi.org/10.5194/bg-14-3715-2017, 2017.
- 1315 Sauer, P. E., Miller, G. H. and Overpeck, J. T.: Oxygen isotope ratios of organic matter in arctic lakes as a paleoclimate proxy: field and laboratory investigations, *Journal of Paleolimnology*, 25(1), 43–64, doi:10.1023/A:1008133523139, 2001.
- 1320 Saunio, M., Bousquet, P., Poulter, B., Peregón, A., Ciais, P., Canadell, J. G., Dlugokencky, E. J., Etiope, G., Bastviken, D., Houweling, S., Janssens Maenhout, G., Tubiello, F. N., Castaldi, S., Jackson, R. B., Alexe, M., Arora, V. K., Beerling, D. J., Bergamaschi, P., Blake, D. R., Brailsford, G., Brovkin, V., Bruhwiler, L., Crevoisier, C., Crill, P., Covey, K., Curry, C., Frankenberg, C., Gedney, N., Höglund-Isaksson, L., Ishizawa, M., Ito, A., Joos, F., Kim, H. S., Kleinen, T., Krummel, P., Lamarque, J. F., Langenfelds, R., Locatelli, R., Machida, T., Maksyutov, S., McDonald, K. C., Marshall, J., Melton, J. R.,

- 1325 Morino, I., Naik, V., O&apos;Doherty, S., Parmentier, F. J. W., Patra, P. K., Peng, C., Peng, S., Peters, G. P., Pison, I., Prigent, C., Prinn, R., Ramonet, M., Riley, W. J., Saito, M., Santini, M., Schroeder, R., Simpson, I. J., Spahni, R., Steele, P., Takizawa, A., Thornton, B. F., Tian, H., Tohjima, Y., Viovy, N., Voulgarakis, A., van Weele, M., van der Werf, G. R., Weiss, R., Wiedinmyer, C., Wilton, D. J., Wiltshire, A., Worthy, D., Wunch, D., Xu, X., Yoshida, Y., Zhang, B., Zhang, Z. and Zhu, Q.: The global methane budget 2000–2012, *Earth System Science Data*, 8(2), 697–751, doi:10.5194/essd-8-697-2016, 2016.
- Schindler, D. W., Curtis, P. J., Parker, B. R. and Stainton, M. P.: Consequences of climate warming and lake acidification for UV-B penetration in North American boreal lakes, *Nature*, 379(6567), 705–708, doi:10.1038/379705a0, 1996.
- 1330 Sivan, O., Schrag, D. P. and Murray, R. W.: Rates of methanogenesis and methanotrophy in deep-sea sediments, *Geobiology*, 5(2), 141–151, doi:10.1111/j.1472-4669.2007.00098.x, 2007.
- Staehr, P. A., Testa, J. M., Kemp, W. M., Cole, J. J., Sand-Jensen, K. and Smith, S. V.: The metabolism of aquatic ecosystems: history, applications, and future challenges, *Aquatic Sciences*, 74(1), 15–29, doi:10.1007/s00027-011-0199-2, 2012.
- Thottathil, S. D., Reis, P. C. J. and Prairie, Y. T.: Methane oxidation kinetics in northern freshwater lakes, *Biogeochemistry*, 143(1), 105–116, doi:10.1007/s10533-019-00552-x, 2019.
- 1335 Tipping, E.: Cation binding by humic substances, Cambridge University Press., 2002.
- Turner, A. J., Jacob, D. J., Wecht, K. J., Maasakkers, J. D., Lundgren, E., Andrews, A. E., Biraud, S. C., Boesch, H., Bowman, K. W., Deutscher, N. M., Dubey, M. K., Griffith, D. W. T., Hase, F., Kuze, A., Notholt, J., Ohyama, H., Parker, R., Payne, V. H., Sussmann, R., Sweeney, C., Velazco, V. A., Warneke, T., Wennberg, P. O. and Wunch, D.: Estimating global and North American methane emissions with high spatial resolution using GOSAT satellite data, *Atmospheric Chemistry and Physics*, 15(12), 7049–7069, doi:https://doi.org/10.5194/acp-15-7049-2015, 2015.
- 1340 Ullman, W. J. and Aller, R. C.: Diffusion coefficients in nearshore marine sediments<sup>1</sup>, *Limnology and Oceanography*, 27(3), 552–556, doi:10.4319/lo.1982.27.3.0552, 1982.
- Verpoorter, C., Kutser, T., Seekell, D. A. and Tranvik, L. J.: A global inventory of lakes based on high-resolution satellite imagery, *Geophysical Research Letters*, 41(18), 6396–6402, doi:10.1002/2014GL060641, 2014.
- 1345 Wallin, M. B., Campeau, A., Audet, J., Bastviken, D., Bishop, K., Kokic, J., Laudon, H., Lundin, E., Löfgren, S., Natchimuthu, S., Sobek, S., Teutschbein, C., Weyhenmeyer, G. A. and Grabs, T.: Carbon dioxide and methane emissions of Swedish low-order streams—a national estimate and lessons learnt from more than a decade of observations, *Limnology and Oceanography Letters*, 3(3), 156–167, doi:10.1002/lo2.10061, 2018.
- 1350 Wand, U., Samarkin, V. A., Nitzsche, H. M. and Hubberten, H. W.: Biogeochemistry of methane in the permanently ice-covered Lake Untersee, central Dronning Maud Land, East Antarctica, *Limnology and Oceanography*, 51(2), 1180–1194, doi:10.4319/lo.2006.51.2.1180, 2006.
- Wang, Y. and Van Cappellen, P.: A multicomponent reactive transport model of early diagenesis: Application to redox cycling in coastal marine sediments, *Geochimica et Cosmochimica Acta*, 60(16), 2993–3014, doi:10.1016/0016-7037(96)00140-8, 1996.
- 1355 Whiticar, M. J.: Carbon and hydrogen isotope systematics of bacterial formation and oxidation of methane, *Chemical Geology*, 161(1), 291–314, doi:10.1016/S0009-2541(99)00092-3, 1999.

~~Whiticar, M. J., Faber, E. and Schoell, M.: Biogenic methane formation in marine and freshwater environments: CO<sub>2</sub> reduction vs. acetate fermentation—Isotope evidence, *Geochimica et Cosmochimica Acta*, 50(5), 693–709, doi:10.1016/0016-7037(86)90346-7, 1986.~~

1360 ~~Wuebbles, D. J. and Hayhoe, K.: Atmospheric methane and global change, *Earth Science Reviews*, 57(3), 177–210, doi:10.1016/S0012-8252(01)00062-9, 2002.~~

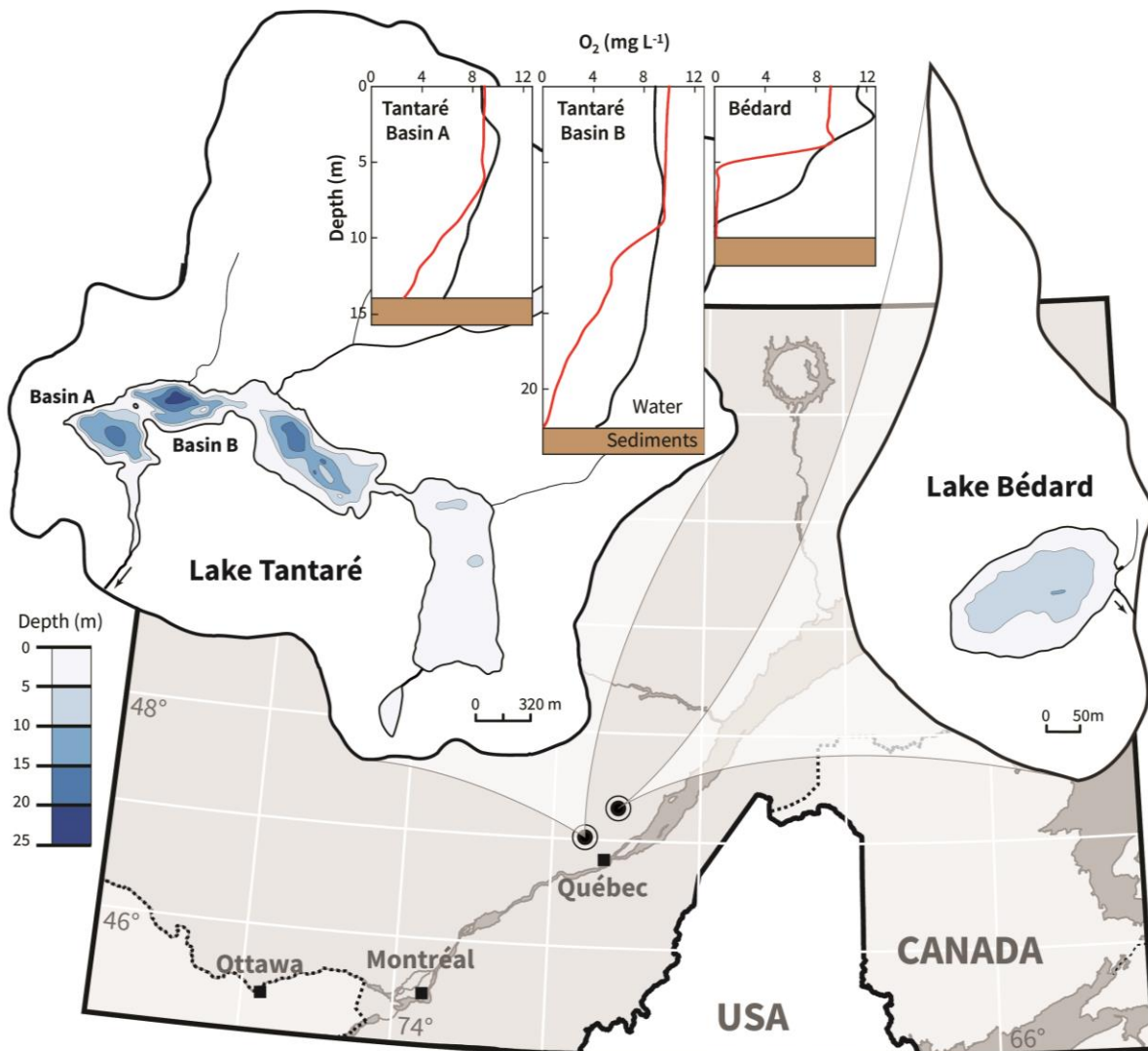
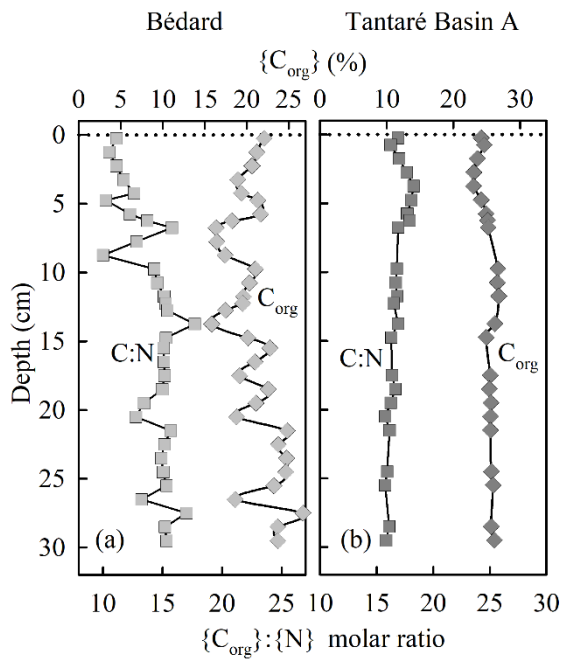
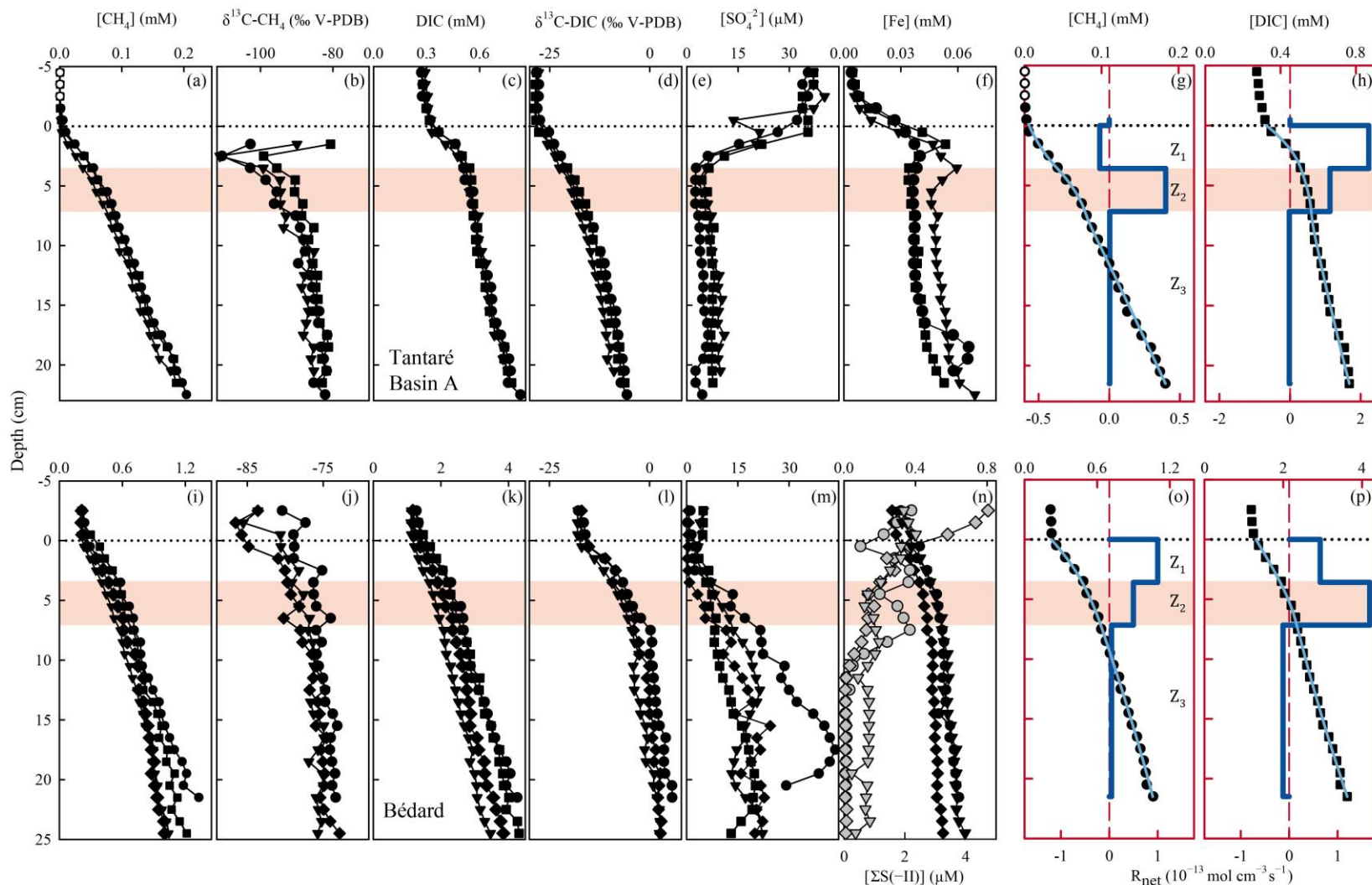


Figure 1: Location map and bathymetry of Lakes Tantaré and Bédard. The bathymetric map of Lake Tantaré was reproduced from the map C-9287 of the Service des eaux de surface of the Québec Ministry of Environment. The map of Lake Bédard was reproduced from D'Arcy (1993). Dioxygen concentrations in the water column of Lake Tantaré basins A and B, and of Lake Bédard are given for June (black lines) and October (red lines).

1365



**Figure 2: Depth profiles of the organic C concentrations and of the C : N molar ratio in sediment cores collected at the deepest sites of Lake Bédard (a) and Lake Tantaré Basin A (b).**



**Figure 2-3:** Replicate porewater profiles of  $\text{CH}_4$  (a and i),  $\delta^{13}\text{C}-\text{CH}_4$  (b and j), DIC (c and k),  $\delta^{13}\text{C}-\text{DIC}$  (d and l),  $\text{SO}_4^{2-}$  (e and m), Fe and  $\Sigma\text{S}(-\text{II})$  (f and n), and comparison of the modeled (blue lines) and average ( $n = 3$ ) measured (symbols) concentration profiles of  $\text{CH}_4$  (g and o) and DIC (h and p) in Lakes Tantaré Basin A (a–h) and Bédard (i–p). Different symbols indicate data from different peepers and empty symbols are for concentrations below detection limit. The horizontal dotted line indicates the sediment-water interface. The thick and thin blue lines represent the net solute reaction rate ( $R_{\text{net}}^{\text{solute}}$ ) and the modeled concentration profiles, respectively. The red area fills correspond to the sediment zones  $Z_1$ .

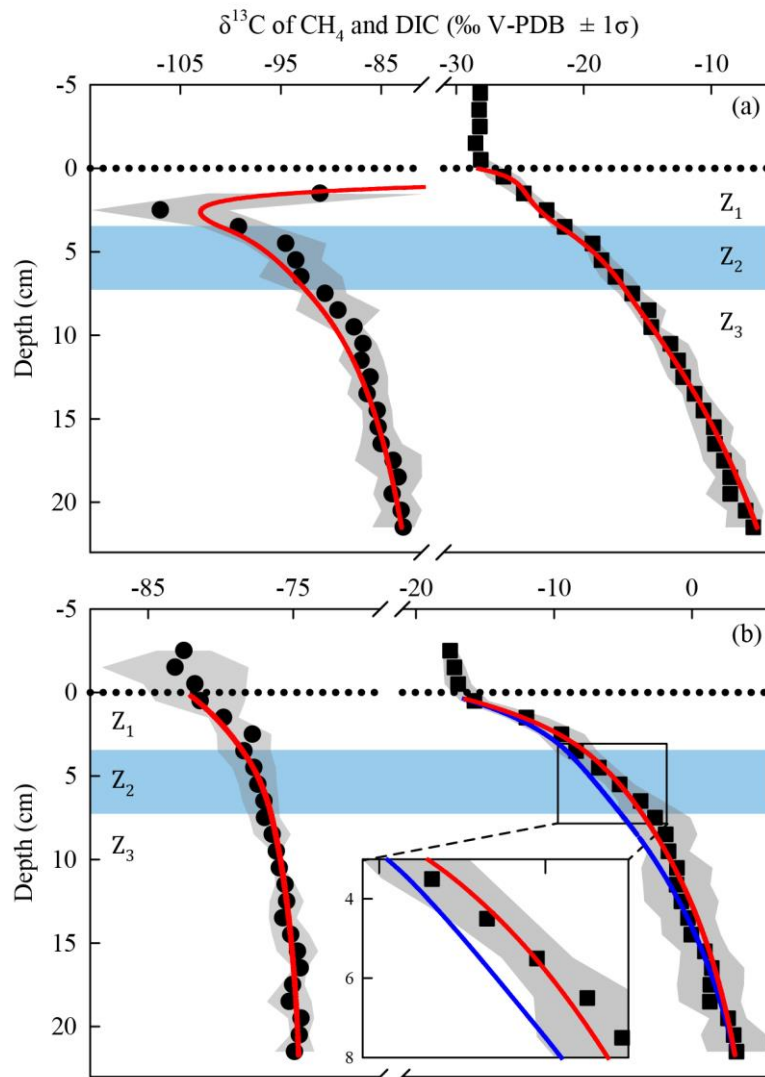


**Figure 3-4:** Comparison of the simulated (lines) and measured average ( $n = 3$ )  $\delta^{13}\text{C}$  profiles of  $\text{CH}_4$  (circles) and DIC (squares) in the porewater of Lake Tantaré Basin A (a) and Lake Bédard (b). The horizontal dotted line indicates the sediment-water interface. The variability in  $\delta^{13}\text{C}$  values ( $\pm$  one standard deviation  $-\sigma$ ) related to the spatial heterogeneity within the sampling area is shown by the grey area fills. The zone  $Z_2$  is delimited by the blue area fill. In panel b, the blue lines are the profiles simulated with the default rate values and optimal  $\alpha_1$  and  $f$  values as described in section S2.2.1. The red lines in panel (b) are the profiles simulated with  $\alpha_2$  values of 0.980–0.984 (see section 4.1 for details).

1395

CH<sub>4</sub> -□- and DIC -○- concentrations (mM)

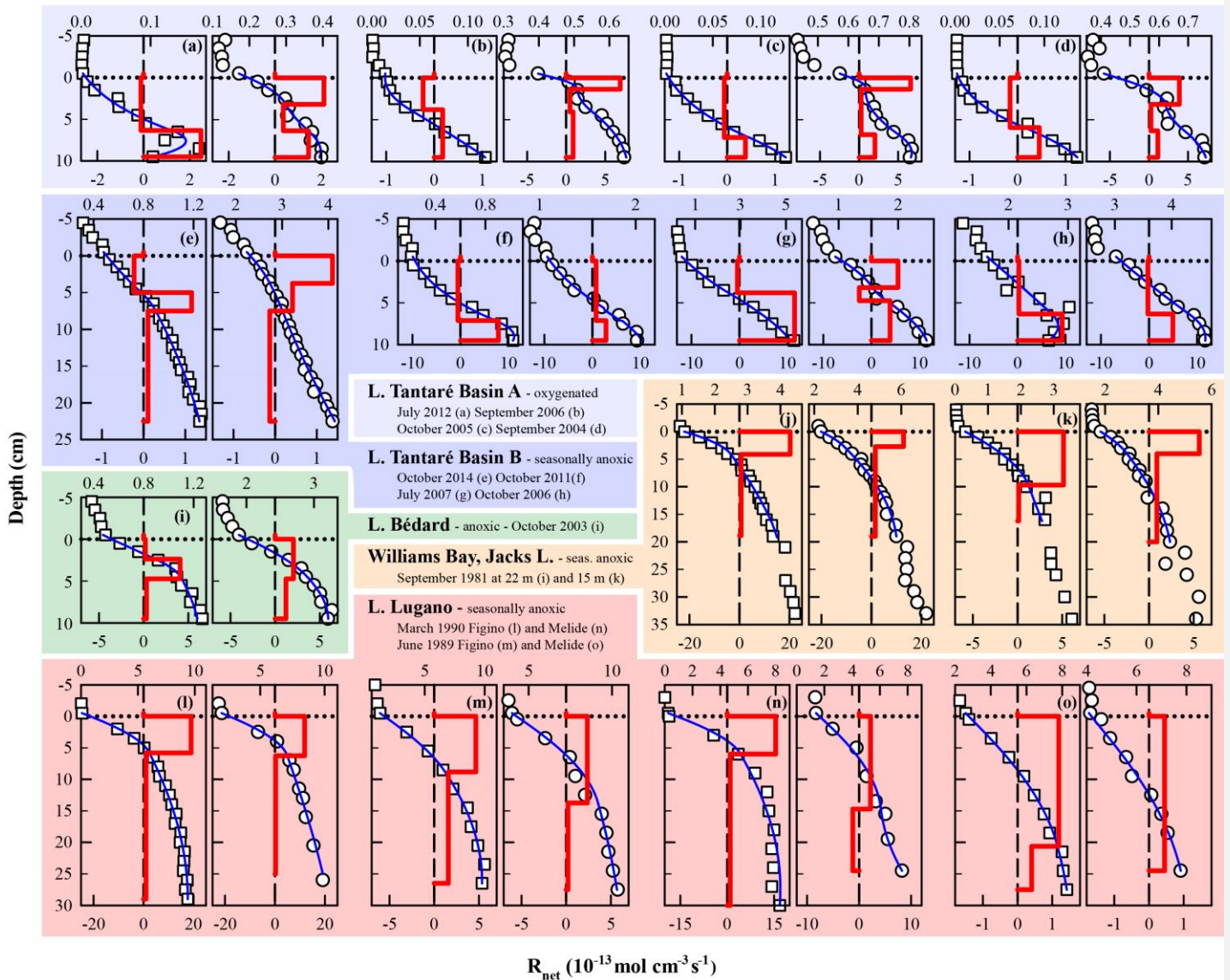


**Figure 4-5:** Comparison of the modeled (blue lines) and average ( $n = 3$ ) measured concentration profiles of CH<sub>4</sub> (squares) and DIC (circles) in Lakes Tantaré Basin A (a–d) and Basin B (a–h), Bédard (i), Jacks Lake (j–k) and Lake Lugano (l–o) at various sampling dates. The thick red lines represent the net solute reaction rate ( $R_{net}^{solute}$ ).



**Table 1: Reactions (r1–r8) considered, their reaction rates ( $R_1$ – $R_8$ ) and carbon isotopic fractionation factors ( $\alpha_1$ – $\alpha_7$ ).**

Description	Reaction	ID
<b>CO<sub>2</sub> production due to complete fermentation of labile OM <sup>a</sup></b>		
	$C_xH_yO_z + (x + v_1 - z)H_2O \xrightarrow[\alpha_1]{R_1} \left(\frac{x - v_1}{2}\right)CH_3COOH + v_1CO_2 + \left(\frac{y}{2} - z + 2v_1\right)H_2$	r1
<b>CO<sub>2</sub> production due to partial fermentation of HMW OM <sup>a,b</sup></b>		
	$v_2HMW\ OM \xrightarrow[\alpha_2]{R_2} v_3\ LMW\ OM + v_4CO_2$	r2
<b>Methanogenesis via</b>		
acetoclasty	$CH_3COOH \xrightarrow[\alpha_3]{R_3} CH_4 + CO_2$	r3
hydrogenotrophy	$CO_2 + 4H_2 \xrightarrow[\alpha_4]{R_4} CH_4 + 2H_2O$	r4
<b>CO<sub>2</sub> production due to</b>		
methanotrophy	$CH_4 + 2\ Oxidants \xrightarrow[\alpha_5]{R_5} CO_2 + 2\ Reducers$	r5
OM oxidation	$OM + Oxidant \xrightarrow[\alpha_6]{R_6} CO_2 + Reducer$	r6
<b>Precipitation of siderite</b>	$Fe^{2+} + CO_2 + H_2O \xrightarrow[\alpha_7]{R_7} FeCO_{3(s)} + 2H^+$	r7
<b>H<sub>2</sub> production through a Fe-S cryptic cycle <sup>a,c</sup></b>		
	$(16 + v_5)H_2S + 8FeOOH \xrightarrow{R_8} 8FeS_2 + v_5SO_4^{2-} + (4 + 4v_5)H_2 + (16 - 4v_5)H_2O + 2v_5H^+$	r8

<sup>a</sup> where  $v_1$  can have any value between 0 and x, values for  $v_2$ – $v_4$  are unknown and  $v_5$  can have any value between 0 and 1.

<sup>b</sup> HMW OM and LMW OM designate high and lower molecular weight organic matter, respectively.

<sup>c</sup> adapted from Holmkvist et al. (2011)

**Table 2: Net production rates ( $R_{\text{net}}^{\text{solute}}$ ) of CH<sub>4</sub>, DIC and oxidants obtained with the code PROFILE in the three CH<sub>4</sub> consumption/production zones (Z<sub>1</sub>, Z<sub>2</sub> and Z<sub>3</sub>) for both sampling sites.**

Sampling site	Zones	Depth	$R_{\text{net}}^{\text{DIC}}$	$R_{\text{net}}^{\text{CH}_4}$	$R_{\text{net}}^{\text{Ox}}$
([O <sub>2</sub> ] in mg L <sup>-1</sup> )		(cm)	(fmol cm <sup>-3</sup> s <sup>-1</sup> )		
Tantaré Basin A (2.5)	Z <sub>1</sub>	0–3.6	223	-7	-335
	Z <sub>2</sub>	3.6–7.2	113	39	-103
	Z <sub>3</sub>	7.2–21.5	-2	1	
Bédard (<0.1)	Z <sub>1</sub>	0–3.6	65	100	-6.5
	Z <sub>2</sub>	3.6–7.2	167	50	-4.5
	Z <sub>3</sub>	7.2–21.5	-13	5	

1425

**Table 3: Molecular diffusivity ratio of CH<sub>4</sub> (f-CH<sub>4</sub>) as well as the isotopic fractionation factors ( $\alpha_1$ ,  $\alpha_2$ ,  $\alpha_4$ – $\alpha_7$ ), the fraction of oxidant used by methanotrophy ( $\chi_M$ ) and rates (R<sub>1</sub>, R<sub>2</sub>, R<sub>4</sub>–R<sub>7</sub>; fmol cm<sup>-3</sup> s<sup>-1</sup>) of each reaction involved in OM mineralization in each zone and for the whole sediment column ( $\Sigma R_i$ ; fmol cm<sup>-2</sup> s<sup>-1</sup>) corresponding to the lowest values of N<sub>res</sub>. At both study sites, R<sub>3</sub> was shown to be negligible. See section S2 of the SI for details.**

Study site	Zones	f-CH <sub>4</sub>	$\alpha_1$	$\alpha_2$	$\alpha_4$	$\alpha_5$	$\alpha_6$	$\alpha_7$	R <sub>1</sub>	R <sub>2</sub>	R <sub>4</sub>	R <sub>5</sub>	R <sub>6</sub>	R <sub>7</sub>	$\chi_M$
Tantaré Basin A	Z <sub>1</sub>	1.003	1.000	-	1.094	1.024	1.000	-	132	-	119	126	84	-	<u>0.75</u>
	Z <sub>2</sub>	1.003	1.000	-	1.087	1.005	1.000	-	126	-	78	39	26	-	<u>0.75</u>
	Z <sub>3</sub>	1.003	-	-	1.085	-	-	-	-	-	1	-	-	-	-
	$\Sigma R_i$								931	-	721	592	394	-	-
Bédard	Z <sub>1</sub>	1.003	1.000	-	1.074	-	-	-	165	-	100	-	-	-	-
	Z <sub>2</sub>	1.003	-	0.984 <sup>a</sup>	1.074	-	-	-	72 <sup>b</sup>	145 <sup>b</sup>	50	-	-	-	-
	Z <sub>3</sub>	1.003	-	-	1.074	-	-	0.995	-	-	5	-	-	8	-
	$\Sigma R_i$								853	522	612	-	-	114	-

<sup>a</sup>the optimal value of  $\alpha_2$ , given here ~~is~~ for a COS value of -1.5, varies slightly with the COS value (see section S2.2.2.3 of the SI).

1430

<sup>b</sup>the ~~value~~ values of R<sub>1</sub> and R<sub>2</sub>, given here ~~is~~ for a COS value of -1.5, ~~varies~~ vary with the COS value (see section S2.2.2.3 of the SI).

**Table 4: Net reaction rates ( $R_{\text{net}}^{\text{solute}}$ ;  $\text{fmol cm}^{-3} \text{ s}^{-1}$ ) of  $\text{CH}_4$ , DIC and oxidants in the zone with the highest production rate of  $\text{CH}_4$  as well as the  $\text{O}_2$  concentration in the bottom water ( $[\text{O}_2]$  in  $\text{mg L}^{-1}$ ), the  $R_2$  rates ( $\text{fmol cm}^{-3} \text{ s}^{-1}$ ) and the average carbon oxidation state (COS) of the fermenting OM at the origin of  $\text{CH}_4$  calculated with Eq. (129) at both study sites, Lake Tantaré Basin B (Fig. 1), Jacks Lake (Carignan and Lean 1991) and Lake Lugano (Lazzaretti-Ulmer & Hanselmann 1999) for various sampling dates.**

Lake Basin	Sampling date	$[\text{O}_2]$	$R_{\text{net}}^{\text{DIC}}$	$R_{\text{net}}^{\text{CH}_4}$	$R_{\text{net}}^{\text{Ox}}$	$R_2$	Reference	COS <sup>a</sup>	
								Min.	Max.
Tantaré Basin A, 15 m	Oct 2015 – Z <sub>1</sub>	3.5	223	-7	-335	0	this study	-3.2	-3.2
	Oct 2015 – Z <sub>2</sub>	3.5	113	39	-103	0	this study	-0.9	-0.9
	Jul 2012	6.0	143	245	-66	-	1	-2.1	-1.7
	Sep 2006	4.0	89	33	-45	-	1	0.4	0.6
	Oct 2005	3.1	202	48	-44	-	1	1.8	2.1
	Sep 2004	4.6	99	45	-60	-	1	-0.3	-0.2
Tantaré Basin B, 22 m	Oct 2014	< 0.1	42	116	-1	-	2	-1.9	-1.9
	Oct 2011	0.4	279	783	-12	-	1	-2.0	-1.9
	Jul 2007	4.1	283	1147	-20	-	1	-2.5	-2.5
	Oct 2006	< 0.1	442	825	-2	-	1	-1.2	-1.2
Bédard, 10 m	Oct 2015 – Z <sub>1</sub>	< 0.1	65	100	-6.5	0	this study	-1.1	-1.0
	Oct 2003	< 0.1	205	408	-13	-	3	-1.4	-1.4
Jacks Lake, 15 m	Sep 1981	na	284	514	-	-	4	-1.2	-1.2
Jacks Lake, 22 m	Sep 1981	na	904	2030	-	-	4	-1.5	-1.5
Lugano, Melide, 85 m	Mar 1989	2.0	228	388	-83	-	5	-1.8	-1.6
Lugano, Melide, 85 m	Jun 1989	< 0.1	45	97	-1	-	5	-1.5	-1.5
Lugano, Figino, 95 m	Mar 1989	4.0	1168	1903	-234	-	5	-1.4	-1.3
Lugano, Figino, 95 m	Jun 1989	< 0.1	237	355	-19	-	5	-1.0	-0.9

<sup>a</sup> Minimum and Maximum COS values were obtained by setting  $\chi_M$  to 0 and 1 in Eq. (129), except for Tantaré Basin A in October 2015 for which  $\chi_M$  is known to be 0.75.

References: (1) Clayer et al. (2016), (2) Clayer et al. (2018), (3) see Supporting Information, (4) Carignan and Lean (1991), (5) Lazzaretti-Ulmer & Hanselmann (1999).